BMR JOURNAL

OF AUSTRALIAN GEOLOGY & GEOPHYSICS

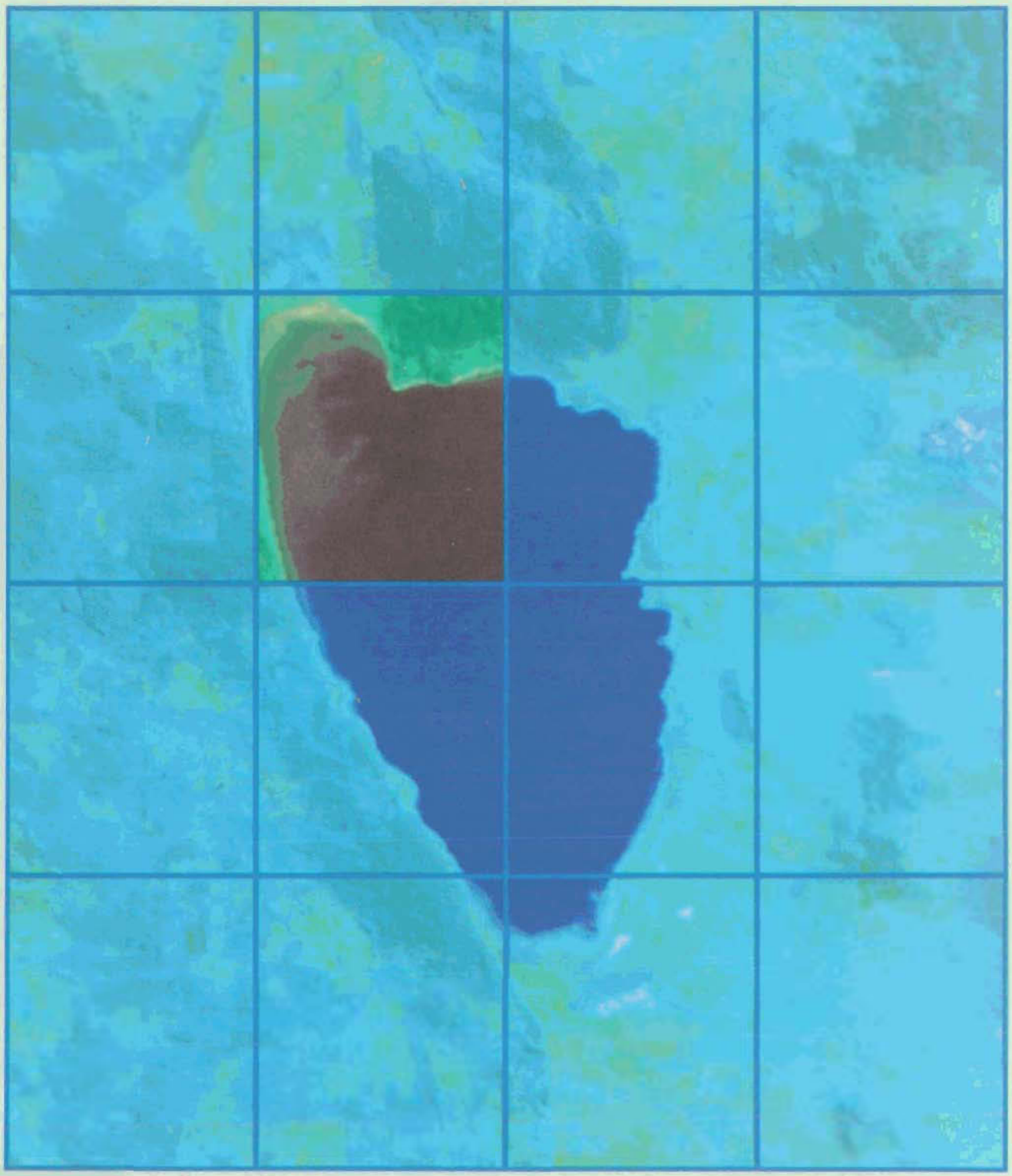

VOLUME 12 NUMBER 2

1991

BMR Journal of Australian Geology & Geophysics Volume 12 (2) 1991

BMR JOURNAL

OF AUSTRALIAN GEOLOGY & GEOPHYSICS

VOLUME 12 NUMBER 2 1991

CONTENTS

Front cover: A Landsat image of Lake George, New South Wales, showing the lake under 'lake-full' conditions, with water up to 3 m deep. The scarp of the Lake George Fault is prominent along the western shore of the lake, with darker toned forested areas to the west. The area covered by the image is about 30 km (east–west) by 35 km (north–south). The hydrogeology of Lake George is described in a paper by Jacobson & others in this issue. [Landsat data provided by the Australian Centre for Remote Sensing, Department of Administrative Services]

Editor, BMR Journal: Bernadette Hince

Cover design by Saimonne Bissett.

Figures prepared by BMR Cartographic Services Unit unless otherwise indicated.

AUSTRALIAN GOVERNMENT PUBLISHING SERVICE CANBERRA 1991

ISSN 0312–9608

Month of issue: June

Subscriptions to the BMR Journal are available through the BMR (GPO Box 378, Canberra ACT 2601; tel. (06) 249 9642, fax (06) 257 6466) or the Australian Government Publishing Service (Mail Order Sales, GPO Box 84, Canberra, ACT 2601; telephone (06) 295 4485).

Other matters concerning the Journal should be sent to the Editor, BMR Journal.

Typeset by Adtype Graphics Pty Ltd, North Sydney, NSW

Printed in Australia by P. J. GRILLS, Commonwealth Government Printer, Canberra

BMR Journal of Australian Geology & Geophysics, 12, 119–144

Application of sequence stratigraphic concepts to Middle Cambrian phosphogenesis, Georgina Basin, Australia

P.N. Southgate[1] & J.H. Shergold[1]

The stratigraphic and spatial distributions of phosphatic and organic-matter rich Middle Cambrian sediments of the Georgina Basin are outlined in terms of sequence stratigraphic concepts. This approach has permitted an integrated analysis of Middle Cambrian depositional patterns and their time constraints. It has also provided insights into aspects of the basin's structure, the timing of subsidence of its primary components, and frequency of relative sea level fluctuations. Middle to early Late Cambrian sediments of the Georgina Basin are interpreted to occur in two stratigraphic sequences. In each sequence phosphorites, phosphatic limestones and organic-matter rich shales comprise a suite of repeating lithofacies restricted to retrogradational parasequence sets of the transgressive systems tract. The position of facies within each transgressive systems tract depends on relative sea level, palaeogeography and palaeotectonics. In sequence 1 (early Middle Cambrian), phosphogenesis is related to gradual transgression of a continent with irregular palaeotopography. Sequence 1a is interpreted to be of local significance, related to early subsidence of the Mt Isa Block during the late Ordian to early Templetonian. A rapid fall in relative sea level terminated sediment accumulation in sequence 1 and led to the development of a subaerial exposure surface. Sediments of the transgressive systems tract in stratigraphic sequence 2 are of late Templetonian to early Undillan age. Deposition in sequence 2 ceased in the Mindyallan. Rocks of the transgressive systems tract occur in three retrogradational parasequence sets. Recognition of sequence boundaries has helped clarify lateral biofacies, leading to improved reconstructions of the palaeogeographic distribution of the phosphorites and organic-matter rich shales.

Introduction

In this paper we explore the application of sequence stratigraphic concepts to explain Middle Cambrian phosphogenetic events in the Georgina Basin, north-western Queensland and east central Northern Territory (Figs 1, 2). In so doing, we reassess the correlation of lithostratigraphic units throughout the basin, re-evaluate the currently available biochronology (Figs 3, 4), suggest revised palaeogeographic models, and conclude with palaeotectonic observations on the structure of the basin.

The Georgina Basin is a broad intracratonic depression covering some 325 000 km^2 of central northern Australia (Fig. 1). The eastern and northern margins abut Proterozoic rocks of the Mt Isa Block and Lawn Hill Platforms, while to the south and west the basin sequence is bounded by Proterozoic rocks of the Tennant Creek and Arunta Blocks. Rather than defining a palaeogeographic margin, the present outline is an erosional remnant of a much larger early Palaeozoic sedimentary province that once covered much of central and northern Australia.

Subsidence in the Georgina Basin followed a Late Proterozoic phase of crustal extension, now represented by volcanics of the Antrim Plateau Basalts and their correlatives (Lindsay & others, 1987). Although sediments of Early Cambrian age are found in the south (Walter & others, 1979), it was not until the Middle Cambrian that marine depositional environments prevailed throughout the basin (Shergold & Druce, 1980). A suite of anomalous chemical sediments locally rich in phosphate, organically-derived carbon, and noble metals was deposited during this Middle Cambrian transgression (Shergold, 1985; Donnelly & others, 1988). Eighteen phosphate deposits have been recognised in this transgressive sequence. The associated organic-matter rich shale facies has a total organic content (TOC) of 1–16%.

[1] Onshore Sedimentary & Petroleum Geology Program, Bureau of Mineral Resources, Geology & Geophysics, GPO Box 378, Canberra ACT 2601

Whitehouse (1936) and Öpik (1956, 1960, 1961 & 1979) provided the initial stratigraphic subdivision of the basin. It was based on biostratigraphic concepts, and resulted in a multitude of stratigraphic units which frequently lacked a clearly defined lithostratigraphic identity. De Keyser (1973) clearly demonstrated difficulties in the biostratigraphic classification, but a lack of detailed sedimentological information resulted in similar difficulties with his lithosome-based subdivisions. As a result, phosphate deposits of the Georgina Basin were until 1983 regarded as uniformly Templetonian in age, and placed in the Beetle Creek Formation (Russell, 1967; de Keyser & Cook, 1973). However, there is a laterally persistent erosion surface on top of the Thorntonia Limestone, and it has correlatable lithofacies associated with the Beetle Creek Formation in the type areas of these formations (Southgate, 1983, 1986a,b,c, 1988; Fig. 3). This raises doubts about the contemporaneity of phosphogenesis. An integrated sedimentological and palaeontological study of selected Middle Cambrian sediments investigated the implications of this disconformity to models of phosphogenesis. Although detailed biostratigraphic, lithostratigraphic and petrographic studies showed phosphorites of three different ages in a mosaic of repeating lithofacies and biofacies (Shergold & Southgate, 1988; Shergold & others, 1989), poor regional outcrop and the lack of data suitable for seismic stratigraphic interpretation prevented the use of this work in a regional model. However, using the predictive model of sequence stratigraphy (e.g. Van Wagoner & others, 1988; Sarg, 1988), data from geographically isolated areas have been integrated into a depositional model with implications for basin architecture and subsidence history.

Sequence stratigraphic concepts

Lack of outcrop continuity and the complexities of facies patterns often inhibit the regional correlation of units in sedimentary basins. Even though facies models constitute a predictive tool for interpreting facies patterns, they do not provide integrated models for basin development. Furthermore, difficulties arising from possible faunal element facies control, lack of fauna in some facies, and the possibility that faunal resolution is

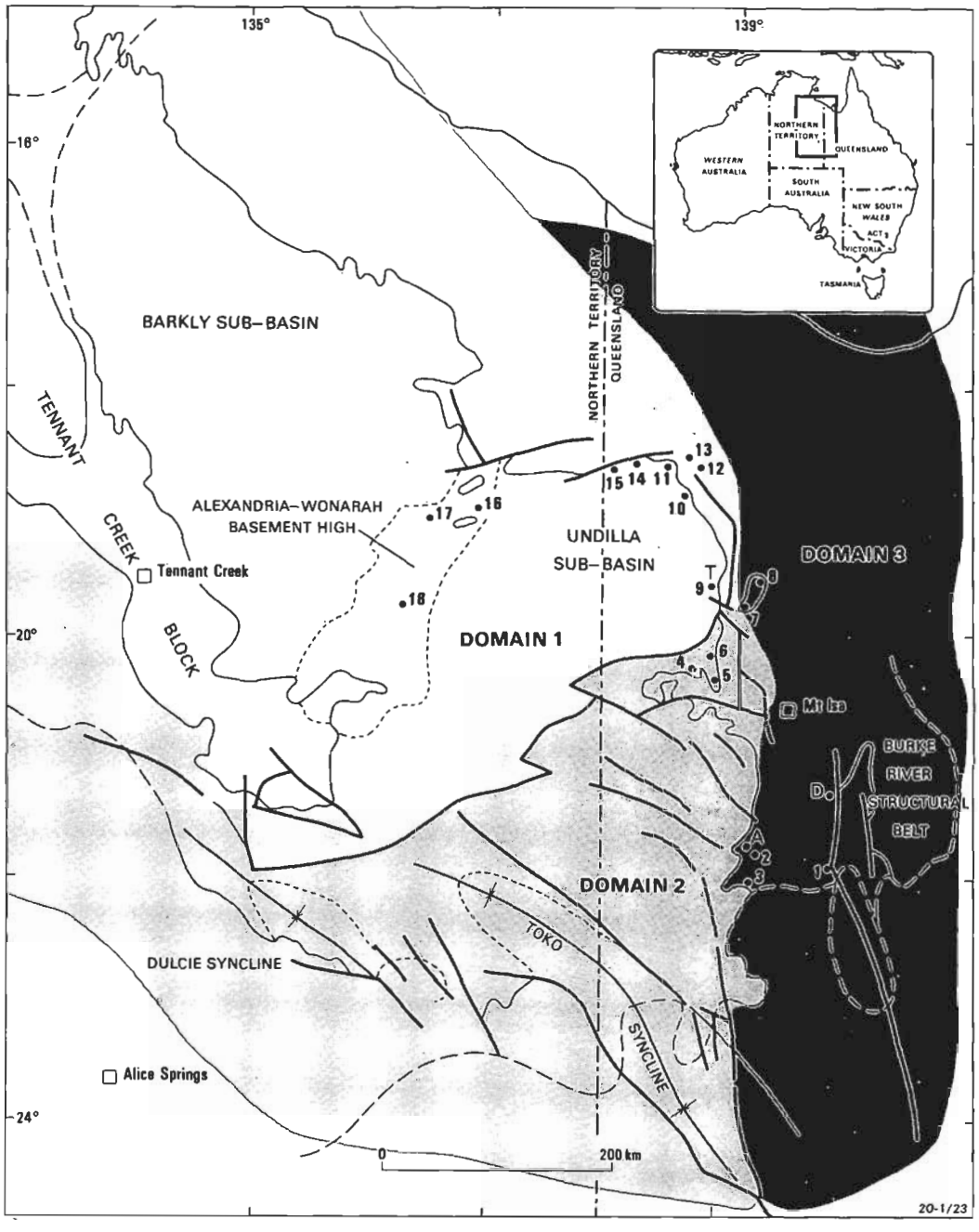

Figure 1. Principal structural features of the Georgina Basin, location of the respective domains, and geographic distribution of the phosphate deposits.

Numbered phosphate deposits: 1 Phosphate Hill, 2 Ardmore, 3 Quita Creek, 4 Lily Creek, 5 Sherrin Creek, 6 Yelvertoft, 7 Lady Annie, 8 Lady Jane, 9 D Tree, 10 Riversleigh, 11 Babbling Brook Hill, 12 Phantom Hills (Lawn Hill), 13 Mount Jennifer, 14 Mount O'Connor, 15 Highland Plains, 16 Alexandria, 17 Alroy, 18 Wonarah.

not at an appropriate scale to recognise genetically-related sedimentary units, have always hampered the correlation of sedimentary rocks on a regional scale.

Sequence stratigraphic interpretation of seismic data provides a predictive framework for combining lithostratigraphic and biostratigraphic data into regional models for basin development. In sequence stratigraphy, a complex sedimentary package is divided into chronostratigraphically-constrained, genetically-related strata, bounded either by surfaces of erosion or non-deposition, or by their correlative conformities (Van Wagoner & others, 1988). The fundamental unit of sequence stratigraphy is the sequence, a unit bounded by unconformities and their correlative conformities and containing systems tracts which are defined by the parasequences they contain (Van Wagoner & others, 1988). Although sequence stratigraphic studies have typically been based on seismic data, the model derived from sequence stratigraphy can also be a predictive tool where such data are unavailable. Sequence boundaries in seismic sections are normally recognised by stratal terminations. Such terminations are used to recognise unconformities in the field. However, disconformities and their correlative surfaces of non-deposition are often more difficult to recognise, both in seismic sections and in the field. Faunal breaks can be used to identify sequence boundaries of greater magnitude than the faunal resolution. Discontinuities in facies may indicate a sequence boundary, a change in systems tract, or

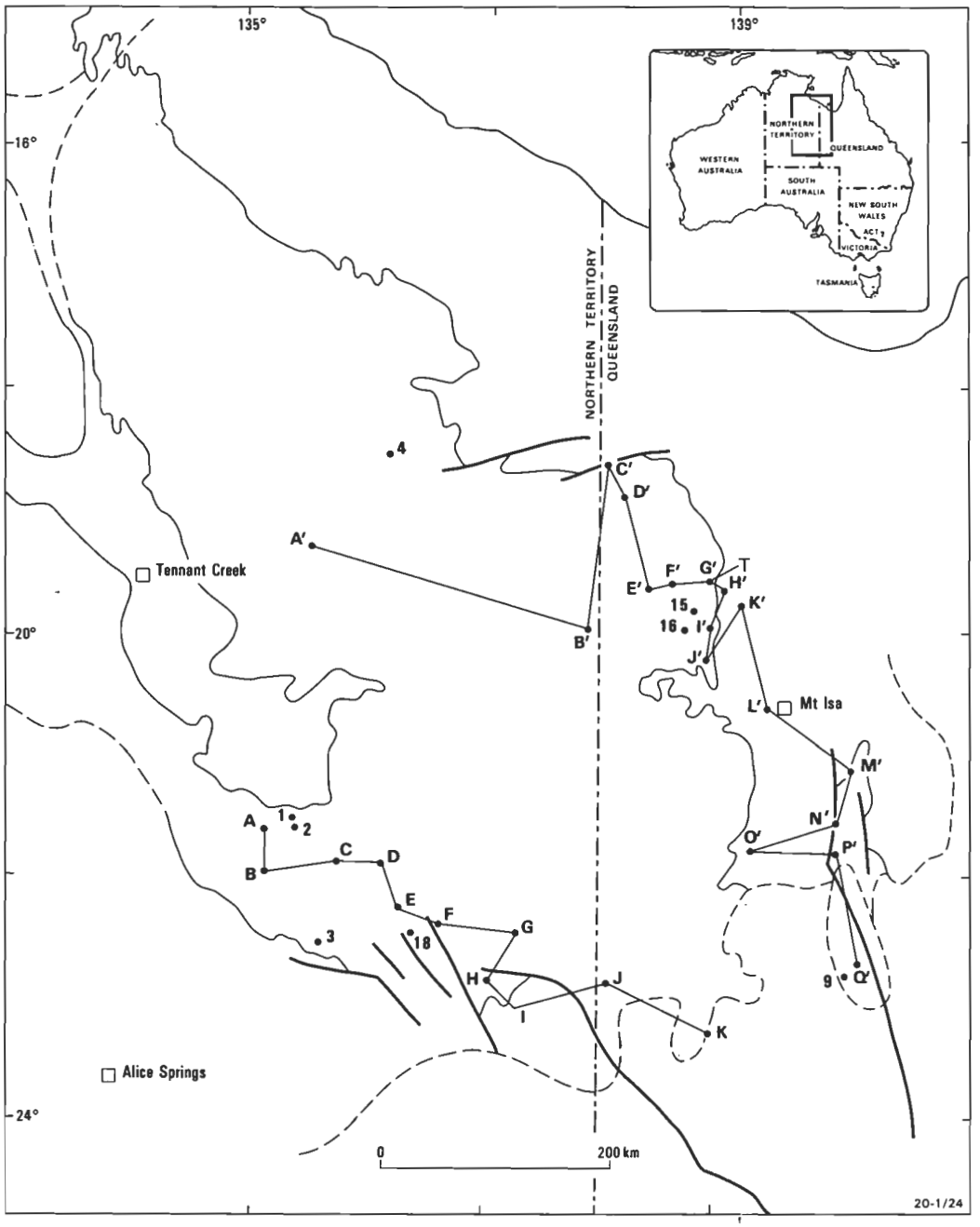

Figure 2. Distribution of stratigraphic and oil exploration wells, areas of principal outcrop, transects, and geographic localities used in the study.

A′	Frewena No. 1	A	NTGS Elkedra No. 7	1	Ammaroo No. 1
B′	BMR Cattle Creek No. 1	B	NTGS Elkedra No. 6	2	Ammaroo No. 2
C′	Highland Plains	C	NTGS Elkedra No. 3	3	Huckitta No. 1
D′	Lawn Hill	D	BMR Sandover No. 13	4	Brunette Downs No. 1
E′	Totts Creek	E	NTGS Huckitta No. 1	10	The Brothers No. 1
F′	Morstone No. 1	F	Lucy Creek No. 1	14	Marduroo No. 1
G′	Thorntonia West	G	BMR Cockroach No. 1	15	Elizabeth Springs No. 1
H′	Thorntonia East	H	BMR Tobermory No. 14	16	Canary No. 1
I′	D Tree	I	BMR Hay River No. 11	18	Beantree No. 1
J′	Yelvertoft	J	Netting Fence No. 1	Numbers: Data points or localities.	
K′	Lady Annie	K	GSQ Mt Whelan No. 1	Letters: Transects.	
L′	May Downs				
M′	Roaring Bore				
N′,	Monastery Creek				
O′	Ardmore				
P′	BMR Duchess No. 18				
Q′	Black Mountain No. 1				

a parasequence set. In each of these cases the facies are a response to, and a record of, changes in relative sea level. This contrasts with sedimentation within a parasequence, where changes in relative sea level are gradational and facies patterns predictable. Similar relationships also occur in those parts of a systems tract where the magnitude of relative sea level fluctuation is minor compared with the absolute water depth.

Domains

To simplify description of the Middle Cambrian sedimentary package, the sediments are grouped into geophysically defined and geographically and sedimentologically delineated areas, hereafter referred to as domains (Fig. 1). This terminology follows the work of Tucker & others (1979), who distinguished three structural domains within basement to the Georgina Basin. Regional differences in the sedimentary sequences recognised in the present study occur between these domains, suggesting that basement structures controlled subsidence patterns during the early stages of basin formation. The recrystallised dolostones of Domain 1 form a thin veneer of Middle, and possibly Upper, Cambrian sediment deposited in predominantly shallow shelf and peritidal environments (Shergold & Druce, 1980) on a stable carbonate platform undergoing comparatively little subsidence. In Domain 2, linear doublets of lows and highs, trending east–southeast but swinging more southerly farther east, characterise the gravity pattern (Fig. 1). The principal faults in this domain, and the associated Toko and Dulcie Synclines, parallel the gravity trends and contain some of the thickest Cambro-Ordovician sequences known in the basin. Domain 3 is defined by linear southerly to south–southeasterly trending gravity highs and lows. Its western margin is a major geophysical feature which in outcrop corresponds with the edge of the Mt Isa Block. Cambro-Ordovician sediments in Domain 3 occur in the Burke River Structural Belt, a graben-like structure parallel to the principal structural trends of the domain.

Biochronological framework

To make the present synthesis in the absence of seismic stratigraphy, great reliance has been placed on biostratigraphy to identify and correlate sequences and parasequence sets (Figs 3–6). In places, as the accompanying palaeogeographic reconstructions show, the information is inadequate and we have extrapolated observations from better known areas. These are the areas that have permitted the development of a Middle Cambrian biostratigraphy which is more complete and more intensively investigated than any other area in Australia. They have yielded the characteristic faunal assemblages which Öpik (1968a,b, 1979) used to define his Ordian, Templetonian, Floran, Undillan and Boomerangian Cambrian Stages. Original definitions made use of trilobite assemblages, particularly those of agnostoid trilobites, which evolved rapidly and had a wide geographic distribution (Öpik, 1979). Descriptions of these Middle Cambrian stages and evaluation of their concepts, including the need for revision, have been published elsewhere (Shergold, 1989). The Ordian and Templetonian Stages are particularly problematical and difficult to maintain in their original concepts (Shergold, 1989). When current basic taxonomic revisions (Laurie, 1988, 1989) are completed on materials originally used for definition by Whitehouse (1936, 1939) and Öpik (1961, 1970a,b, 1975, 1979), more refinement will be possible at this level. Here we foreshadow potential change by uniting the Ordian with the early Templetonian Stage, and the late Templetonian with the Floran. This has been brought about partly by the perceived contemporaneity of the Thorntonia Limestone and Beetle Creek Formation alluded to above, and the need to distinguish the latter (*sensu stricto*) from similar rocks in the Burke River Structural Belt and Huckitta–Elkedra regions.

In consequence the faunas of the Ordian Stage, characterised by biofacies based on *Redlichia chinensis*, must be regarded as coeval with the *Xystridura templetonensis* biofacies which characterises the Beetle Creek Formation (*sensu stricto*). The latter may then be discriminated from the *Xystridura*-bearing strata which additionally contain agnostoid trilobites of the *Triplagnostus gibbus* Zone occurring later elsewhere. Previously Shergold (1989) had considered that the *Xystridura*-bearing sequences of the Barkly Tableland and Elkedra area in the southwest Georgina Basin, for instance (which Öpik (1979) assigned to the *Peronopsis longinqua* Zone), could be a third contemporaneous Ordian/early Templetonian biofacies. Material recently determined from the NTGS Elkedra No. 3 borehole suggests that the *Peronopsis longinqua* Zone is more probably of late Templetonian age, perhaps equivalent to the early *Triplagnostus gibbus* Zone. Equally possible is the correlation of the *P. longinqua* Zone with an interval characterised by *Pentagnostus praecurrens* which predates and overlaps the range of *Triplagnostus gibbus* in the Great Basin (USA) and Scandinavia. Since *T. gibbus* is a long-ranging species and continues on into the overlying *Acidusus atavus* Zone, the existence of an independent zone of *T. gibbus* may be called into question. No continuously fossiliferous core is available to assist in the solution of such biostratigraphic problems. Nevertheless, as a result of current biostratigraphic revisions, it is possible to date the occurrence of phosphate deposits in all three geophysical domains, and in association with each of the stratigraphic sequences identified here. The faunas upon which these dates are based are listed in Appendices 1–3.

Sequence stratigraphy

Based on sequence stratigraphic concepts and predictable geometric relationships between facies, Middle Cambrian sediments of the Georgina Basin may be subdivided into two stratigraphic sequences (Figs 3 and 4; Table 1). Both sequences are of basin-wide extent and are subdivided into transgressive and highstand systems tracts. Sequence No. 1a is restricted to parts of Domain 3, and extends to the major geophysical feature that defines the western margin of this domain. In order to synthesise the facies information, the data are described in terms of the two transects shown in Figs 2, 5 and 6.

Stratigraphic sequence 1

Terrigenous clastic rocks, peritidal and shelf carbonate rocks, phosphorites and phosphatic carbonate rocks, and restricted basinal sediments occur in this stratigraphic sequence (Figs 5–7; Table 1). In the southern and central parts of the basin (transect 2, Domain 2), where outcrop is poor, biostratigraphic and lithostratigraphic data are from stratigraphic and oil

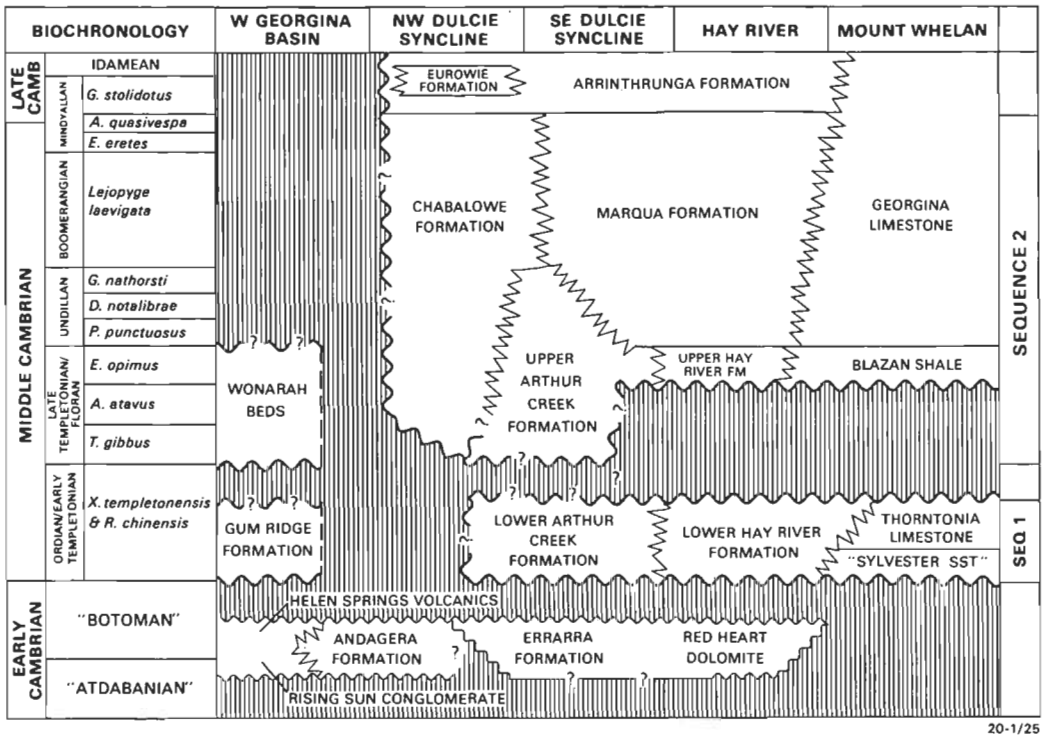

Figure 3. Sequence stratigraphic distribution of formations, northern transect.

exploration wells (Fig. 2). The best outcrop is in the northeast of the basin (transect 1, Figs 5, 7).

Sedimentation in sequence 1 commenced with gradual onlap of the palaeocontinent during the earliest Middle Cambrian (Ordian). It is not possible to estimate average sediment thickness because faulting (southern margin) and post-Tertiary erosion (northeastern margin) have removed parts of the sequence. Furthermore, the absence of sediments of appropriate age in some parts of the basin suggests that initial topographic relief on the palaeocontinent exceeded the rise in relative sea level. The thickest sections, 120–150 m, are in the northeastern parts of the basin in Domain 1. Along the northern transect (Fig. 5) sequence 1 sediments onlap in a southerly direction toward the May Downs area (Fig. 2 L′), where they terminate in shoreline facies. Along the remaining part of transect 1 and along transect 2, onlap occurs in a northerly direction, with shoreline facies developed in the northern parts of the Burke River Structural Belt and in the far southwest (Figs 5, 6). We interpret early subsidence of parts of the Mt Isa Block in Domain 3 as the cause of changed depositional patterns in stratigraphic sequence 1 (Fig. 7). This led to the accumulation of sediments in stratigraphic sequence 1a, a tectonically induced sequence, of local significance and major economic importance. A subaerial exposure surface, which indicates a major lowering in relative sea level, terminates deposition in stratigraphic sequences 1 and 1a (Fig. 8).

Lowstand systems tract. Terrigenous clastic sediments occur at the base of sequence 1 (Figs 5, 6; Table 1). Along the northern transect, poorly sorted conglomerate, sandstone, siltstone and shale beds of local provenance form thin, laterally discontinuous scree deposits and fluvial sequences which partly fill depressions in the irregular basement (Howard & Cooney, 1976; Rogers & Keevers, 1976). Over most of the Burke River Structural Belt, a soil profile caps red siltstone of the Mt Birnie Beds (de Keyser, 1968). The soil profile has a sharp upper contact with marine carbonate rocks of the Thorntonia Limestone. Along the southern transect, red to green terrigenous siltstone, mudstone, minor sandstone and marl rocks underlie sediments of the transgressive systems tract and have conformable contacts with them.

Transgressive systems tract — northern transect. Between Highland Plains (Fig. 2 C′) and May Downs Station (Fig 2 L′), phosphorite, phosphatic limestone and limestone were deposited during gradual onlap of an irregular basement. Rocks of the transgressive systems tract accumulated in peritidal, embayed and littoral environments (de Keyser & Cook, 1973) as shallowing upward cycles. Descriptions of these facies are given in de Keyser (1969) and Southgate (1986a,b, 1988). The six small phosphate deposits between Highland Plains and Riversleigh (Fig 2 D′; de Keyser & Cook, 1973) occur in this transgressive systems tract (Fig. 8).

Highstand systems tract — northern transect. Non-phosphatic dolostone overlies cyclic phosphatic sediment of the transgressive systems tract (Figs 5, 7, 8). In the northern parts of the transect, medium to thick peloid packstone and wackestone beds accumulated in deeper water platform environments. Later, as water depths decreased, peloid, ooid and oncolitic grainstone, packstone and wackestone and laminoid fenestral packstone accumulated in shallow submergent and emergent environments as progradational shallowing-upward cycles (Southgate, 1988). A shoreline for the lower parts of the highstand systems tract probably formed around a topographic high in the May Downs

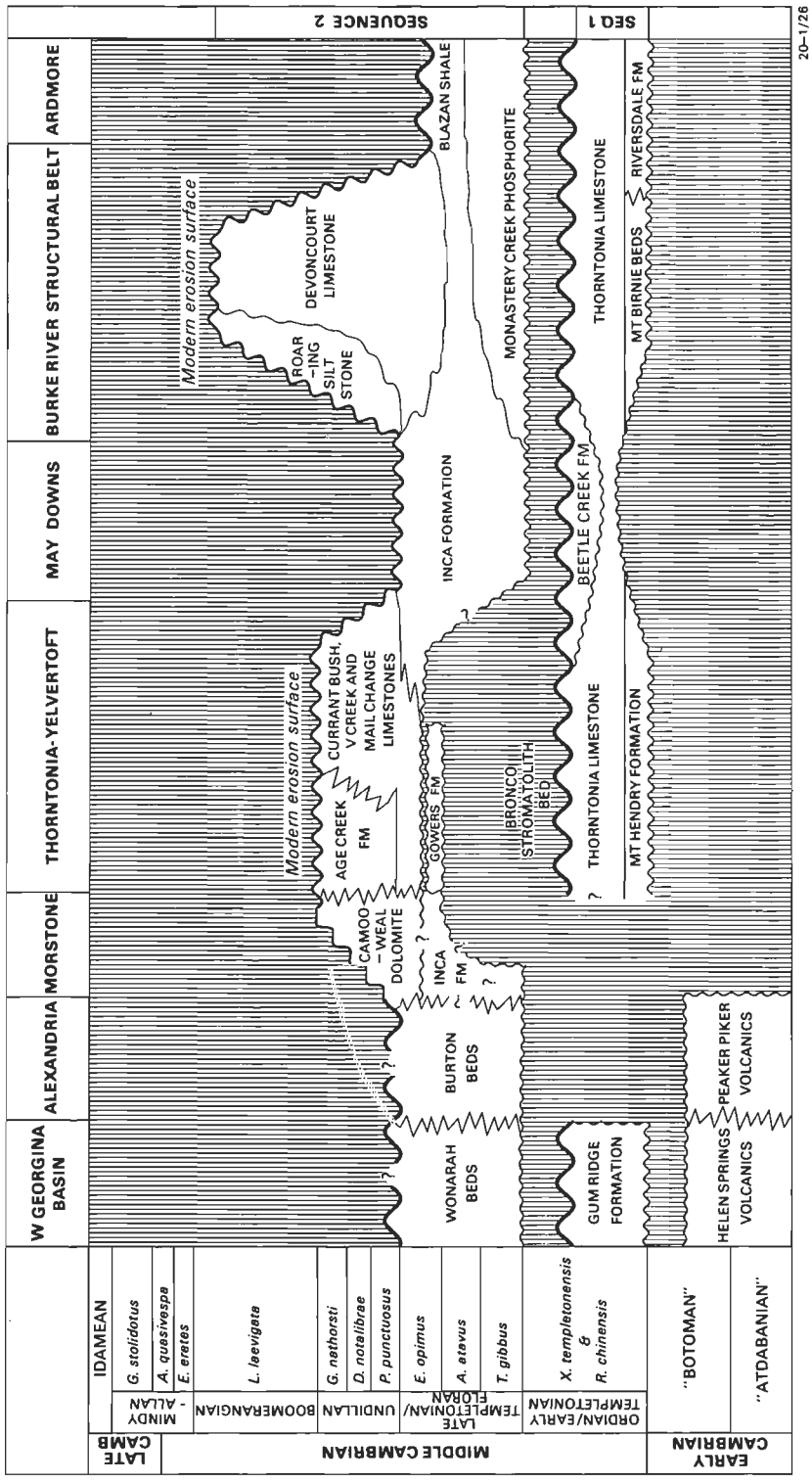

Figure 4. Sequence stratigraphic distribution of formations, southern transect.

area (Fig. 7). Here a 2–8 m thick interval of stromatolitic dolostone and chert of peritidal origin onlaps basement. This shoreline facies prograded in a northerly direction toward Yelvertoft (Fig. 2 J′).

Whereas the northern parts of the transect contain predominantly shallow water facies that onlap in a southerly direction, facies belts in the southern parts of the transect contain deeper water sediments that onlap in a northerly direction (Figs 5, 7). In the Burke River Structural Belt, the contact between the Thorntonia Limestone and coastal plain clastics of the Mt Birnie Beds is generally sharp and erosional. Retrogradational transgressive cycles are thin and poorly developed, suggesting that a rapid rise in relative sea level took place. This contrasts with the northern parts of the transect, where some 40–90 m of sediment is attributed to a keep-up transgressive systems tract (see Sarg, 1988). Such

Table 1. Distribution of Middle Cambrian formations in the Georgina Basin with respect to their stratigraphic sequence, depositional environment and domain.

Environments	*Domain 1*	*Domain 2*	*Domain 3*
Sequence 1			
Coastal plain clastics and carbonates	Mt Hendry Formation	Riversdale Formation, Sylvester Sandstone, Lower Arthur Creek Formation	Mt Birnie Beds
Peritidal carbonates	Thorntonia Limestone	Lower Arthur Creek Formation	Thorntonia Limestone and Ardmore Chert Mbr. Thorntonia Limestone
Platform carbonates	Thorntonia Limestone	Thorntonia Limestone, Lower Arthur Creek Formation	Thorntonia Limestone
Peritidal phosphorites and phosphatic limestones	Border Waterhole Formation, Thorntonia Limestone	—	? Black Mountain No. 1
Shelf phosphorites and phosphatic limestones	Border Waterhole Formation, Thorntonia Limestone	—	? Black Mountain No. 1
Black recrystallised dolostones	—	—	Thorntonia Limestone
Organic matter rich shales with a planktonic and benthonic fauna	Border Waterhole Formation	Lower Hay River Formation	? Black Mountain No. 1
Organic matter rich shales with a planktonic fauna	—	Lower Hay River Formation	? Black Mountain No. 1
Sequence 1a			
Coastal plain clastics and carbonates	—	—	Bronco Stromatolith Bed
Peritidal phosphorites and phosphatic limestones	Thorntonia Limestone & Beetle Creek Formation	—	Thorntonia Limestone and Beetle Creek Formation
Shelf phosphorites and phosphatic limestones	Thorntonia Limestone and Beetle Creek Formation	—	Thorntonia Limestone and Beetle Creek Formation
Organic matter rich shales with a planktonic and benthonic fauna	—	—	Siltstone Member Beetle Creek Formation
Organic matter rich shales with a planktonic fauna	—	—	Siltstone Member Beetle Creek Formation
Sequence 2			
Coastal plain clastics and carbonates	Bronco Stromatolith Bed	Upper Chabalowe Formation	—
Peritidal carbonates	Camooweal Dolomite	Hagen Member Chabalowe Formation	—
Platform carbonates	Camooweal Dolomite	Chabalowe Formation	—
Platform edge grainstones	Age Creek Formation	Steamboat Sandstone	—
Ramp carbonates	Currant Bush, V Creek and Mail Change Limestones	Georgina Limestones, Marqua Formation and Upper Hay River Formation	Devoncourt Limestone
Peritidal phosphorites and phosphatic limestones	Gowers Formation	Upper Arthur Creek Formation	Thorntonia Limestone and Monastery Creek Formation
Shelf phosphorites and phosphatic limestones	—	Upper Arthur Creek Formation	Monastery Creek Formation
Organic matter rich shales with a planktonic and benthonic fauna	—	Upper Arthur Creek Formation	Siltstone Member Monastery Creek Formation
Organic matter rich shale with a planktonic fauna	Inca Formation	Upper Arthur Creek Formation	Inca Formation, Blazan Shale, Roaring Siltstone

differences in sedimentation patterns suggest that sediment accumulation rates and/or subsidence rates varied across the basin.

Black recrystallised dolostone of the highstand systems tract (Thorntonia Limestone) accumulated in quiet-water environments, possibly below wave-base (Nordlund & Southgate, 1988). Slump folds infer deposition on an inclined or unstable substrate possibly affected by penecontemporaneous faulting. The lack of trace and shelly fossils infers restricted conditions of sedimentation. At Rogers Ridge (Fig. 2 P′), silicified fragments of the trilobite *Redlichia* sp., hyolithids and brachiopods are found in the uppermost 2 m of the black recrystallised dolostone (Fig. 5). This sparse shelly fauna heralds the rapid shallowing event that resulted in the deposition of an 8 m thick peritidal sequence of laminoid fenestral dolostone, peloid ooid grainstone, stromatolite and evaporite as the terminal sediments of this stratigraphic sequence. In the Burke River Structural Belts the peritidal dolostone sequence has a sharp lower contact with the recrystallised dolostone unit, suggesting that a rapid fall in relative sea level caused the deeper water facies to be succeeded by peritidal and emergent environments without a gradual change in corresponding facies (Fig. 8). A similar facies succession occurs in the Ardmore Outlier (Fig. 2 O′), where recrystallised black dolostone is succeeded by chert that contains the trilobite *Redlichia chinensis*, stromatolites and pseudomorphs of halite crystals which grew in brine pools on subaerially exposed flats (Southgate, 1982). North of Rogers Ridge, the Thorntonia Limestone is replaced by an interval of chert rubble interpreted by de Keyser (1968) as a Middle Cambrian regolith derived by dissolution and silicification of a precursor limestone.

Transgressive and highstand systems tracts — southern transect. Along the southern transect, sediments onlap in a northwesterly direction (Fig. 6). The deepest water and most restricted conditions of sedimentation occur in the Toko Syncline (Fig. 1). Here organic-matter rich shale and weakly phosphatic micritic dolostone of the Lower Hay River Formation form a condensed sequence (Fig. 8). The organic-matter rich shale, with TOC content of up to 16% in the Inca Formation and 6% in the Hay River Formation, accumulated in an oxygen minimum zone beneath an anoxic watercolumn (Donnelly & others, 1988). The associated laminated and concretionary phosphatic mudstone, in which phosphatic hardgrounds and skeletal debris occur, was deposited in

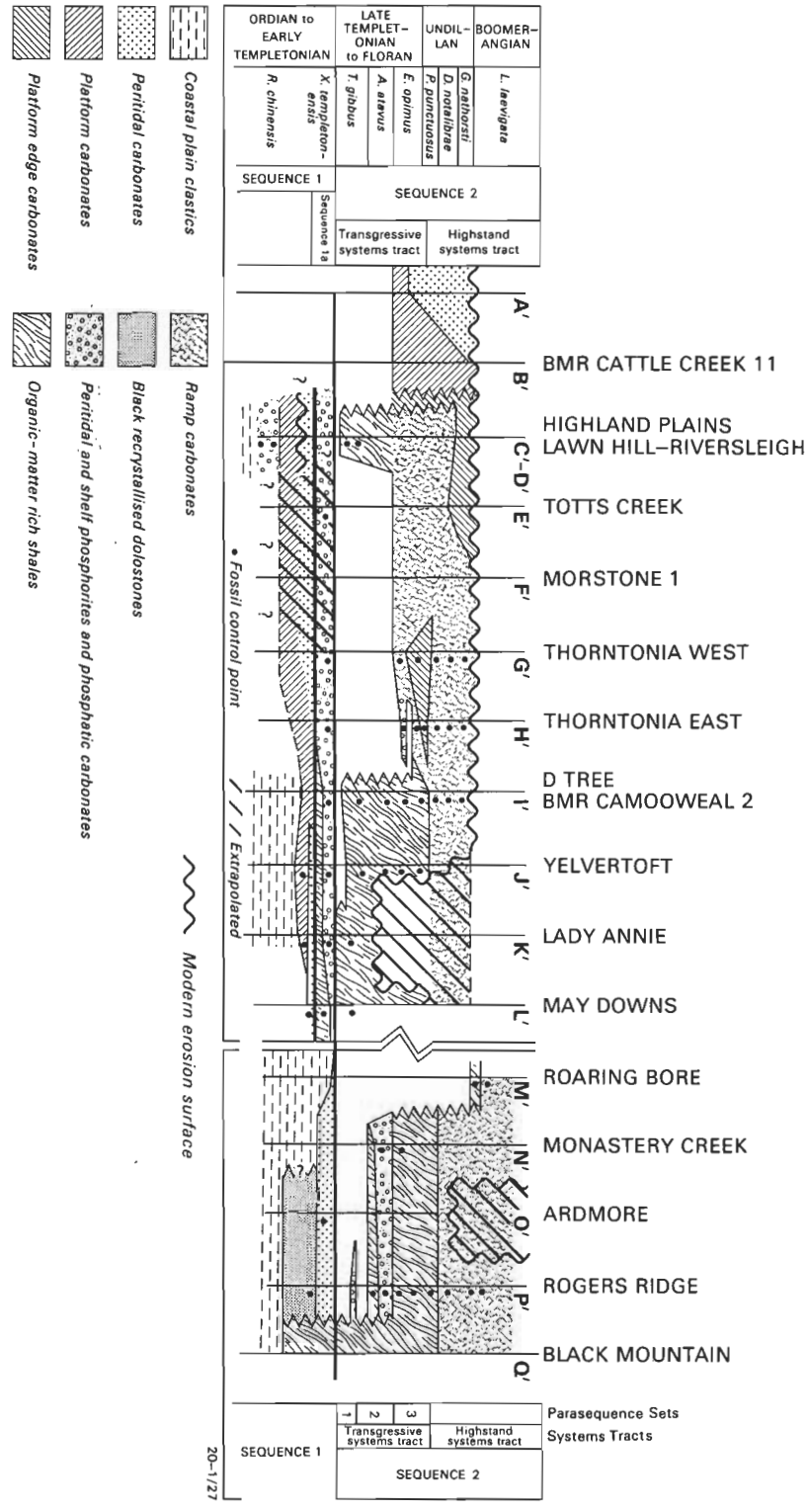

Figure 5. Sequence stratigraphic distribution of principal lithologies and interpreted depositional environments, northern transect. Cross-section plotted against time.

environments of fluctuating oxygen concentrations close to the upper boundary of the oxygen minimum zone (Donnelly & others, 1988). In BMR Hay River No. 11A (Fig. 2 I), dysaerobic phosphatic mudstone occurs in two retrogradational cycles at the base of the sequence, suggesting that transgression was rapid in this part of the basin and that euxinic conditions suitable for the deposition of organic-matter rich sediment were quickly established.

Because the sequence in Hay River No. 11A is incomplete, and a fault separates organic-matter rich shale in

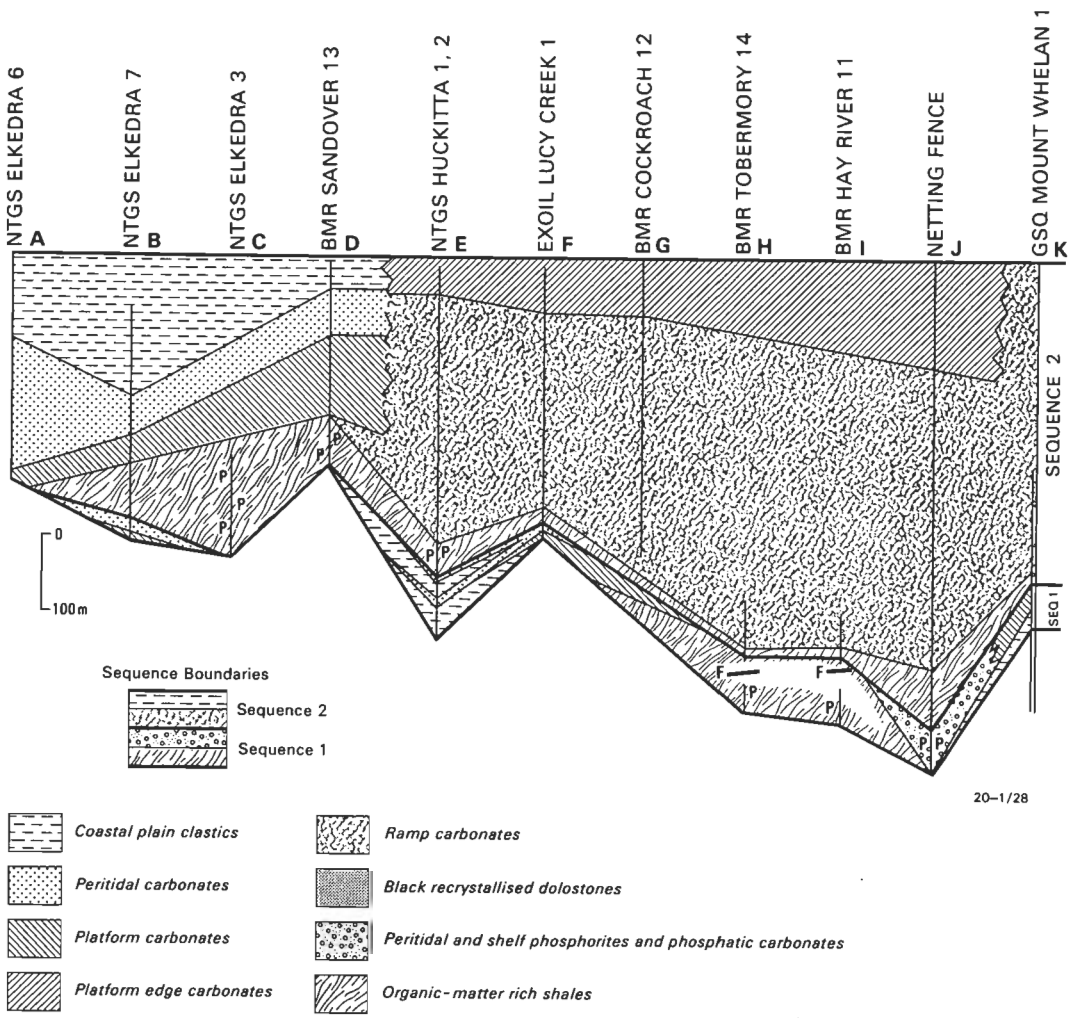

Figure 6. Sequence stratigraphic distribution of principal lithologies and interpreted depositional environments, southern transect. Cross-section plotted against sediment thickness.

this hole from similar rocks at the base of BMR Hay River No. 11, it is not possible to determine an accurate thickness for the organic-matter rich shale (Fig. 6). The presence of shale beneath 0.5 m of weathered, brown and grey laminated mudstone marking the top of this stratigraphic sequence indicates that a rapid fall in relative sea level terminated deposition (Fig. 8). Alternatively, any overlying peritidal facies indicative of shallowing may have been removed by erosion, but the absence of such sediments in outcrop makes this unlikely.

Rocks of stratigraphic sequence 1 age are poorly represented in the southwestern parts of the basin. Although their absence may be partly due to poor outcrop, it is likely that rocks of this age were only sporadically deposited in this part of the basin. Where palaeontological control exists (e.g. NTGS Elkedra No. 3; Figs 2 C, 6) organic-matter rich shale of sequence 2 age disconformably overlies archaeocyathan-bearing dolostone of Early Cambrian age. Elsewhere an interval of terrestrial clastic sediment and/or peritidal dolostone and limestone separates Lower Cambrian dolostone from sequence 2 organic-matter rich shale. As this intervening sequence has both upper and lower disconformable contacts it is assigned to sequence 1. Thus a shoreline for sequence 1 probably occurs in the vicinity of NTGS Huckitta No. 1 (Fig. 2 E), where a 60 m thick sequence of terrestrial clastics with thin interbeds of fenestral and stromatolitic dolostone occurs. Slightly deeper water conditions existed in the Dulcie Syncline in the vicinity of NTGS Elkedra No. 7 (Fig. 2 A), where peritidal fenestral dolostone and grainstone rather than terrestrial clastics sediments are found.

Summary

By associating facies patterns in sequence 1 with the principal structural elements in which they occur, the following conclusions can be drawn:

1. The most restricted and deepest water conditions of sedimentation in sequence 1 occur in the Toko Syncline, which suggests that this area underwent rapid subsidence in the early Middle Cambrian. Such a conclusion is consistent with the thin retrogradational cycles found at the base of the transgressive systems tract in this area, and the

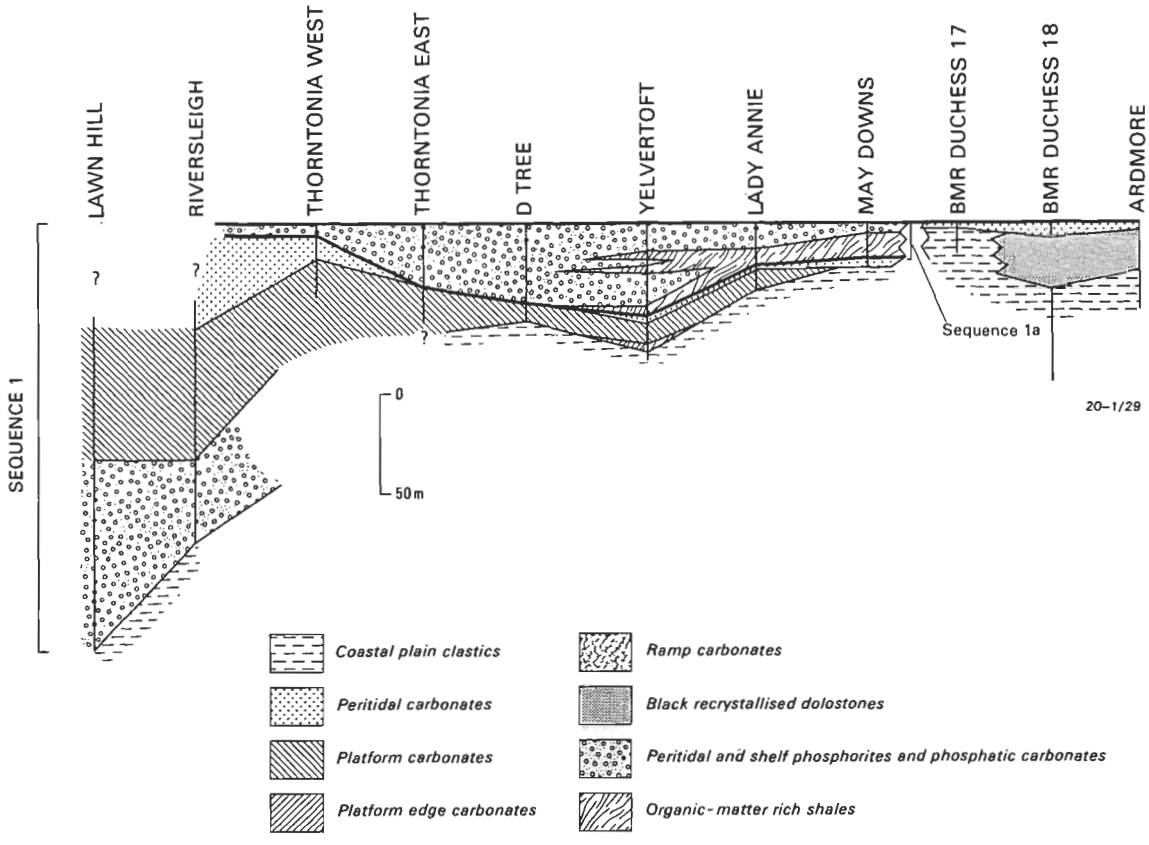

Figure 7. Sequence stratigraphic distribution of principal lithologies and interpreted depositional environments for the Lawn Hill–Thorntonia–May Downs region showing relationships between sequences 1 and 1a.
Note that sequence 1a forms a thin veneer of onlapping phosphatic sediment in the Thorntonia West region.

shallower water platform and peritidal facies found in GSQ Mount Whelan No. 1 (Fig. 2 K) and Exoil Lucy Creek No. 1 (Fig. 2 F) boreholes on the eastern and western flanks of this structure, respectively.

2. Rapid subsidence may also have taken place in the Burke River Structural Belt, permitting deposition of the recrystallised black dolostone, which also lacks a well developed transgressive systems tract at its base.
3. This scenario contrasts with that in Domain 1. In the northeast of the basin subsidence was much slower, permitting the development of a keep-up transgressive systems tract and the formation of several minor phosphate deposits.
4. In the southwest of the basin, sequence 1 sediments are best developed in the Dulcie Syncline. Elsewhere, this interval is represented by either an erosion surface, or terrestrial redbed sedimentation with minor marine incursions leading to the deposition of peritidal dolostone.
5. A rapid fall in relative sea level terminated sedimentation in sequence 1.

Tectonically enhanced stratigraphic sequence 1a

Sediments in sequence 1a form a parasequence set interpreted as accumulating in response to early subsidence of the Mt Isa block during the late Ordian/early Templetonian. Organic-matter rich shale and phosphorite of sequence 1a attains a maximum thickness of approximately 50 m, and onlaps platform and peritidal facies attributed to the previously described highstand (Figs 5, 7, 9b). Onlap is interpreted to have taken place in a northwesterly direction, thus reversing the shallowing trend previously described from sequence 1. The D Tree, Lady Annie and Yelvertoft phosphate deposits (Fig. 2 I', K', J') belong in this stratigraphic sequence.

Northern transect — May Downs to Thorntonia West. Phosphatic limestone and phosphorite deposition in sequence 1a coincided with a return to some of the facies patterns and faunal elements previously attributed to the transgressive systems tract of sequence 1. The deepest water and most restricted conditions occurred in the May Downs area, where organic-matter rich shale and siltstone, containing whole and fragmented trilobites referred to *Xystridura* spp. (Appendix 2) accumulated in dysaerobic to anaerobic environments. To the north, at Yelvertoft, Lady Annie and D Tree, organic-matter rich shale interfingers with phosphatic, siliceous and calcareous rocks and phosphorites deposited in shallow water aerobic environments (Howard & Cooney, 1976; Cook & Elgueta, 1986). At Yelvertoft (Fig. 7), the phosphatic rocks occur in three shallowing upward

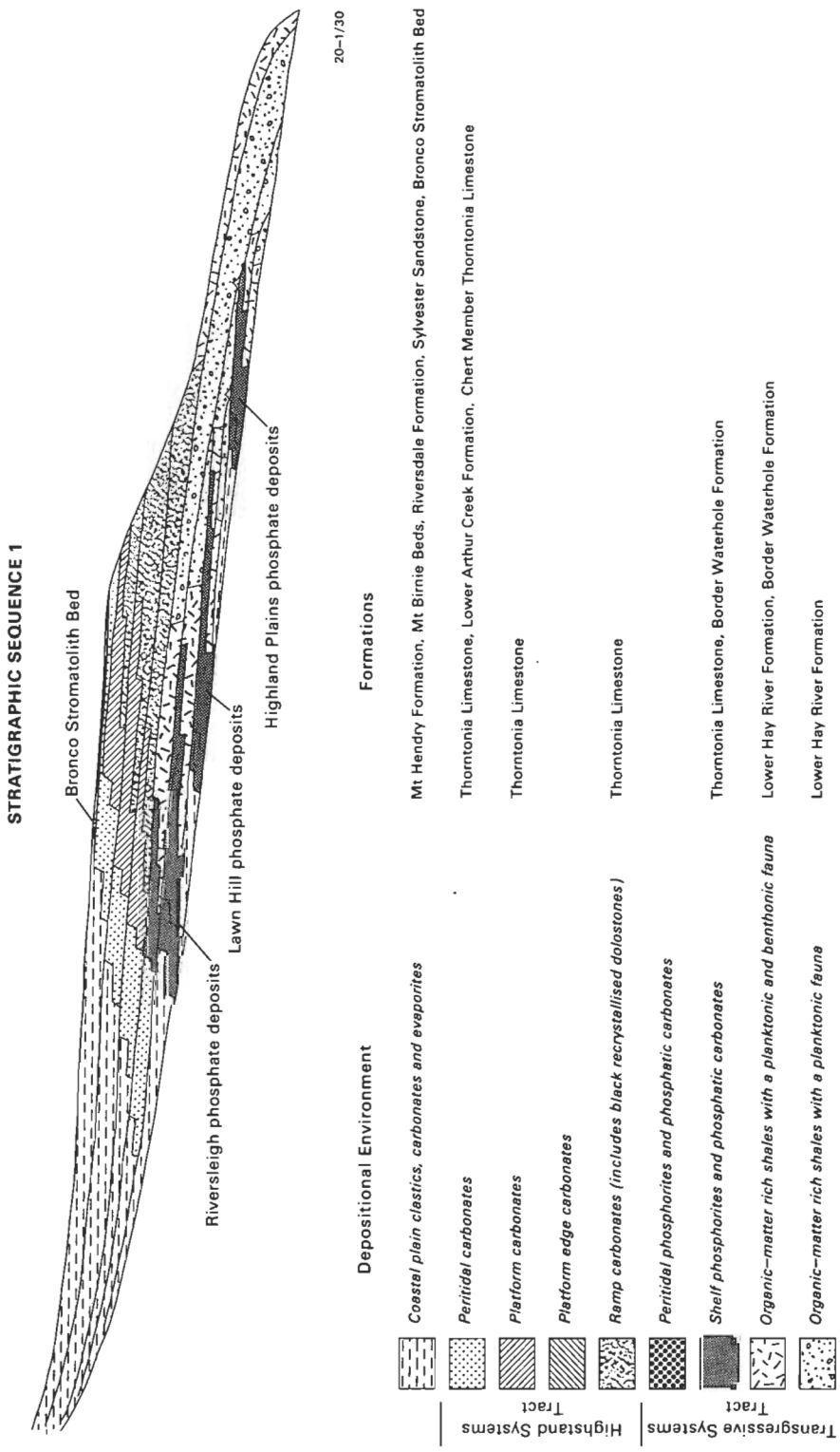

Figure 8. Sequence stratigraphic cross-section showing the relative positions of formations and their constituent facies in stratigraphic sequence 1 (after Van Wagoner & others, 1988).

cycles. Organic-matter rich shale and phosphatic mudstone dominate the lower parts of each cycle. Cycles culminate in the deposition of phosphatic grainstone, coquinite and phosphorite. Howard & Cooney (1976) recognised three organic-matter rich shale–phosphorite sequences in the D Tree deposit, and Cook & Elgueta (1986) described similar sediments in the Lady Annie deposit. In the uppermost parts of the D Tree deposit phoscrete crusts, laminoid fenestral phosphorite and desiccated mudstone phosphorite collectively indicate emergent conditions representing the cessation of sedimentation in this sequence. Between Thorntonia Station

and Thorntonia West (Fig. 2 G), phosphatic coquinite forms a thin veneer of sediment onlapping emergent laminoid fenestral dolostone of the previously described highstand. Phoscrete crusts, vertically stacked coquinite and stromatolites indicating deposition in an algal marsh (Southgate, 1988) demonstrate emergent conditions associated with the boundary that terminates this sequence.

Summary

The changes in sediment mineralogy and facies patterns between non-phosphatic sediments of the highstand systems tract in sequence 1 and the overlying phosphatic sediments of sequence 1a are interpreted as related to subsidence of the Mt Isa block and the creation of a new seaway, through which nutrient-rich oceanic waters entered the May Downs–Yelvertoft–D Tree–Lady Annie areas (Figs 9, 12). Before this switch in facies patterns the sea shallowed in a southeasterly direction toward May Downs. At May Downs, the change from shoreline aerobic conditions to deeper water dysaerobic environments suitable for the accumulation of organic-matter rich shale indicates rapid subsidence and an accompanying change in current circulation patterns. At Yelvertoft, D Tree and Lady Annie, peloidal phosphorite and the associated phosphatic sediment accumulated in shallow, nutrient-rich, oxygenated waters. The change from non-phosphatic calcareous peritidal facies in the older *Redlichia*-bearing sequence to the phosphatic and skeletal-rich facies of the younger sequence provides evidence for a dramatic increase in the nutrient content of the flooding waters.

Stratigraphic sequence 2

Sediments of stratigraphic sequence 2 accumulated in terrestrial, shoreline, peritidal, platform, platform edge, ramp and basinal environments. The relative rise in sea level responsible for sequence 2 inundated the continent and resulted in the deepest water conditions attained in the Georgina Basin (Figs 6, 7, 12). The transgressive systems tract is considered in terms of the three parasequence sets thus far recognised. Each parasequence set comprises a repeating mosaic of lithofacies related to onlap during one or more of the three stepped rises in relative sea level. Rocks of parasequence set 1 contain agnostoid trilobites of late Templetonian age close to the overlap of the *Pentagnostus praecurrens* and *Triplagnostus gibbus* Zones (Appendix 3). Parasequence set 2 contains agnostoid and polymeroid trilobites which give an age at the overlap of the *Triplagnostus gibbus* and *Acidusus atavus* Zones within the late Templetonian/early Floran passage. Agnostoid trilobites in parasequence set 3 are of Floran age.

Transgressive systems tract

Northern Transect — Highland Plains to May Downs. Subsidence of the Mt Isa block controlled sedimentation in this area. In consequence, facies variations occur on the eastern and western sides of the prominent geophysical feature forming the western boundary of Domain 3. Organic-matter rich shale belonging to parasequence sets 1, 2 and 3 occurs in Domain 3 on the eastern side of this structure (Fig. 5). To the west, in Domain 1, rocks belonging to parasequence sets 1 and 2 are replaced by the Bronco Stromatolith Bed (Figs 5, 9, 10).

At Lady Annie and May Downs, laminated organic-matter rich shale of the Inca Formation overlies phosphorite, phosphatic carbonate rock and shale of sequence 1a age. Shale in the Beetle Creek Formation (sequence 1a) contains elements of a benthonic and planktonic trilobite fauna which indicate dysaerobic conditions. The overlying organic-matter rich shale of the Inca Formation only contains planktonic agnostoid trilobites, suggesting anaerobic bottom conditions. In the May Downs area, a limonitic horizon separates sequence 1a sediments from organic-matter rich shale of sequence 2. At Lady Annie, a chert-mudstone facies separates sequence 1a phosphorite from sequence 2 organic-matter rich shale (Cook & Elgueta, 1986). The mudstone facies has a blanket-like geometry that lacks both interfingering and gradational relationships with the underlying phosphorite, yet contains lithological and faunal elements which suggest it is associated with them.

The limonitic horizon at May Downs is interpreted as the transgressive sediment bypass surface at the base of sequence 2. The chert–mudstone facies at Lady Annie is interpreted as a transgressive interval at the base of the Inca Formation. At Lady Annie and May Downs, the lack of a subaerial exposure surface at the sequence boundary separating sequence 1a from sequence 2 (coupled with the trend from shallow water phosphatic sediments and phosphorites of sequence 1a to restricted deeper water organic-matter rich shale of sequence 2) suggests that in these areas a relative rise in sea level terminated the shallowing trends present in the upper parts of sequence 1a. Although outcrop on the eastern side of West Thornton Creek (Fig. 2 G′) is generally poor, the sequence in this area is similar to that at Lady Annie, and once again a subaerial exposure surface on top of sequence 1a is missing. Thus sedimentation across the boundary between stratigraphic sequences 1a and 2 was continuous in this part of Domain 3, and the sequence boundary is represented by a correlative conformable surface. However, on the western side of West Thornton Creek a different sedimentary record is found.

Between Yelvertoft and Thorntonia West, sediments belonging to parasequence sets 1 and 2 are represented by the Bronco Stromatolith Bed, a 1–30 cm thick stratigraphic interval representing minor deposition and erosion on a subaerial exposure surface (Southgate, 1986c, fig. 10). In this part of the basin, transgression commenced in parasequence set 3 time and resulted in onlap of a palaeogeographic high (Figs 5, 12). Near Thorntonia Station, phosphatic limestone and dolostone

Figure 9. Schematic development of stratigraphic sequences 1 and 2 in the northeastern parts of the basin between Lawn Hill and May Downs.

a. Stratigraphic sequence 1. Gradual inundation of the palaeocontinent. Phosphate deposits occur where retrogradational cycles of the transgressive systems tract impinge upon the irregular basement palaeotopography.

b. Stratigraphic sequence 1a. Subsidence of the Mt Isa Block (shown schematically as several half grabens) results in the deposition of organic-matter rich shales and their associated phosphorites.

c. Stratigraphic sequence 2. Continued subsidence during a period of fall in relative sea level results in the deposition of organic-matter rich shale and the development of a subaerial disconformity surface.

d. A gradual rise in relative sea level completely floods the Mt Isa block. This structural area (Domain 3) forms a carbonate ramp to a stable platform area to the west (Domain 1). Cross-bedded grainstone of the Age Creek Formation was deposited at the edge of the ramp.

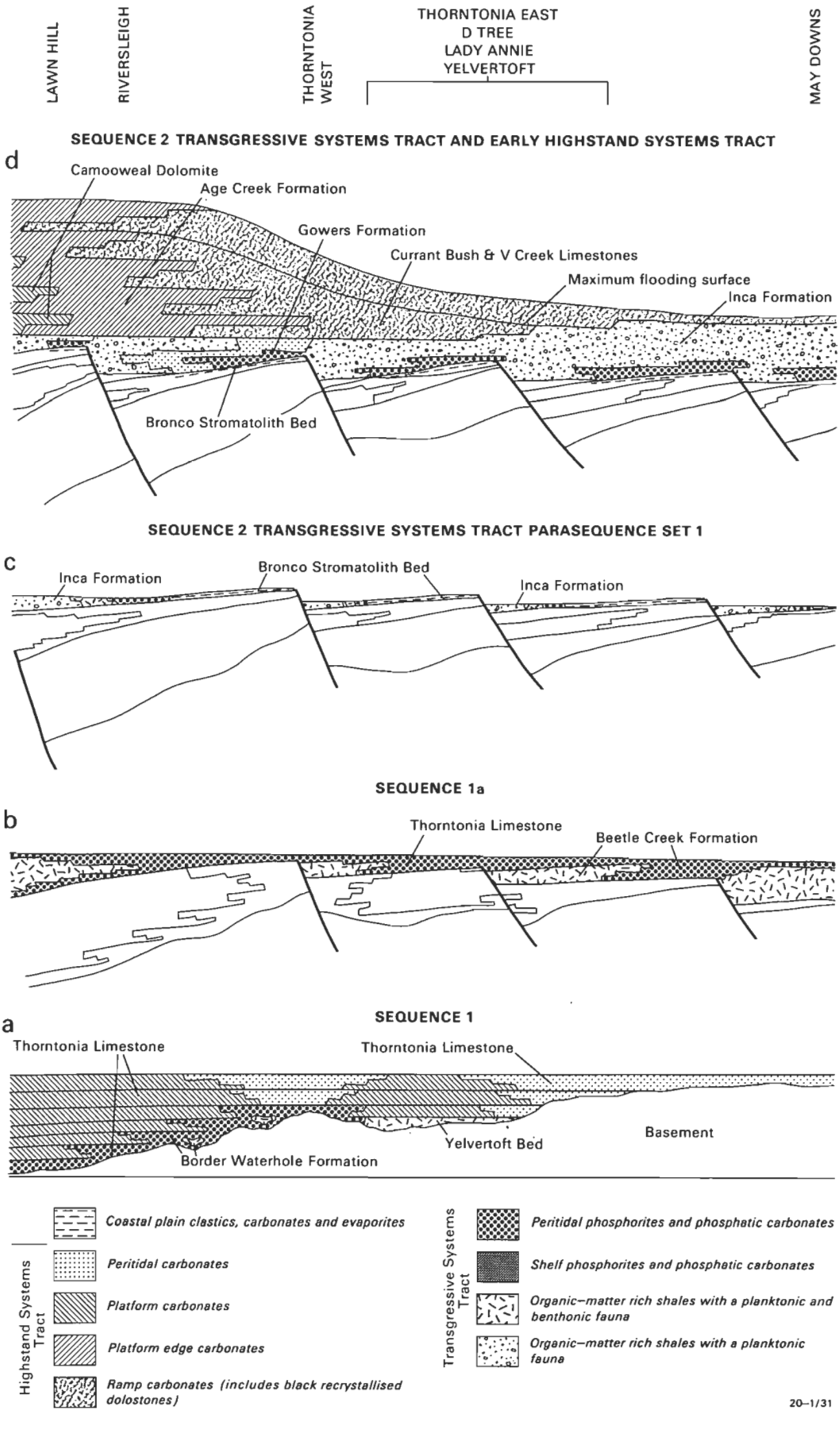
LAWN HILL
RIVERSLEIGH
THORNTONIA WEST
THORNTONIA EAST
D TREE
LADY ANNIE
YELVERTOFT
MAY DOWNS
SEQUENCE 2 TRANSGRESSIVE SYSTEMS TRACT AND EARLY HIGHSTAND SYSTEMS TRACT
d
Camooweal Dolomite
Age Creek Formation
Gowers Formation
Currant Bush & V Creek Limestones
Maximum flooding surface
Inca Formation
Bronco Stromatolith Bed
SEQUENCE 2 TRANSGRESSIVE SYSTEMS TRACT PARASEQUENCE SET 1
c
Inca Formation
Bronco Stromatolith Bed
Inca Formation
SEQUENCE 1a
b
Thorntonia Limestone
Beetle Creek Formation
SEQUENCE 1
a
Thorntonia Limestone
Thorntonia Limestone
Yelvertoft Bed
Basement
Border Waterhole Formation
Highstand Systems Tract
Coastal plain clastics, carbonates and evaporites
Peritidal carbonates
Platform carbonates
Platform edge carbonates
Ramp carbonates (includes black recrystallised dolostones)
Transgressive Systems Tract
Peritidal phosphorites and phosphatic carbonates
Shelf phosphorites and phosphatic carbonates
Organic–matter rich shales with a planktonic and benthonic fauna
Organic–matter rich shales with a planktonic fauna
20–1/31

of the Gowers Formation forms a 0.1–15 m thick parasequence set that onlaps the Bronco Stromatolith Bed (Southgate, 1986c, fig. 9). A subaerial exposure surface caps the Gowers Formation and separates this phosphatic parasequence set from the overlying Currant Bush Limestone. Continued transgression drowned the northeastern parts of the basin and led to the deposition of (1) organic-matter rich shale–chert retrogradational cycles with caps of concretionary, glauconitic and phosphatic limestone, and (2) interbedded ribboned limestone and organic-matter rich shale. Slump folds in the organic-matter rich shale, and intervals of intraclast breccia up to 4 m thick, that are traceable over distances of 5–6 km, provide evidence for sediment deposition on an inclined seafloor and/or possible synsedimentary faulting during deposition of parasequence sets 2 and 3.

Northern transect — Roaring Bore to Black Mountain. The three parasequence sets recognised in the Burke River Structural Belt onlap in a northerly direction (Fig. 5). In consequence, all three parasequence sets are found in the southern parts of the transect (Black Mountain, Fig. 2 Q′, and Rogers Ridge, Fig. 2 P′) but only two parasequence sets occur at Monastery Creek (Fig. 2 N′) and Ardmore (Fig. 2 O′), and one at Roaring Bore (Fig. 2 M′).

Onlap during parasequence set 1 time deposited shoreline facies in the Rogers Ridge area (Figs 5, 10). Here, a 12 m thick interval of cyclic phosphatic limestone of peritidal origin rests disconformably on the Thorntonia Limestone (Nordlund & Southgate, 1988). These rocks are correlated with the Siltstone Member of the Monastery Creek Formation[2] which outcrops in the southern parts of the Duchess phosphate deposit and in turn correlates with the organic-matter rich shale intersected in Black Mountain 1. Thus the thin phosphatic interval at Rogers Ridge represents a shoreline facies for a sea that deepened to the south (Fig. 12).

Rocks of the Monastery Creek Formation and its accompanying Siltstone Member, which comprise the phosphate deposits in the Duchess and Ardmore areas, belong to parasequence set 2. North of Rogers Ridge and at Ardmore, rocks of parasequence set 2 overlie the sequence boundary (subaerial exposure surface) that caps sequence 1; to the south these rocks overlie phosphatic limestone and organic-matter rich shale belonging to parasequence set 1 (Figs 5, 11). At Rogers Ridge, phosphatic and glauconitic hardgrounds attest to sediment starvation on the transgressive surface of parasequence set 2 (Fig. 10). After the transgression, four facies belts were established. Intraclastic, bioclastic and siliceous phosphorite accumulated on structural highs and their attendant slopes; phosphorite of the micritic calcareous facies accumulated in sub-basins or structural lows (Russell & Trueman, 1971). In deeper water settings, or in areas of restricted circulation, organic-matter rich shale of the Siltstone Member was deposited in predominantly dysaerobic environments. Organic-matter rich shale devoid of a benthonic fauna, but containing elements of a planktonic fauna, accumulated in deeper and more restricted anaerobic environments.

Parasequence set 2 has both conformable and disconformable relationships with onlapping organic-matter rich shale of parasequence set 3 (Rogers & Crase, 1980; Soudry & Southgate, 1989). Soudry & Southgate (1989) interpreted mudstone phosphorites and their associated vadose miniprofiles in the uppermost unit of the Monastery Creek Formation as forming on subaerially exposed coastal flats during vadose diagenesis. In the phosphate pits, at the Duchess deposit, the contact with the Inca Formation is gradational. Packstone and wackestone phosphorite initially interbed with, but are rapidly succeeded by, finely laminated non-phosphatic shale. In the Rogers Ridge area, five retrogradational transgressive cycles form a gradational sequence, some 8 m thick, at the base of parasequence set 3 (Fig. 10). In each cycle, thin beds of black chert and siliceous mudstone with graded phosphatic laminae overlie the basal erosion surface and pass upwards into phosphatic and glauconitic, grain-supported limestone concretions. Thin crusts of mudstone phosphorite coat the eroded upper surfaces of some concretions (Fig. 10). In the uppermost retrogradational cycle (50 cm thick) organic-matter rich shale of the Inca Formation overlies the concretions.

The concretions are interpreted as sediment-starvation surfaces (marine flooding surfaces of Van Wagoner & others, 1988). They formed on the seafloor during times of sediment starvation and cementation, and underwent penecontemporaneous erosion and phosphate encrustation. Following each transgressive pulse, anoxic conditions prevailed on the seafloor and fine-grained siliceous sediments were deposited. Subsequent shallowing and minor progradation of the nearby shelf sediments resulted in the accumulation of granular phosphatic sediments in the upper parts of each retrogradational cycle.

Southern transect. In the southern parts of the basin, poor outcrop makes the regional correlation of rock units difficult. However, parasequence sets 2 and 3 are recognised in parts of the Dulcie Syncline, and parasequence set 3 occurs in the Toko Syncline (Figs 6, 12). Near the Dulcie Syncline, at the westernmost end of the transect, rocks of parasequence sets 2 and 3 onlap in a northwesterly direction. The oldest sediments are found in Elkedra No. 3 (Fig. 2 C) and Huckitta No. 1 (Fig. 2 E), where sedimentation started with the accumulation of lithoclastic and intraclastic grainstone in two retrogradational transgressive cycles (Fig. 10). In Huckitta No. 1 the grainstone is glauconitic and phosphatic. Following the initial transgression, organic-matter rich shale and interbedded phosphatic mudstone of parasequence sets 2 and 3 (anaerobic facies of Stidolph & others, 1988) accumulated in anaerobic and dysaerobic basinal environments. Phosphatic hardgrounds in the organic-matter rich shale and mudstone probably formed during times of sediment starvation when the sea floor was locally cemented by phosphate. Similar sediments are found to the northwest in Elkedra No. 7a (Fig. 2 A), but poor faunal resolution in this area and the lack of retrogradational cycles suggest that this interval of organic-matter rich shale belongs to parasequence set 3. Further to the north, in Elkedra No. 6 (Fig. 2 B), organic-matter rich shale is absent (Fig. 6). Here, carbonate rocks interpreted as deposited in shallow water platform environments overlie Proterozoic basement. These rocks pass rapidly upwards into carbonate rocks and sulphate evaporites of peritidal and sabkha facies, here interpreted as deposited in the overlying highstand systems tract. This suggests that inundation of Proterozoic basement in the northern parts of the Dulcie Syncline coincided with the maximum flooding surface (Fig. 11).

[2] Formerly referred to in the literature as the Beetle Creek Formation (e.g. Russell, 1967; Russell & Trueman, 1971).

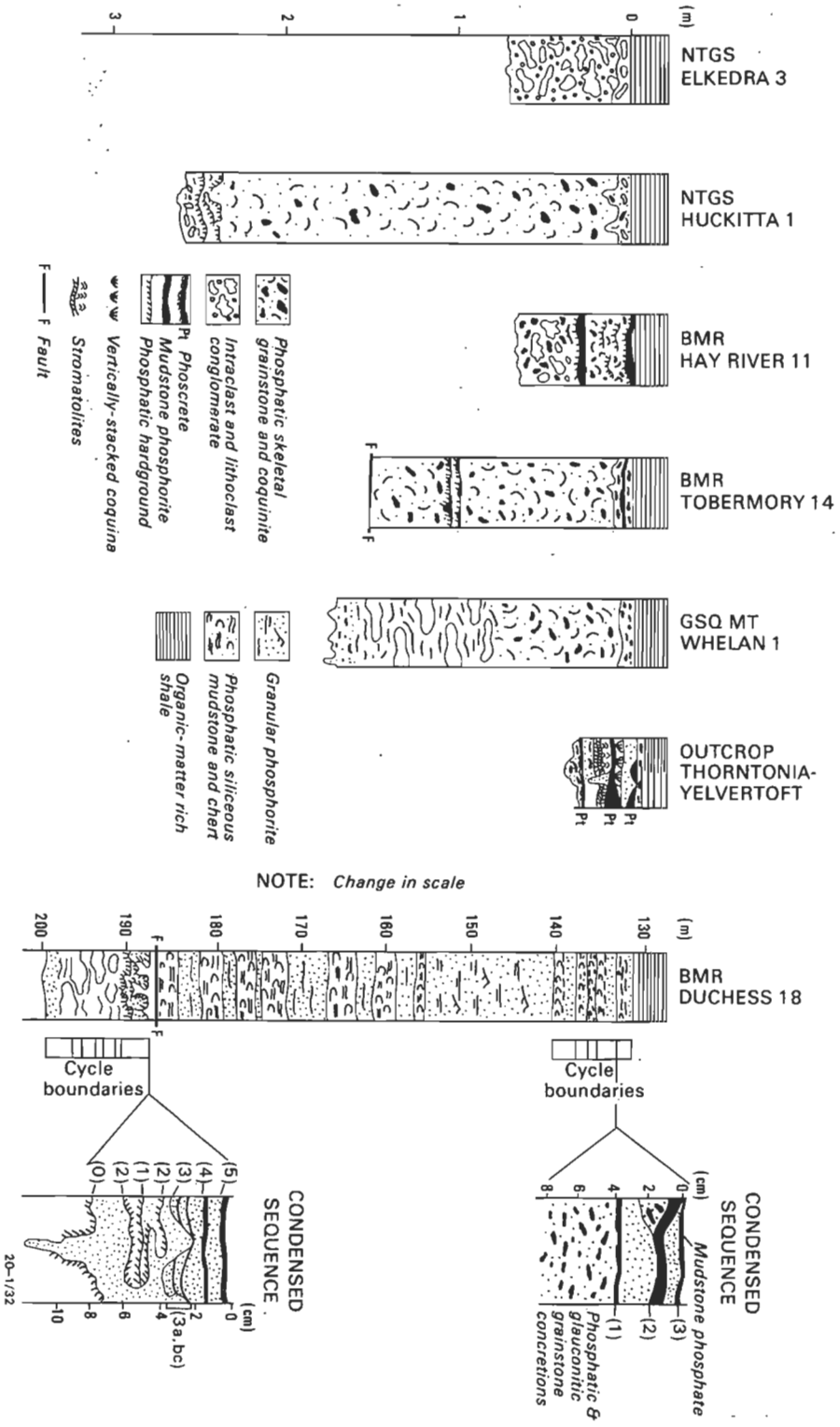

Figure 10. Distribution of phosphatic coquinite, skeletal grainstone and intraclastic conglomerate in drill core and outcrop for the first couple of retrogradational parasequences at the bottom of sequence 2.

The column shown for Duchess No. 18 depicts the three parasequence sets recognised in this hole. The interval from 187.73 m to 199.52 m shows a typical parasequence in parasequence set 1; the boundaries of individual cycles are shown on the right hand side. Parasequence set 2 (140.72–187.73 m) commences with the development of a condensed interval with a complex array of sediment bypass surfaces (right hand side). In the drill core, most of the organic-matter rich shale (dysaerobic depositional environments) that normally occurs beneath a deposit is missing due to faulting; it outcrops elsewhere on Rogers Ridge. Parasequence set 3 (140.72 m and upwards) consists of 5 retrogradational transgressive cycles between 140.72 m and 132.50 m. Above this, organic-matter rich shale of the Inca Formation passes gradationally upwards into Devoncourt Limestone.

East of the Dulcie Syncline, organic-matter rich shale in BMR Sandover No. 13 (Fig. 2 D) and Exoil Lucy Creek No. 1 (Fig. 2 F) is correlated with the previously described sediments (Fig. 6). Further east, in the Toko Syncline, sediment deposition in sequence 2 began in parasequence set 3 time, with the accumulation of reworked lag deposits and coquinite in thin retrogradational transgressive cycles (Fig. 10). This phase of rapid transgression deposited organic-matter rich shale of the Inca Formation and Blazan Shale, which correlates with similar facies to the west.

Summary

Three faunal assemblages occur in the regionally extensive blanket of organic-matter rich shale that characterises the transgressive systems tract of sequence 2 (Figs 4, 6, 11). As each assemblage coincides with a period of rapid onlap, followed by aggradation and progradation, the faunal assemblages are used to define the three parasequence sets. Similar facies patterns characterise each parasequence set. Reworked lag deposits, often phosphatic and coquinitic, and phosphate-encrusted sediment starvation surfaces occur at the base of each parasequence set (Fig. 10). In deeper water settings, these sediments are rapidly succeeded by anaerobic or dysaerobic organic-matter rich shale and siltstone (Fig. 11). Phosphatic limestone and phosphorite was initially deposited in laterally equivalent, shallower water environments. Later, as shallowing took place, these sediments prograded over the organic-matter rich shale facies. The initial flooding surface occurs in the basal lag. Subsidiary flooding surfaces occur in the organic-matter rich shale facies, the associated, spicular and concretionary limestone facies or the laterally equivalent phosphorite facies. The phosphatic rocks accumulated as aggradational and progradational parasequences in the upper parts of the parasequence set. Phosphate sedimentation ceased when the next rise in relative sea level resulted in the deposition of organic-matter rich shale.

Highstand systems tract

Although phosphate deposition is restricted to the transgressive systems tract, rocks of the highstand systems tract in sequence 2 are included in this study, to place the phosphatic interval in its stratigraphic context and to illustrate the dramatic changes that take place in Cambrian palaeogeography at this time (Figs 5, 6, 11, 12). Rocks of the highstand systems tract were deposited over the entire basin. The maximum flooding surface, which defines its lower boundary, is interpreted to occur within the organic-matter rich shale facies. The upper boundary coincides with the base of the Arrinthrunga Formation and its correlative formations (Fig. 4). Along the northern and southern transects, shallow water platform facies are found in the north and west in Domain 1; deeper water ramp and basinal facies occur in the south and east in Domains 2 and 3.

Northern Transect — Frewena to May Downs. Sediments of the highstand systems tract were deposited on a shallow water platform and a drowned ramp (Figs 5, 11, 12). De Keyser & Cook (1973) interpreted the Camooweal Dolomite as a large carbonate platform or shoal dominated by shallow water and supratidal hypersaline environments. The Age Creek Formation, a thick to thinly bedded grainstone unit present in foresets that dip to the southeast at 5–30° (Randal & Brown, 1962), is interpreted as defining the eastern margin of this platform. To the east, rocks of the Age Creek Formation interfinger with, and eventually pass into, nodular, ribbon and parted limestone and dolomitic limestone of the Currant Bush, V Creek and Mail Change Limestones (terminology after James & Stevens, 1986). These cherty mud-supported rocks contain articulated trilobites (which indicate an open marine fauna) and thin beds of skeletal debris. Burrows are common, and some lithified beds are punctured by *Trypanites* sp. borings to form hardgrounds. Thin beds of flat pebble conglomerate and intraclast breccia are interbedded with the mud-supported rocks, which lack features indicating subaerial exposure. Collectively, these features suggest deposition in comparatively deep water in a ramp setting.

Stratigraphic drilling in the Totts Creek area (Fig. 2 E'), close to the boundary of Domains 1 and 2 on the northern transect, intersected carbonate rocks which show a transition from ribbon and parted limestone at the base (Currant Bush, V Creek and Mail Change Limestones), through cross-bedded grainstone (Age Creek Formation) into recrystallised dolostone (Camooweal Dolomite). Such a transition is interpreted as a catch-up carbonate system (Sarg, 1988). Initial sediment aggradation took place in comparatively deep water below fair weather wave base (cf. Read, 1985) on a drowned ramp inclined in a southeasterly direction (Figs 11, 12). Water depths increased towards the present Mt Isa Block. Cross-bedded grainstones of the Age Creek Formation defined the edge of the platform and separated mud-supported carbonate rocks deposited in a ramp setting in Domain 3, from platform dolostone of the Camooweal Dolomite in Domain 1. Post-Cambrian erosion has removed the upper parts of this systems tract.

Northern Transect — Roaring Bore to Black Mountain. With the exception of the Burke River Structural Belt and its northern extension, the Landsborough Trough, post-Cambrian uplift of the Mt Isa Block and subsequent erosion has removed sediments of the highstand systems tract deposited north of present latitude 22°S. In the Burke River Structural Belt, laminated and concretionary limestone of the highstand systems tract (Devoncourt Limestone) was deposited in deep water outer-ramp environments. In parts of the Burke River Structural Belt there is evidence for synsedimentary tectonism at this time. At Rogers Ridge, organic-matter rich shale and phosphorite of the transgressive systems tract has an early to late Floran age. These same sediments have conformable and gradational contacts with rhythmically laminated and concretionary limestone of the highstand systems tract (Devoncourt Limestone). However, some 50 km north, at Roaring Bore (Fig. 2 M'), a hiatus spanning the Templetonian, Floran and Undillan stages of the Middle Cambrian separates dolostones of sequence 1 from organic-matter rich shale of the transgressive systems tract of sequence 2. Such a marked hiatus in an area of deep water sedimentation suggests that tectonic subsidence partly controlled relative sea level in this part of the basin.

Southern Transect. In the northwestern parts of this transect, organic-matter rich shale of the transgressive systems tract passes both vertically and laterally into carbonate rocks deposited in shelf and peritidal environments (Fig. 6). Thinning of this sequence in a westerly direction suggests progressive onlap over a basement high (Fig. 12). Sediment progradation, initially as a

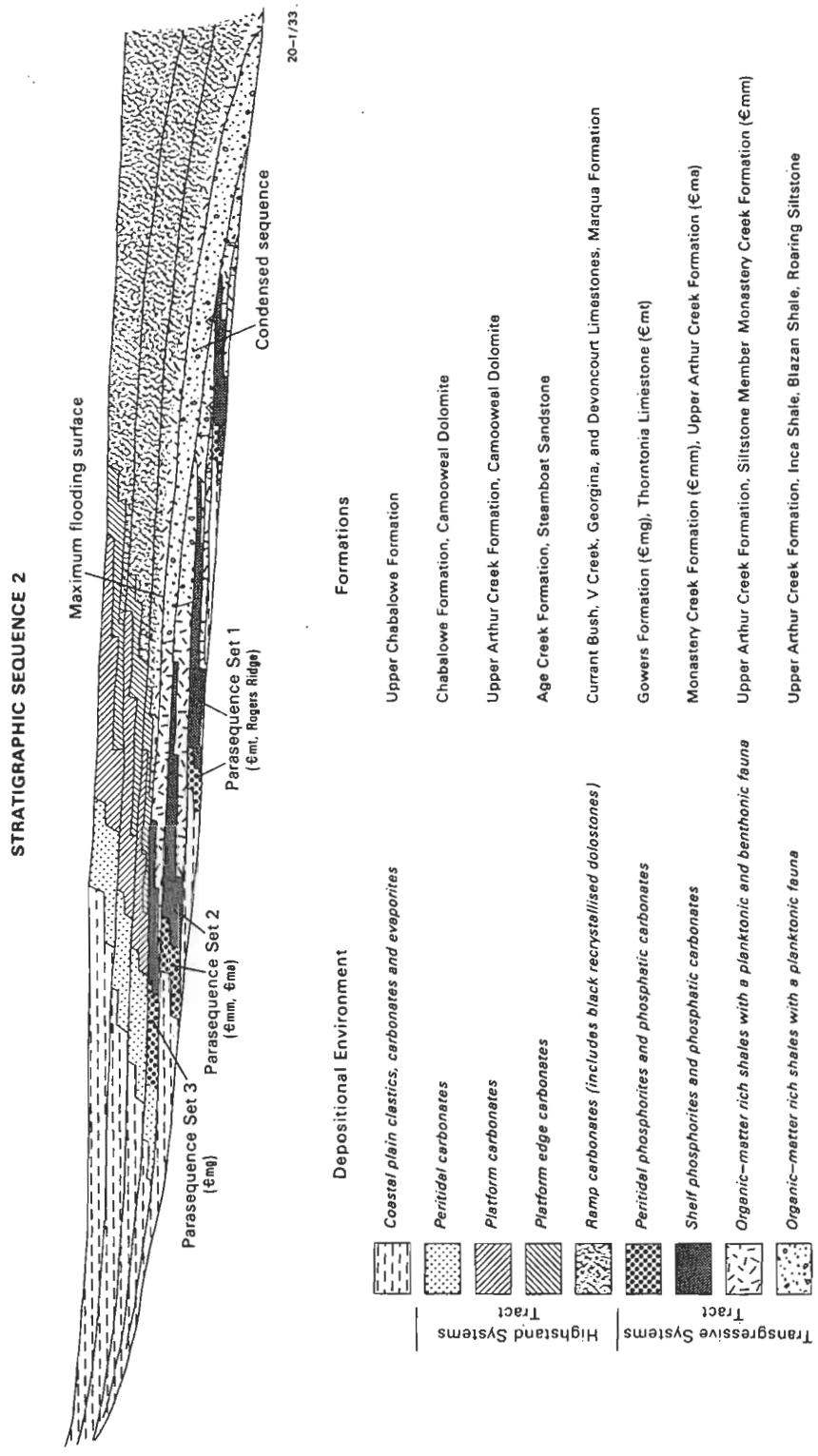

Figure 11. Modified sequence stratigraphic cross-section, showing the relative positions of formations and their constituent facies in stratigraphic sequence 2.
After Van Wagoner & others, 1988.

probable barrier-bar and lagoon system associated with the basement high, and later from other shoaling areas, eventually produced supratidal conditions and the accumulation of sulphate evaporite minerals in sabkha settings (Hagen Member of the Chabalowe Formation, Stidolph & others, 1988). As progradation continued, cross-laminated sandstone and desiccated, thinly bedded siltstone and mudstone accumulated in marginal marine playas and ephemeral streams of the coastal plain facies belt, landward of the previously described sabkhas. Periodic marine incursions promoted a return to lagoonal and sabkha environments. In Elkedra No.

7 (Fig. 2 A), these stromatolitic interbeds become progressively less frequent in the upper parts of the Chabalowe Formation.

Between Exoil Lucy Creek No. 1 (Fig. 2 F) and GSQ Mt Whelan No. 1 (Figs 2 K, 6) organic-matter rich shale of the transgressive systems tract grades into nodular, ribbon, parted and rhythmically laminated carbonate rocks of the highstand systems tract (Upper Hay River Formation, Georgina Limestone and Marqua Beds), and cross-stratified quartzitic carbonate rocks and sandstone of the Marqua Beds and Steamboat Sandstone. In this part of the basin, rocks of the highstand systems tract

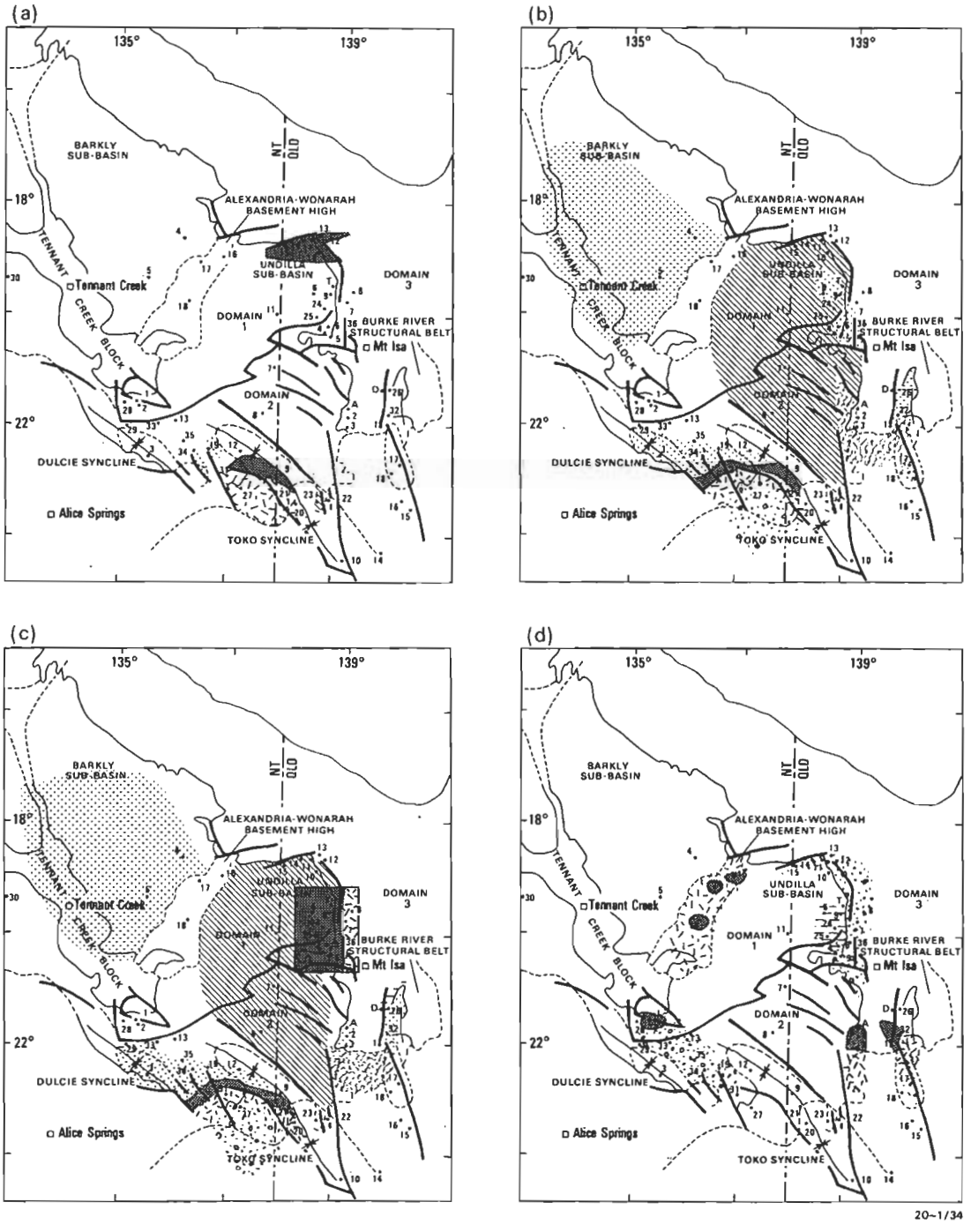

Figure 12. Palaeogeographic maps for stratigraphic sequences 1 and 2 structural elements and domains have been used to constrain boundaries on the maps.

Sequence 1a is shown as an inset in 12c, to emphasise the local tectonically induced aspect of this sequence and place it in its regional context.

a. Sequence 1, early transgressive systems tract. Initial onlap took place from the north in the Highland Plains to Riversleigh region to form the phosphate deposits. Transgression also occurred in the Toko Syncline region.

b. Sequence 1, highstand systems tract. Continued gradual onlap produced a mosaic of lithofacies in the early Middle Cambrian. Organic-matter rich shale accumulated in possible structural compartments in the southern parts of the basin.

c. Sequence 2. Rapid subsidence of the Mt Isa Block led to local tectonically enhanced onlap and the deposition of phosphatic sediments and their associated source rocks.

d. Sequence 2, parasequence set 2. Following a regional lowering in relative sea level, organic-matter rich source rocks and associated phosphorites were deposited in a number of structurally defined compartments.

thicken in a southerly direction. In PAP Netting Fence No. 1 (Fig. 2 J), they attain a maximum thickness of 600 m (Fig. 6). A BMR seismic survey of the Toko Syncline identified a 400 m thick southeasterly prograding sequence referred to the Marqua Beds and Steamboat Sandstone (Harrison, 1979). The gradual passage from fine-grained micritic and silty carbonate sediments deposited on a drowned platform or ramp, to shallower water and coarser grained sandy limestone and sandstone of the prograding sequence infers initial sediment aggradation in relatively deep water, followed by rapid progradation in shallower water (Figs 11, 12). Harrison (1979) interpreted the prograding sequence as indicating high sediment supply, slow basin subsidence

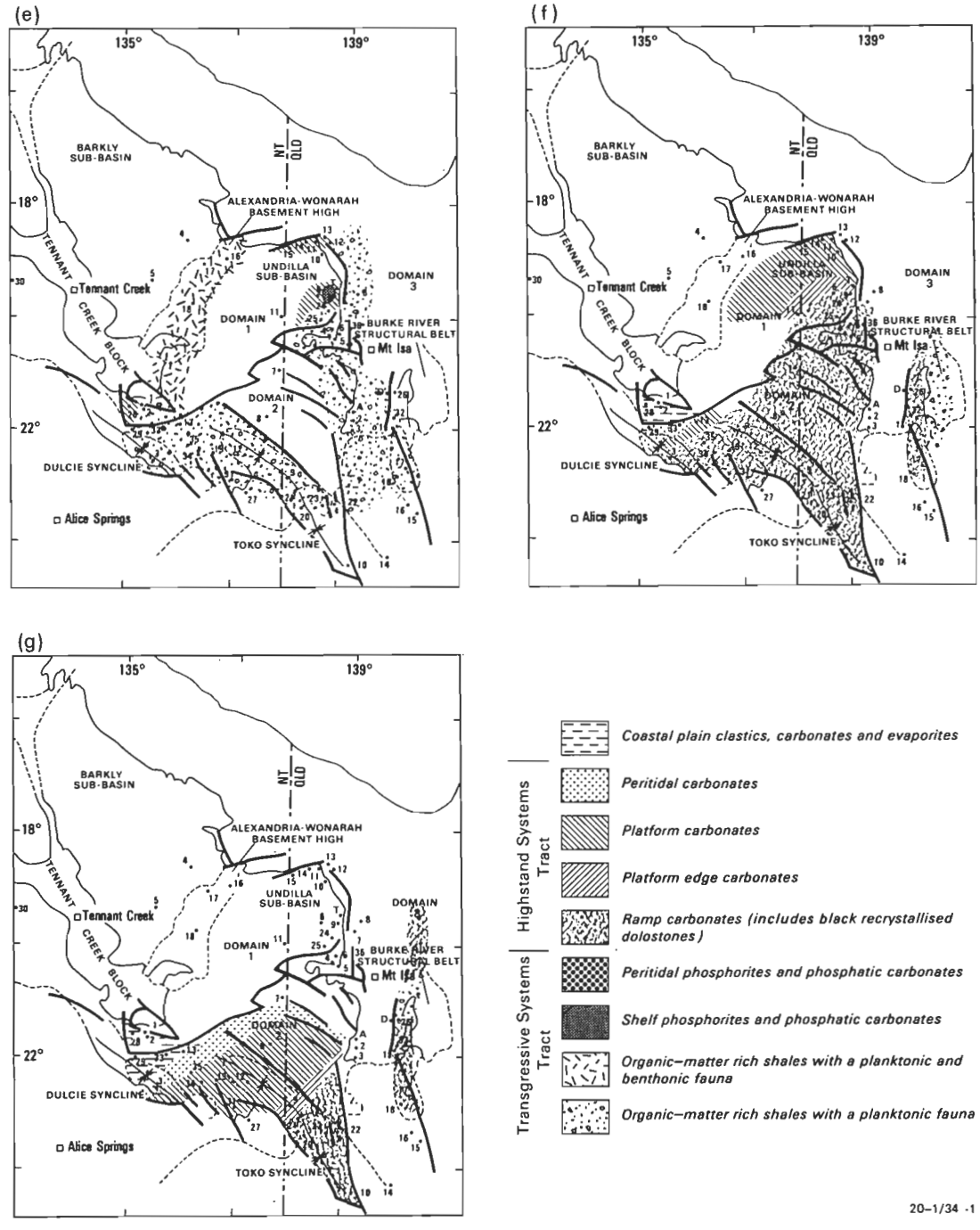

Figure 12 (continued)

e. Sequence 2, parasequence set 3. Continued onlap led to further deposition of organic-matter rich shale and associated phosphorite in structurally defined compartments. Clear water carbonate deposition commenced in structurally stable platform settings. Phosphatic limestone of the Gowers Formation was deposited during onlap of a structural high in the vicinity of Thorntonia Station.

f. Early highstand systems tract. A stable platform area developed in Domain 1. Deeper water carbonates accumulated on a southeasterly dipping ramp.

g. Sediment accumulation and a possible relative lowering in relative sea level resulted in gradual regression in a southeasterly direction. Mixed carbonates and siliciclastics formed a southeasterly dipping and prograding sequence in the region of the Toko Syncline.

and a stillstand of sea level. Such conditions are compatible with sedimentation in a highstand systems tract.

Thus, on the southern transect, water depths gradually increased from west to east (Figs 11, 12). In the west, peritidal carbonate sediments accumulated in shoal and sabkha environments on a carbonate platform, and a shoreline probably existed to the west of Elkedra No. 6 (Fig. 2 B). Gradual sediment accumulation during the highstand systems tract led to progradation of this shoreline in an easterly direction toward BMR Sandover No. 13 (Fig. 2 D; correlations in Stidolph & others, 1988). To the east, deeper water micritic and silty limestone accumulated on a southeasterly dipping drowned ramp (Figs 11, 12). The platform–ramp transition probably lay along the southern boundary of Domain 1. Quartz grains in the Marqua Beds and Steamboat Sandstone were probably derived from emergent basement in this domain.

The upper sequence boundary with the Arrinthrunga Formation and its correlatives changes in character from west to east. This reflects the change from terrestrial environments in the west to progressively deeper water platform and ramp settings in the east. In the west, peloid grainstones of the Arrinthrunga Formation (Kennard, 1981) onlap emergent coastal plain and peritidal sediments of the Chabalowe Formation. Further east, a gradational contact up to several metres thick occurs between peloid grainstones of the Arrinthrunga Formation and submergent platform carbonates and siliciclastics of the Arthur Creek and Marqua Formations (Kennard, 1981). In the far east, the Arrinthrunga Formation correlates with the outer ramp, nodular and rhythmically laminated carbonate rocks of the Georgina, Devoncourt and Selwyn Range Limestones.

Implications for phosphogenesis and organic-matter rich shale deposition

Riggs (1979) classified sedimentary phosphorites into two broad categories, (1) phosphate deposits of economic significance which form during periods of abnormal sedimentation, and (2) phosphatic occurrences associated with unconformities or surfaces of sediment bypass and non-deposition. Analysis of the distribution of economic phosphate deposits (Cook & McElhinny, 1979) supported the ideas of Riggs (1979), indicating that economic phosphate deposits have an episodic distribution, with peaks in the Late Proterozoic–Middle Cambrian, Ordovician, Permian, Jurassic, Late Cretaceous to Eocene and Miocene. With the advent of sequence stratigraphy (Van Wagoner & others, 1988), the regional importance of phosphatic hardgrounds associated with surfaces of sediment bypass, as indicators of condensed sections, and surfaces of maximum flooding, became apparent (Loutit & others, 1988).

The position of major economic phosphate deposits within the stratigraphic sequence model proposed by the EXXON group remained unclear. Sedimentological studies of economic phosphate deposits of Proterozoic and Cambrian age (Cook & Shergold, 1986), those of Late Cretaceous to Eocene age (Slansky, 1980; Soudry, 1987) and the Miocene deposits of Florida (Riggs, 1979) all indicate deposition in shallow submergent and, at times, emergent environments. Such shallow water environments appear incompatible with the deeper water continental margin settings considered as the depositional sites for phosphatic condensed sequences (Loutit & others, 1988). Yet the mineral and facies assemblages in both environmental settings are similar. Like phosphatic rocks in condensed sequences (Loutit & others, 1988), economic phosphate deposits are usually associated with the authigenic mineral glauconite and organic-matter rich sediments with anomalously high concentrations of noble metals (e.g. Shergold, 1985).

Sequence stratigraphic analysis of Middle Cambrian sediments in the Georgina Basin may provide an answer to some of these questions. In stratigraphic sequence 1, phosphate deposits in the Highland Plains to Riversleigh region are related to gradual onlap of the palaeocontinent (Figs 8, 9, 12). In sequence 1a, phosphate deposits in the Thorntonia, D Tree, Yelvertoft and Lady Annie areas occur in the transgressive systems tract and are related to early subsidence of the Mt Isa block and the creation of a new seaway deepening in a southeasterly direction (Figs 8, 9, 12). Phosphate deposits and occurrences in the Burke River Structural Belt, Ardmore, the southwestern parts of the basin and Thorntonia, found in stratigraphic sequence 2, are related to gradual onlap of the palaeocontinent during a second major rise in relative sea level (Figs 11, 12). The confinement of phosphate deposits and occurrences to retrogradational parasequence sets of the transgressive systems tract provides a link with the condensed sequences of Loutit & others (1988). Whereas condensed sequences occur in deep water environments with slow sedimentation rates, phosphate deposits in the Georgina Basin formed in shallow water environments in areas of more rapid sedimentation. Facies analysis of the phosphatic suite of sediments indicates that they were deposited in a range of environments varying from shallow shelf and emergent (economic phosphate deposits) to outer shelf and possibly basinal (condensed sequences).

In stratigraphic sequence 1, phosphatic sediments in the Highland Plains to Riversleigh region accumulated in a variety of semi-emergent to submergent peritidal environments (Southgate, 1988). At the same time, the organic-matter rich shale facies, with its interbedded glauconitic and phosphatic wackestone laminae and associated phosphatic hardgrounds (condensed sequence), formed in deeper water restricted environments in the Tobermory and Hay River areas (Figs 8, 12). Similar relationships occur in sequence 1a, where semi-emergent to shallow submergent phosphorites of the Lady Annie, D Tree and Yelvertoft deposits overlie and pass laterally into organic-matter rich shale of the Beetle Creek Formation (Fig. 9). The shale contains a rich fauna of benthonic and planktonic organisms. This suggests that, in proximal shallower water conditions, oxygen concentrations in the bottom waters fluctuated, permitting periodic colonisation by a benthonic fauna, subsequently killed by increasing anoxia. In sequence 2, the facies mosaic is once again repeated (Figs 11, 12). Continued transgression here eventually led to complete drowning of the continent, and the formation of depositional environments unsuitable for economic phosphate deposition.

Examination of the three parasequence sets in sequence 2 shows how this process takes place. During parasequence set 1 time, phosphatic limestone rocks at

Rogers Ridge accumulated in semi-emergent and shallow submergent environments, while organic-matter rich shale accumulated in deeper water environments to the south (Figs 11, 12). The next phase of onlap resulted in the deposition of parasequence set 2. At Rogers Ridge, these sediments overlie the transgressive surface, a 5 cm thick condensed interval of phosphatic and glauconitic wackestone and packstone cemented by phosphate to form phosphatic hardgrounds and crusts. Siliceous, organic-matter rich shale with interbedded packstone and mudstone phosphorite and a benthonic and planktonic trilobite fauna accumulated above the transgressive surface. The maximum flooding surface for this parasequence set probably lies within the siliceous shale beds, which grade both vertically and laterally into phosphatic grain-supported and mud-supported rocks forming the deposits.

These sediments accumulated in a variety of semi-emergent to submergent environments. The deposition of mud-supported and grain-supported phosphorite in the Burke River Structural Belt and at Ardmore coincided with accumulation of deeper water organic-matter rich shale and phosphorite, with interlaminated phosphatic hardgrounds, in the Huckitta and Elkedra areas in the southwest of the basin. At Rogers Ridge, the next phase of onlap resulted in five cycles, each capped by concretions of phosphatic and glauconitic spicular wackestone and packstone. Some of these concretions have eroded upper surfaces and associated phosphate crusts, thus inferring that each of these cycles is capped by a sediment starvation surface, and that the boundary between parasequence sets 2 and 3 is a condensed interval.

In the Rogers Ridge area, the transgression responsible for parasequence set 3 resulted in the termination of phosphate deposition and the accumulation of an organic-matter rich shale facies with a planktonic fauna (Figs 5, 11, 12). Elsewhere, phosphatic sediments of the Gowers Formation were deposited on a palaeohigh to the south of Thorntonia Station, while in the southwest and south of the basin the organic-matter rich shale facies, in which planktonic faunal elements are found but benthonic faunal components are lacking, accumulated above sediments of parasequence 1 or the transgressive surface.

As transgression continued, and water depths increased, anaerobic conditions responsible for the preservation of organic-matter rich shale were replaced by dysaerobic and aerobic bottom waters. Rhythmically laminated, nodular, ribbon and parted limestone was deposited there (Figs 11, 12). This sequence of events is probably related to changes in productivity and preservation potential of the organic matter. As water depths increased, the residence time for planktonic organic matter in the oxygenated portion of the water column also increased. This resulted in elevated levels of organic matter degradation before it reached the sea floor, a decline in bottom water anoxia, and eventually an oxic watercolumn. As onlap took place, oceanic circulation patterns would have changed, enabling cold, nutrient-rich waters to upwell on to the former continent.

The most vigorous upwelling and highest productivity probably coincided with the initial phases of transgression, resulting in the accumulation of organic-matter rich shale and phosphorite in shallow water embayed environments. Dysaerobic, and periodically aerobic, conditions permitted the development of a benthonic fauna in the near-shore shale facies, possibly as upwelling events increased in intensity and later decayed. Subsequent onlap led to deeper water and permanently anaerobic bottom waters in which organic-matter rich shale devoid of a benthonic fauna accumulated. Later, as water depth increased, circulation patterns stabilised, upwelling declined and productivity decreased. This resulted in a decline in organic material available for preservation on the seafloor, and as a consequence a return to more oxygenated bottom waters.

The sequence of events outlined above, although doubtless simplified, explains the consistent facies patterns observed in the transgressive systems tracts. Phosphorite, and its associated organic-matter rich shale facies that contains a benthonic fauna, accumulated in shallow water embayed and locally restricted environments subject to rapid fluctuations in oxygen concentrations, probably caused by variations in the intensity of upwelling events. With continuing onlap and increased water depth, the zone of vigorous upwelling moved shoreward, permitting the establishment of an oxygen minimum zone in the region of former phosphorite sedimentation. This in turn resulted in the accumulation of organic-matter rich shale devoid of a benthonic fauna. Subsequent onlap led to increased water depths, less vigorous upwelling and a gradual return to aerobic bottom water conditions in which deeper water ramp carbonate of the highstand systems tract accumulated.

Riggs (1979, 1984) has proposed an integrated model to explain the genesis of economic phosphate deposits of Neogene age in Florida and North Carolina. Although these deposits are much younger than the Cambrian sediments discussed here, many aspects of phosphate deposition in the southeastern USA are similar to those of the Georgina Basin. Riggs (1984) relates phosphate deposition to eustatic changes in relative sea level during the Neogene. Specifically, phosphate deposits of the southeastern USA accumulated during times of transgression when the Gulf Stream and its associated nutrient-rich waters moved on to the continental shelf, permitting the formation of shallow water environments suitable for phosphate deposition. Periods of maximum sea level rise coincide with the deposition of carbonate sediments and correspond with a cessation in phosphorite deposition. Riggs (1984) related Miocene phosphogenesis of the southeastern USA to the interplay of a variety of factors, including glacial eustatic sea level oscillations, bathymetric configuration, changes in the dynamics of the Gulf Stream and climate.

Although it is not possible to reconstruct Middle Cambrian palaeo-oceanographic conditions in the same detail, there are many similarities between the two suites of phosphatic sediments. In both cases phosphate deposits occurred during periods of major transgression, and phosphate deposition was greatest on the flanks of palaeobathymetric highs. Spatial positioning of phosphate deposits in sequence 1 was controlled by the interaction between relative sea level rise and palaeotopography (Southgate, 1988). Russell & Trueman (1971) interpreted similar relationships for the Duchess deposits and phosphatic limestone in the Gowers Formation also occurs on a palaeotopographic high.

Cyclical processes in deposition are recognised in Middle Cambrian and Neogene deposits, although a

hierarchical system has not been established for the Cambrian cycles. In the Georgina Basin deposits, the transgressive systems tract in sequence 2 is divided into 3 parasequence sets. In sequence 1, onlap of phosphatic facies attributed to the highstand systems tract resulted in the inclusion of sequence 1a, a parasequence set, in the upper parts of sequence 1.

Each of these parasequence sets has its own transgressive surface, followed by several thin retrogradational cycles and an interval of organic-matter rich shale accumulation. The uppermost part of the parasequence set is then characterised by the aggradational and progradational accumulation of packstone and grainstone phosphorite. This suggests that each parasequence set may represent a lower order sequence. If this scenario is correct, the two sequences discussed here may be at the supercycle scale (Haq & others, 1988), and the parasequence sets may be comparable to the third order cycles of Haq & others (1988). This problem will be resolved when there is consensus on the age of the base of the Cambrian (e.g. Conway Morris, 1988) and additional sequence stratigraphic studies are undertaken in central Australia.

Conclusions

1. Phosphate deposits and occurrences of Middle Cambrian age in the Georgina Basin occur in two stratigraphic sequences. In each sequence they are restricted to the upper, progradational parts of retrogradational parasequence sets of the transgressive systems tract.
2. Phosphate deposits in sequence 1 are restricted to the northeast of the basin, between Highland Plains and Riversleigh. These deposits are related to gradual transgression of an irregular palaeotopography by a sea that deepened to the north.
3. Phosphate deposits in tectonically enhanced sequence 1a are restricted to the northeast of the basin between Thorntonia and Yelvertoft. These deposits accumulated in response to the synsedimentary subsidence of the Mt Isa block, creating a seaway that deepened to the southeast.
4. Phosphate deposits in sequence 2 are found in the Burke River Structural Belt, Ardmore Outlier, Huckitta–Elkedra region, along the Alexandria–Wonarah Basement High and near Thorntonia Station. These deposits are related to a stepped rise in relative sea level that completely inundated and drowned the palaeocontinent.
5. Carbonate rocks are the principal lithological component of the highstand systems tract in both stratigraphic sequences.
6. In the highstand systems tract of sequence 2, carbonate rocks, evaporites and mixed siliciclastics accumulated in coastal plain, platform and ramp depositional environments.
7. Organic-matter rich shale is best developed in the transgressive systems tract. Shale with benthonic and planktonic faunal components accumulated in dysaerobic environments close to the upper boundary of the oxygen minimum zone. These shale facies usually underlie phosphate facies of the same parasequence or parasequence set. Organic-matter rich shale with planktonic faunal components, but lacking benthos, accumulated in anaerobic bottom waters within the oxygen minimum zone. These sediments usually overlie phosphorites and as such occur in the next parasequence or parasequence set.
8. Difficulties in correlating sequences between structural domains, and across major structural features within domains, suggest that sedimentary facies are controlled by structural compartments. Lack of facies continuity is most pronounced in sediments of the transgressive systems tract, where phosphorites and organic-matter rich shales are the principal sediments.

Acknowledgements

Many people have provided assistance during the course of this work. Discussions with John Kennard and John Laurie helped us evolve some of the ideas presented here. The manuscript was improved by the constructive criticisms of Colin Gatehouse and David Feary. The assistance and support provided by Peter Cook and Malcolm Walter throughout the project are gratefully acknowledged.

References

Conway Morris, S., 1988 — Radiometric dating of the Precambrian–Cambrian boundary in the Avalon Zone. *In* Landing, E., Narbonne, G.M. & Myrow, P. (editors), Proceedings, Trace fossils, small shelly fossils and the Precambrian–Cambrian boundary, 1987, Memorial University. *New York State Geological Survey, Bulletin* 463, 53–58.

Cook, P.J. & Elgueta, S.A., 1986 — Proterozoic and Cambrian phosphorites - deposits: Lady Annie, Queensland, Australia. *In* Cook, P.J. & Shergold, J.H. (editors), Phosphate deposits of the world. 1: Proterozoic and Cambrian phosphorites. *Cambridge University Press, Cambridge*, 132–148.

Cook, P.J. & McElhinny, M.W., 1979 — A re-evaluation of the spatial and temporal distribution of sedimentary phosphate deposits in the light of plate tectonics. *Economic Geology*, 74, 315–330.

Cook, P.J. & Shergold, J.H., 1986 — Proterozoic and Cambrian phosphorites — nature and origin. *In* Cook, P.J. & Shergold, J.H. (editors), Phosphate deposits of the world. 1: Proterozoic and Cambrian phosphorites. *Cambridge University Press, Cambridge*, 369–386.

de Keyser, F., 1968 — The Cambrian of the Burke River outlier. *Bureau of Mineral Resources, Australia, Record* 1968/67.

de Keyser, F., 1969 — The phosphate-bearing Cambrian formations in the Lawn Hill and Lady Annie districts, northwestern Queensland. *Bureau of Mineral Resources, Australia, Record* 1969/147.

de Keyser, F., 1973 — A review of the Middle Cambrian stratigraphy in the Queensland portion of the Georgina Basin. *Bureau of Mineral Resources, Australia, Bulletin* 139, 13–27.

de Keyser, F. & Cook, P.J., 1973 — Geology of the Middle Cambrian phosphorites and associated sediments in northwestern Queensland. *Bureau of Mineral Resources, Australia, Bulletin* 138, 79 pp.

Donnelly, T.H., Shergold, J.H. & Southgate, P.N., 1988 — Anomalous geochemical signals from phosphatic Middle Cambrian rocks in the southern Georgina Basin, Australia. *Sedimentology*, 35, 549–570.

Fleming, P.J.G., 1971 — *In* Hill, D., Playford, G. & Woods J.T. (editors), Cambrian fossils of Queensland. *Queensland Palaeontographical Society, Brisbane*, 32 pp., 15 pl.

Fleming, P.J.G., 1973 — Bradoriids from the *Xystridura* Zone of the Georgina Basin, Queensland. *Geological Survey of Queensland, Publication* 356, *Palaeontological Papers*, 31, 9 pp.

Freeman, M.J., 1986 — Huckitta SF53-11, 1:250 000 Geological Map Series Explanatory Notes. *Northern Territory Geological Survey, Darwin*, 58 pp.

Green, P.M. & Balfe, P.E., 1980 — Stratigraphic drilling report — GSQ Mt Whelan 1 and 2. *Queensland Government Mining Journal*, 81 (941), 162–178.

Haq, B.U., Hardenbol, J. & Vail, P.R., 1988 — Mesozoic and Cenozoic chronostratigraphy and eustatic cycles. *In* Wilgus, C.K. & others (editors), Sea-level changes : an integrated approach. *Society of Economic Paleontologists and Mineralogists, Special Publication* 42, 71–108.

Harrison, P.L., 1979 — Recent seismic studies upgrade the petroleum prospects of the Toko Syncline, Georgina Basin. *The APEA Journal*, 19 (1), 30–42.

Henderson, R.A. & McKinnon, D.I., 1981 — New Cambrian inarticulate Brachiopoda from Australasia, and the age of the Tasman Formation. *Alcheringa*, 5(3), 289–310.

Henderson, R.A. & Shergold, J.H., 1971 — *Cyclocystoides* from early Middle Cambrian rocks of northwestern Queensland, Australia. *Palaeontology*, 14(4), 704–710, pl. 138.

Howard, P.E. & Cooney, A., 1976 — D Tree phosphate deposit, Georgina Basin, Queensland. *In* Knight, C.L. (editor), Economic geology of Australia and Papua New Guinea. 4. Industrial minerals and rocks. *Australasian Institute of Mining and Metallurgy, Melbourne, Monograph* 8, 273–278.

James, N.P & Stevens, R.K., 1986 — Stratigraphy and correlation of the Cambro-Ordovician Cow Head Group Western Newfoundland. *Geological Survey of Canada, Bulletin* 366, 143 pp.

Jell, P.A., 1970 — *Pagetia ocellata*, a new Cambrian trilobite from northwestern Queensland. *Memoirs of the Queensland Museum*, 15, 303–313, pl. 23–24.

Jell, P.A., 1975 — Australian Middle Cambrian eodiscoids with a review of the Superfamily. *Palaeontographica* [A] 150, 97 pp.

Jell, P.A., Burrett, C.F. & Banks, M.R., 1985 — Cambrian and Ordovician echinoderms from eastern Australia. *Alcheringa*, 9, 183–208.

Jones, P.J. & McKenzie, K.G., 1980 — Queensland Middle Cambrian Bradoriida (Crustacea): new taxa, palaeobiogeography, and biological affinities. *Alcheringa*, 4(3), 203–225.

Kennard, J.M., 1981 — The Arrinthrunga Formation — Upper Cambrian epeiric carbonates in the Georgina Basin, central Australia. *Bureau of Mineral Resources, Australia, Bulletin* 211, 61 pp.

Laurie, J.R., 1988 — Revision of some Australian Ptychagnostinae (Agnostida, Cambrian). *Alcheringa*, 12, 169–205.

Laurie, J.R., 1989 — Revision of species of *Goniagnostus* Howell and *Lejopyge* Corda from Australia (Agnostida, Cambrian). *Alcheringa*, 13, 175–191.

Lindsay, J.F., Korsch, R.J. & Wilford, J.R., 1987 — Timing the breakup of a Proterozoic supercontinent: evidence from Australian intracratonic basins. *Geology*, 15, 1061–1064.

Loutit, T.S., Hardenbol, J., Vail, P.R. & Baum, G.R., 1988 — Condensed sections: the key to age determination and correlation of continental margin sequences. *In* Wilgus, C.K. & others (editors), Sea-level changes: an integrated approach. *Society of Economic Palaeontologists and Mineralogists, Special Publication*, 42, 183–213.

Nordlund, U. & Southgate, P.N., 1988 — Depositional environments and importance of the early Middle Cambrian sequence at Rogers Ridge, Georgina Basin, W. Queensland. *Acta Universitatis Upsaliensis, Comprehensive Summaries of Uppsala Dissertations from the Faculty of Science*, 170(6), 19 pp.

Öpik, A.A., 1956 — Cambrian geology of Queensland. *20th Session International Geological Congress, Mexico*, 2, 1–24.

Öpik, A.A., 1960 — Cambrian and Ordovician geology (of Queensland). *Geological Society of Australia, Journal*, 7, 89–109.

Öpik, A.A., 1961 — Geology and palaeontology of the headwaters of the Burke River, Queensland. *Bureau of Mineral Resources, Australia, Bulletin* 53, 249 pp., 24 pl.

Öpik, A.A., 1968a — The Ordian Stage of the Cambrian and its Australian Metadoxididae. *Bureau of Mineral Resources, Australia, Bulletin* 92, 133–170, pl. 19–20.

Öpik, A.A., 1968b — Ordian (Cambrian) Crustacea Bradoriida of Australia. *Bureau of Mineral Resources, Australia, Bulletin* 103, 37 pp., 4 pl.

Öpik, A.A., 1970a — Nepeiid trilobites of the Middle Cambrian of northern Australia. *Bureau of Mineral Resources, Australia, Bulletin* 113, 48 pp., 17 pl.

Öpik, A.A., 1970b — *Redlichia* of the Ordian (Cambrian) of northern Australia. *Bureau of Mineral Resources, Australia, Bulletin* 114, 66 pp., 14 pl.

Öpik, A.A., 1975 — Templetonian and Ordian xystridurid trilobites of Australia. *Bureau of Mineral Resources, Australia, Bulletin* 121, 84 pp., 32 pl.

Öpik, A.A., 1979 — Middle Cambrian agnostids: systematics and biostratigraphy. *Bureau of Mineral Resources, Australia, Bulletin* 172 (2 vols), 188 pp., 67 pl.

Öpik, A.A., 1982 — Dolichometopid trilobites of Queensland, Northern Territory and New South Wales. *Bureau of Mineral Resources, Australia, Bulletin* 175, 85 pp., 32 pl.

Öpik, A.A., Carter, E.K. & Noakes, L.C., 1961 — Mt Isa — 1:250 000 Geological Series Explanatory Notes, Sheet F/54-1. *Bureau of Mineral Resources, Australia*, 20 pp.

Randal, M.A. & Brown, G.A., 1962 — Additional notes on the geology of the Camooweal 4-mile sheet area. *Bureau of Mineral Resources, Australia, Record* 1962/49.

Read, J.F., 1985 — Carbonate platform facies models. *American Association of Petroleum Geologists, Bulletin* 69, 1–21.

Riggs, S.R., 1979 — Phosphorite sedimentation in Florida — a model phosphogenetic system. *Economic Geology*, 74, 285–314.

Riggs, S.R., 1984 — Paleoceanographic model of Neogene phosphorite deposition, US Atlantic continental margin. *Science*, 233 (4632), 123–131.

Rogers, J.K. & Crase, N.J., 1980 — The Phosphate Hill rock phosphate deposit, northwest Queensland, Australia — an outline of geological development. *In* Sheldon, R.P. & Burnett, W.C. (editors), Fertilizer mineral potential in Asia and the Pacific. Proceedings of the Fertilizer Raw Materials Resources Workshop, August 20–24, 1979, Honolulu, Hawaii. *East-West Resource Systems Institute, Honolulu*, 307–328.

Rogers, J.K. & Keevers, R.E., 1976 — Lady Annie — Lady Jane phosphate deposits, Georgina Basin, Queensland. *In* Knight, C.L. (editor), Economic geology of Australia and Papua New Guinea. 4. Industrial minerals and rocks. *Australasian Institute of Mining and Metallurgy, Melbourne, Monograph* 8, 251–265.

Runnegar, B.N. & Jell, P.A., 1976 — Australian Middle Cambrian molluscs and their bearing on early molluscan evolution. *Alcheringa*, 1(2), 109–138.

Russell, R.T., 1967 — Discovery of a major phosphate deposit in northwest Queensland. *Queensland Government Mining Journal*, 68, 153–157.

Russell, R.T. & Trueman, N.A., 1971 — The geology of the Duchess phosphate deposits, northwest Queensland, Australia. *Economic Geology*, 66, 1186–1214.

Sarg, J.F., 1989 — Carbonate sequence stratigraphy. *In* Wilgus, C.K. & others (editors), Sea-level changes: an integrated approach. *Society of Economic Paleontologists and Mineralogists, Special Publication* 42, 155–181.

Schmitt, M. & Southgate, P.N., 1982 — A phosphatic stromatolite, *Ilicta* cf. *composita* Sidorov, from the Middle Cambrian of northern Australia. *Alcheringa*, 6, 175–183.

Shergold, J.H., 1968 — Appendix: Cambrian Palaeontology. *In* de Keyser, F., The Cambrian of the Burke River outlier. *Bureau of Mineral Resources, Australia, Record* 1968/67.

Shergold, J.H., 1969 — Oryctocephalidae (Trilobita: Middle Cambrian) of Australia. *Bureau of Mineral Resources, Australia, Bulletin* 104, 66 pp., 12 pl.

Shergold, J.H., 1985 — Notes to accompany the Hay River–Mount Whelan Special 1:250 000 Geological Sheet, southern Georgina Basin. *Bureau of Mineral Resources, Australia, Report* 251, 47 pp.

Shergold, J.H., 1989 — Australian Phanerozoic timescales. 1, Cambrian. *Bureau of Mineral Resources, Australia, Record* 1989/31.

Shergold, J.H. & Brasier, M.D., 1986 — Proterozoic and Cambrian phosphorites — specialist studies: biochronology of Proterozoic and Cambrian phosphorites. *In* Cook, P.J. & Shergold, J.H. (editors), Phosphate deposits of the world. 1. Proterozoic and Cambrian phosphorites. *Cambridge University Press, Cambridge*, 295–326.

Shergold, J.H. & Druce, E.C., 1980 — Upper Proterozoic and Lower Palaeozoic rocks of the Georgina Basin. *In* Henderson, R.A. & Stephenson, P.J. (editors), The geology and geophysics of northeastern Australia. *Geological Society of Australia, Queensland Division, Brisbane*, 149–174.

Shergold, J.H. & Laurie, J.R., 1986 — Appendix 5: Palaeontological determinations from selected formations and field localities. *In* Shergold, J.H. & Southgate, P.N. (editors), Middle Cambrian phosphatic and calcareous lithofacies along the eastern margin of the Georgina Basin, Western Queensland. Australasian Sedimentologists Group, Field Guide Series 2. *Geological Society of Australia, Sydney*, 88–89.

Shergold, J.H. & Southgate, P.N. (editors), 1986 — Middle Cambrian phosphatic and calcareous lithofacies along the eastern margin of the Georgina Basin, western Queensland. Australasian Sedimentologists Group, Field Guide Series 2. *Geological Society of Australia, Sydney*, 89 pp.

Shergold, J.H. & Southgate, P.N., 1988 — Timing and distribution of Middle Cambrian phosphogenetic events in the Georgina Basin Australia. *In* A decade of phosphorite research and development. *11th International Field Workshop and Symposium, IGCP Project 156, Extended Abstracts*, 27–28.

Shergold, J.H., Southgate, P.N. & Cook, P.J., 1988 — Middle Cambrian phosphogenic system in Australia. BMR Research Symposium 88, Extended Abstracts. *Bureau of Mineral Resources, Australia, Record* 1988/42, 78–81.

Shergold, J.H., Southgate, P.N. & Cook, P.J., 1989 — New facts on old phosphates: Middle Cambrian, Georgina Basin. *BMR Research Newsletter, 10*, 14–15.

Slansky, M., 1980 — Géologie des phosphates sedimentaires. *Mémoire du BRGM*, 114, 92 pp.

Soudry, D., 1987 — Ultra-fine structures and genesis of the Campanian Negev high-grade phosphorites (southern Israel). *Sedimentology*, 34, 641–660.

Soudry, D. & Southgate, P.N., 1989 — Ultrastructure of a Middle Cambrian primary nonpelletal phosphorite and its early transformation into phosphate vadoids: Georgina Basin, Australia. *Journal of Sedimentary Petrology*, 59(1), 53–64.

Southgate, P.N., 1982 — Cambrian skeletal halite crystals and experimental analogues. *Sedimentology*, 29, 391–407.

Southgate, P.N., 1983 — Middle Cambrian phosphatic and calcareous depositional environments, Undilla region of the Georgina Basin, Australia. *Ph.D. thesis, Australian National University, Canberra.*

Southgate, P.N., 1986a — Cambrian phoscrete profiles, coated grains, and microbial processes in phosphogenesis: Georgina Basin, Australia. *Journal of Sedimentary Petrology*, 56(3), 429–441.

Southgate, P.N., 1986b — Proterozoic and Cambrian phosphorites – specialist studies: Middle Cambrian phosphatic hardgrounds, phoscrete profiles and stromatolites and their implications for phosphogenesis. *In* Cook, P.J. & Shergold, J.H. (editors), Phosphate deposits of the World. 1. Proterozoic and Cambrian phosphorites. *Cambridge University Press, Cambridge*, 327–351.

Southgate, P.N., 1986c — The Gowers Formation and Bronco Stromatolith Bed, two new stratigraphic units in the Undilla portion of the Georgina Basin. *Queensland Government Mining Journal, October*, 407–411.

Southgate, P.N., 1988 — A model for the development of phosphatic and calcareous lithofacies in the Middle Cambrian Thorntonia Limestone, northeast Georgina Basin, Australia. *Australian Journal of Earth Sciences*, 35, 111–130.

Southgate, P.N., Laurie, J.R., Shergold, J.H. & Armstrong, K.J., 1988 — Stratigraphic drilling in the Georgina Basin, Burke River Structural Belt, August 1986–January 1987. *Bureau of Mineral Resources, Australia, Record* 1988/1.

Southgate, P.N. & Shergold, J.H., 1988 — Sequence stratigraphy and repeating facies mosaics in Middle Cambrian sediments of the Georgina Basin. *In* A decade of phosphate research and development. *11th International Field Workshop and Symposium, IGCP Project 156, Extended Abstracts*, 31–32.

Stidolph, P.A., Bagas, L., Donnellan, N., Walley, A.M., Morris, D.G. & Simons, B., 1988 — Elkedra SF53–7, 1:250 000 Geological Map Series Explanatory Notes. *Northern Territory Geological Survey, Darwin*, 54 pp.

Tucker, D.H., Wyatt, B.W., Druce, E.C., Mathur, S.P. & Harrison, P.L., 1979 — The upper crustal geology of the Georgina Basin region. *BMR Journal of Australian Geology & Geophysics*, 4, 209–226.

Van Wagoner, J.C., Posamentier, H.W., Mitchum, R.M., Vail, P.R., Sarg, J.F., Loutit, T.S. & Hardenbol, J., 1988 — An overview of the fundamentals of sequence stratigraphy and key definitions. *In* Wilgus, C.K. & others (editors), Sea-level changes: an integrated approach. *Society of Economic Paleontologists and Mineralogists, Special Publication* 42, 40–45.

Walter, M.R., Shergold, J.H., Muir, M.D. & Kruse, P.D., 1979 — Early Cambrian and latest Proterozoic stratigraphy, Desert Syncline, southern Georgina Basin. *Journal of the Geological Society of Australia*, 26, 305–312.

Whitehouse, F.W., 1936 — The Cambrian faunas of northeastern Australia. Part 1 — Stratigraphic outline. Part 2 — Trilobita (Miomera). *Memoirs of the Queensland Museum*, 11(1), 59–112, pl. 8–10.

Whitehouse, F.W., 1939 — The Cambrian faunas of northeastern Australia. Part 3 — The polymerid trilobites (with supplement No. 1). *Memoirs of the Queensland Museum*, 11(3), 179–282, pl. 19–25.

Whitehouse, F.W., 1941 — The Cambrian faunas of northeastern Australia. Part 4 — Early Cambrian echinoderms similar to the larval stages of Recent forms. *Memoirs of the Queensland Museum*, 12(1), 1–28, pl. 1–4.

Appendix 1. Faunas of stratigraphic sequence 1.

1. Thorntonia Limestone

Shelf and peritidal sediments of the Thorntonia Limestone (*sensu stricto*) north and west of Riversleigh belonging to the transgressive and highstand systems tract.

Trilobita *Pagetia* cf. *oepiki* Jell, *Redlichia* sp. cf. *idonea* Whitehouse, *Xystridura* (*Xystridura*) sp. cf. *templetonensis* (Chapman).

Brachiopoda Undetermined acrotretid and oboloid inarticulate brachiopods.

Mollusca Undetermined hyolithids; *Latouchella* sp., *Pelagiella* sp. cf. *deltoides* Runnegar & Jell, *Protowenella* sp. cf. *flemingi* Runnegar & Jell.

Bradoriida Undetermined bradoriid.

Alga *Ilicta* sp. cf. *composita* Sidorov, *Girvanella* sp.

Miscellanea *Chancelloria* sp., sponge spicules

Age Ordian (*sensu* Öpik 1968a, 1979), Ordian/early Templetonian (herein), *Redlichia chinensis* biofacies.

References de Keyser (1969), Jell (1975), Schmitt & Southgate (1982), Shergold & Southgate (1986), Southgate (1983, 1988).

2. Yelvertoft Bed

Shelf and peritidal sediments assigned to the Yelvertoft Bed (*sensu stricto* at May Downs, *sensu lato* elsewhere), belonging to the transgressive systems tract, laterally equivalent to Thorntonia Limestone north and west of Riversleigh.

Trilobita *Onaraspis*? sp., *Pagetia* sp., *Redlichia chinensis* Walcott, *R. creta* Öpik, *R. idonea* Whitehouse, *R. lepta* Öpik, *R. micrograpta* Öpik, *R. myalis* Öpik, *R. venulosa* (Whitehouse), *R. versabunda* Öpik, *R. vertumnia* Öpik, *Xystridura (Xystridura) yaringensis* Öpik.

Brachiopoda Undetermined inarticulate brachiopods.

Mollusca Undetermined hyolithids, *Biconulites* sp. cf. *hardmani* Etheridge.

Echinodermata *Edriodiscus primotica* (Henderson & Shergold).

Bradoriida *Bradoria cornulata* Öpik, *B. curvifrons* Öpik, *B.* sp. cf. *curvifrons* Öpik, *B. petalina* Öpik, *Comptaluta calcarata*

Öpik, *C. profunda* Öpik, *Indota otica* Öpik, *Ophiosema spicatum* Öpik, *Tropidiana cirrata* Öpik.
Alga *Girvanella* sp.
Age Ordian (*sensu* Öpik, 1968a, 1979), Ordian/early Templetonian (herein), *Redlichia chinensis* biofacies.
References Henderson & Shergold (1971), Jell & others (1985), Öpik, (1968a,b, 1970a,b, 1975, 1979), Öpik & others (1961).

Appendix 2: Faunas of stratigraphic sequence 1a.

1. Thorntonia Limestone
Encrinitic, coquinitic 'upper' Thorntonia Limestone sediments of the transgressive systems tract between Thorntonia and Yelvertoft and part of the Bronco Stromatolith Bed, laterally equivalent to Beetle Creek Formation (*sensu stricto*) at May Downs.
Trilobita *Kootenia* sp., *Pagetia howardi* Jell, *P. macrommatia* Jell, Ptychopariida genera et spp. undetermined, *Peronopsis* sp., *Xystridura (Xystridura) hamosa* Öpik, *X. (X.) templetonensis* (Chapman), *X. (X.)* sp.
Brachiopoda Acrotretid and oboloid inarticulate brachiopods.
Molluscs Undetermined hyolithids, *Biconulites* sp.; *Helcionopsis* sp., *Latouchella* sp. cf. *accordionata* Runnegar & Jell, *Mellopegma georginensis* Runnegar & Jell, *Pelagiella* sp. cf. *deltoides* Runnegar & Jell, *Protowenella* sp. cf. *flemingi* Runnegar & Jell, *Yochelcionella* sp. cf. *ostentata* Runnegar & Jell, *Yochelcionella* sp.
Bradoriida *Zepaera* sp.
Alga Undetermined stromatolites.
Miscellanea *Chancelloria* sp., sponge spicules.
Echinodermata *Cymbionites craticula* Whitehouse, *Peridionites navicula* Whitehouse.
Age Early Templetonian (*sensu* Öpik, 1968a, 1979), Ordian/early Templetonian (herein), *Xystridura templetonensis* biofacies.
References de Keyser (1969), Jell (1975), Runnegar & Jell (1976), Öpik (1968a, 1973a,b, 1975, 1979), Shergold & Southgate (1986), Southgate (1983, 1986a, 1988), Whitehouse (1939, 1941).

2. Beetle Creek Formation
Beetle Creek Formation (*sensu stricto*) at its type area in the May Downs inlier and neighbourhood, representing the condensed sequence in the transgressive systems tract.
Trilobita *Chancia vicenalis* Whitehouse, *Chienaspis peregrina* (Whitehouse), *Deiradonyx* sp. aff. *collabrevis* Öpik, *Dinesus ida* Etheridge, *Elrathina* sp., *Kootenia modica* (Whitehouse), *Lyriaspis sigillum* Whitehouse, *Pagetia polygnota* Jell, *P. polymorpha* Jell, *Peronopsis* sp. cf. *P. normata* Whitehouse, *Sestrostega testa* Öpik, *Xystridura* (*Xystridura*) *dunstani* (Chapman), *X.* (*X.*) *milesi* (Chapman), *X.* (*X.*) *saintsmithi* (Chapman), *X.* (*X.*) *templetonensis* (Chapman).
Brachiopoda Undetermined species of *Acrotreta*, *Lingulella* and *Paterina*.
Mollusca *Biconulites* sp.
Age Early Templetonian (*sensu* Öpik 1968a, 1979), Ordian/early Templetonian (herein), *Xystridura templetonensis* biofacies.
References Jell (1975), Öpik (1968a, 1975, 1979, 1982), Öpik & others (1961), Shergold (1969), Whitehouse (1939).

Appendix 3: Faunas of stratigraphic sequence 2.

Transgressive systems tract parasequence set 1.
1. Thorntonia Limestone.
Cyclic, phosphatic, peritidal carbonates assigned to the Thorntonia Limestone (Unit 3), representing parasequence set 1 of the transgressive systems tract at Rogers Ridge, Burke River Structural Belt. Equivalent to black shales in Phillips Sunray Black Mountain No. 1 and Inca Formation at May Downs, Lady Annie and Thorntonia.
Trilobita Oryctocephalid undetermined, *Pagetia ocellata* Jell, *Peronopsis* sp. ex gr. *fallax* (Linnarsson), agnostoid aff. *Pentagnostus*? sp., ptychoparioid undetermined, *Xystridura (Xystridura)* sp.
Brachiopoda Undetermined acrotretid brachiopods.
Mollusca Undetermined hyolithids; *Helcionopsis*? sp., Latouchella? sp., *Pelagiella* sp. aff. *corinthiana* Runnegar & Jell, *Protowenella* sp. cf. *flemingi* Runnegar & Jell, *Tannuella*? sp.
Bradoriida Undetermined comptalutid bradoriid.
Annelida Undetermined annelid.
Echinodermata Echinodermal debris.
Problematica
Miscellanea *Chancelloria* sp., sponge spicules.
Age Late Templetonian (*sensu* Öpik, 1968a, 1979), late Templetonian/early Floran (herein), possibly *Pentagnostus praecurrens* Zone but more probably the *Triplagnostus gibbus* Zone lacking the index species.
References Nordlund & Southgate (1988).

Transgressive systems tract parasequence set 2.
2. Monastery Creek Formation
Parasequence set 2 contains the Monastery Creek Formation of the Burke River Structural Belt. This is equivalent to the 'Simpson Creek Phosphorite' plus underlying coquinite at Ardmore (D41). This set is laterally equivalent to and overlain by black shales.
Trilobita *Acidusus* sp. cf. *atavus* (Tullberg), *Oryctocephalites* sp. cf. *gelasinus* Shergold, *Oryctocephalus* sp., *Pagetia ocellata* Jell, *Pentagnostus* sp. cf. *praecurrens* (Westergård), *Peronopsis* spp., ptychoparioids undetermined, *Thoracocare* sp., *Triplagnostus* sp. cf. ex gr. *gibbus* (Linnarsson), *Xystridura* (*Xystridura*) *carteri* Öpik, *X.* (*X.*) sp. cf. *milesi* (Chapman).
Brachiopoda Species of the inarticulate brachiopods *Acrothele*, acrotretids, *Amictocracens*, *Linnarssonia* and oboloids.
Mollusca Undetermined hyolithids; *Helcionopsis* sp., *Latouchella* sp. cf. *accordionata* Runnegar & Jell, *Mellopegma* sp. cf. *georginensis* Runnegar & Jell, *Pelagiella deltoides* Runnegar & Jell, *Protowenella* sp. cf. *flemingi* Runnegar & Jell.
Bradoriida *Flemingopsis duo* Jones & McKenzie, *Hesslandona* sp., *Indota formosa* Fleming, *Monasterium dorium* Fleming, *M. oepiki* Fleming, *Ovaluta* sp., *Phaseolella dubia* Jones & McKenzie, *P. sestina* (Fleming), *P. sipa* (Fleming), *Svealuta* sp., *Zepaera rete* Fleming.
Annelida, Hyolithelminthida, Conodontophorida Undetermined.
Problematica Aff. *Microdictyon* sp., cf. *Utahphospha* sp., undetermined problematica, *Wiwaxia* sp.
Echinodermata Echinodermal debris.
Miscellanea *Chancelloria* sp., acanthose pentact sponge spicules, lithistid tetrad spicules, *Arborella* sp.
Age Late Templetonian (*sensu* Öpik 1968a, 1979), late Templetonian/early Floran (herein), at overlap of *Triplagnostus gibbus* and *Acidusus atavus* Zones.
References Fleming (1971, 1973), Jell (1970, 1975), Jones & McKenzie (1980), Öpik (1968a,b, 1975, 1979), Shergold & Brasier (1986), Shergold & Laurie (1986), Shergold & Southgate (1986), Southgate & others (1988).

3. Inca Formation
Parasequence set 2 also contains black shales laterally equivalent to the Monastery Creek Phosphorite Formation which have been referred either to the 'Lower Siltstone Member of the Beetle Creek Formation' in the Burke River Structural Belt, or to the Inca Formation at Lady Annie, May Downs, Yelvertoft and D Tree.
Trilobita *Acidusus* sp. cf. *atavus* (Tullberg), *Barklyella expansa* Shergold, *Elrathina* sp., *Galahetes fulcrosus* Öpik, *Lyriaspis* sp., *Oryctocephalites* sp. cf. *gelasinus* Shergold, *Pagetia* spp., *Peronopsis* sp., *Sandoveria* sp., *Triplagnostus* sp. cf. *gibbus* (Linnarsson), *Xystridura* (*X.*) *carteri* Öpik, *X.* (*X.*) *dunstani* (Chapman).
Brachiopoda Undetermined acrotretid and oboloid inarticulate brachiopods.
Bradoriida *Bradoria* sp., *Indota formosa* Fleming.
Mollusca Undetermined hyolithids.
Miscellanea Sponge spicules.
Age Late Templetonian (*sensu* Öpik, 1968a,b, 1979), late Templetonian/early Floran (herein), commencing at the overlap of the *Triplagnostus gibbus* and *Acidusus atavus* Zones as documented here, but ranging into the late Floran *Euagnostus opimus* Zone in the Thorntonia–D Tree area, and early Undillan *Ptychagnostus punctuosus* Zone in the Burke River Structural Belt (for faunal lists see Shergold & Laurie, 1986).
References Jell (1975), Fleming (1973), Öpik (1970a,b, 1979,

1982), Shergold (1968, 1969), Shergold & Laurie (1986), Shergold & Southgate (1986).

Transgressive systems tract parasequence set 3.
4. Concretionary interval
In the Burke River area a condensed interval represented by carbonate concretions, locally mantled by crusts of mudstone phosphate, is found at the base of the Inca Formation. It contains a largely reworked fauna from the Monastery Creek Formation.
Trilobita *Pagetia* sp., *Peronopsis* sp., *Xystridura* (*Xystridura*) sp.
Brachiopoda *Acrothele* sp., *Amictocrasens* sp., undetermined acrotretid and oboloid inarticulate brachiopods.
Bradoriida *Indota formosa* Fleming, *Monasterium dorium* Fleming, *Monasterium* sp. undet., *Phaseolella dubia* Jones & McKenzie, *P. sestina* (Fleming), *P. sipa* (Fleming), *Zepaera rete* Fleming.
Annelida Undetermined.
Conodophorida Undetermined.
Mollusca Undetermined hyoliths; *Latouchella* sp. cf. *accordionata* Runnegar & Jell, *Pelagiella* sp. cf. *deltoides* Runnegar & Jell, *Protowenella* sp. cf. *flemingi* Runnegar & Jell.
Echinodermata Echinodermal debris.
Miscellanea *Chancelloria* sp., sponge spicules.
Age Late Templetonian/early Floran overlap.
Reference Southgate & others (1988).

5. Gowers Formation
In the vicinity of Thorntonia Station this parasequence set is represented by the phosphatic Gowers Formation and overlying carbonate concretions of the Currant Bush Limestone. Contemporary black shales are included in the Inca Formation.
Trilobita *Baltagnostus*? sp., *Doryagnostus*? *deltoides* Robison, *Euagnostus cretus* Öpik, *E. opimus* Whitehouse, *Fuchouia* sp., *Goniagnostus* (*Criotypus*) *lemniscatus* Öpik, *Itydeois* sp., *Onymagnostus hybridus* Brögger, *O. semiermis* Öpik, *Opsidiscus microspinus* Jell, *Pagetia thorntonensis* Jell, *Peronopsis* sp. cf. *quadrata* (Tullberg), *Pseudoperonopsis ancisa* Öpik, *P. perplexa* Robison, *Ptychagnostus affinis* (Brögger), *Ptychopariida* undetermined, *Rhodotypiscus nasonis* Öpik, *Triplagnostus* (*Triplagnostus*) *gibbus* (Linnarsson), *Zeteagnostus scarifatus* Öpik.
Brachiopoda Undetermined species of the inarticulate genera *Acrothele*, *Lingulella*, *Linnarssonia*, *Protorthis*?, *Prototreta*, *Treptotreta*.
Mollusca Undetermined hyolithids; *Eotebenna pontifex* Runnegar & Jell, helcionellid undetermined, '*Latouchella*' sp., *Mellopegma georginensis* Runnegar & Jell, *Myona queenslandica* Runnegar & Jell, *Pelagiella corinthiana* Runnegar & Jell, *P. deltoides* Runnegar & Jell, *Protowenella flemingi* Runnegar & Jell, *Tannuella* sp., *Yochelcionella* sp.
Bradoriida *Oepikaluta dissuta* Jones & McKenzie.
Conodontophorida Undetermined.
Miscellanea *Chancelloria* sp., sponge spicules.
Age Late Floran, late *Euagnostus opimus* Zone (*sensu* Öpik, 1979).
References Henderson & McKinnon (1981), Jell (1975), Jones & McKenzie (1980), Laurie (1988), Öpik (1979, 1982), Shergold & Laurie (1986), Shergold & Southgate (1986), Southgate (1983, 1986c).

BMR Journal of Australian Geology & Geophysics, 12, 145–157

Sequence analysis and depositional models of crinoidal limestones, Permian Yessabah Limestone, Manning–Macleay Basin, eastern Australia

John F. Lindsay[1]

The Permian Yessabah Limestone, a thick crinoidal limestone unit, appears abruptly in the stratigraphic succession over a large area of the Hastings Block in northeastern New South Wales, disconformably overlying clastic rocks with sharply contrasting facies associations. The formation is part of a thick depositional sequence that began with a major sea-level fall at the end of the Carboniferous. The sea-level fall produced a major basinward shift in facies causing rejuvenation of streams and the deposition of braided-stream gravels in the onshore areas while a mass-movement association, the Parrabel Beds, was deposited offshore in the deep basin (the lowstand systems tract). The Yessabah Limestone was deposited as part of the transgressive systems tract in a shallow-marine high-energy environment as sea level again began to rise. The highstand systems tract then prograded over the Yessabah Limestone in the form of a distal turbidite association, the Warbro Formation and associated units, as sea level reached its maximum. The growth of both crinoids and bryozoa was prolific; their two distinctive faunal assemblages alternately dominated the sea floor, producing thick units of well-washed crinoid-rich limestone followed by a bryozoan-rich unit. As sea level rose, conditions became unsuitable for carbonate deposition and the area was again invaded by clastic sediments, forming a distal turbidite association that prograded across the limestones as part of the highstand systems tract.

Introduction

Crinoidal limestones are most common in Late Palaeozoic and Mesozoic rocks of the northern hemisphere (e.g. Moore, 1957; Bathurst, 1958, 1975; Carozzi & Soderman, 1962; Lucia, 1962; Stauffer, 1962; Orme & Brown, 1963; Swarzacher, 1963; Blyth Cain, 1968; Skupin, 1973; Walkden & Berry, 1984), and are relatively rare in the Australian stratigraphic record. The Permian Yessabah Limestone, which is exposed in the Macleay River valley of northeastern New South Wales, is largely crinoidal in origin (Woolnough, 1911; Carne & Jones, 1919; Voisey, 1934, 1936, 1938; Lindsay, 1961, 1964, 1969). This paper develops a depositional model through the application of sequence concepts and a detailed sedimentological analysis of the Yessabah Limestone as an aid in understanding the environmental requirements necessary for the explosive growth and preservation of large volumes of crinoidal materials.

Regional setting

The eastern margin of the Australian continent (Fig. 1) was the site of convergent plate interaction from at least the mid-Cambrian to early Permian (Marsden, 1972; Leitch, 1975; Cawood, 1976, 1980, 1982a,b; Lindsay, 1990). The resulting forearc basin subsided rapidly through most of its history and was filled largely by clastic sediments forming an overall shallowing-upward succession (Lindsay, 1990). Over most of the basin, subsidence and sedimentation had ceased by the end of the Carboniferous but, in the Hastings Block, activity continued into the Permian (Lindsay, 1964, 1969).

The Hastings Block, which is at least 50 km wide in an east–west direction and extends north–south for at least 130 km, is a fault-bounded block of relatively gently deformed sediments. The sediments are structurally isolated and contrast sharply with the much more intensely deformed units exposed on the surrounding blocks (Korsch & Harrington, 1981). Sedimentation probably began in the area during the Devonian and continued until at least early Permian time. Evidence of late Carboniferous shorelines located along both northern (Lindsay, 1964, 1966, 1969) and southern (Voisey, 1950) margins of the Hastings Block indicates that the area was a well defined depositional entity within the confines of the larger forearc basin. It has been referred to by Lindsay (1964, 1969) as the Manning–Macleay Basin.

More than 8230 m of Carboniferous and early Permian sediments were deposited in the Manning–Macleay Basin to form two large-scale depositional successions (Lindsay, 1964, 1969; Lennox & Roberts, 1988). The lower succession is Carboniferous and forms a single shallowing-upward unit, the base of which is not exposed. The oldest exposed sediments of the succession are deep-water, dark, pelagic shales, turbidites and mudflow deposits (Boonanghi Beds) which grade upwards through more massive, immature, volcanic-rich sandstones (Majors Creek Formation) to a shallow-marine clastic rock association (Kullatine and Youdale Formations) (Lindsay, 1966; Bourke, 1971; Northcott, 1973), which is terminated by the Sebastopol Disconformity (Northcott, 1973). The second succession (Fig. 2), which is the focus of this study, is a deepening-upward unit of which the crinoidal Yessabah Limestone is the oldest formation; locally coarse braided-stream conglomerate, sandstone and siltstone (Commong and Mooraback Beds) occur beneath the crinoidal limestone (Lindsay, 1966; Northcott, 1973). Everywhere limestone deposition was followed by the deeper water, mixed turbidite–traction current association of the Warbro Beds. Two other clastic units deposited in similar deeper water settings, the Toorooka and Kempsey Beds, appear to be younger than the Warbro Beds (Lindsay, 1964, 1969). The upper contact of this succession is not exposed because of the structural complexity of the area. The Parrabel Beds, a complex diamictite association in fault contact with the second succession, likewise appear to have a deeper water origin (Lindsay, 1969).

[1] Onshore Sedimentary Geology Program, Bureau of Mineral Resources, GPO Box 378, Canberra, ACT 2601

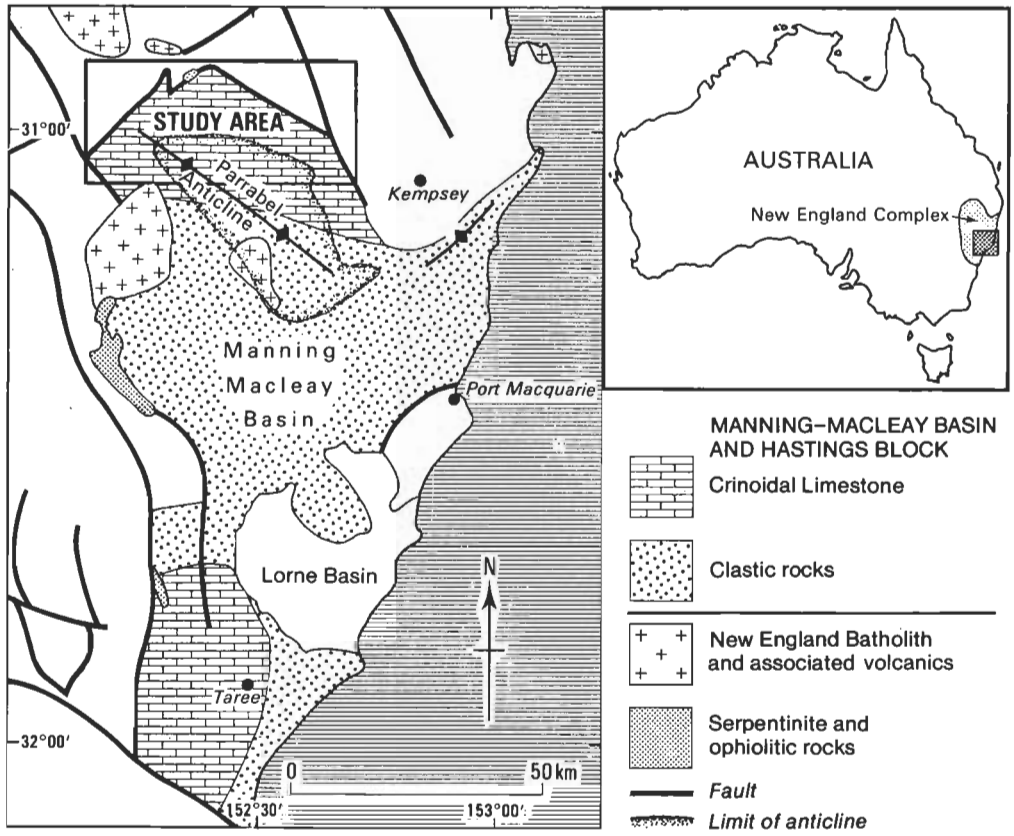

Figure 1. Location map of the Manning–Macleay Basin, showing the study area and the approximate depositional limits of the early Permian crinoidal limestone units. Figures for this paper were drafted by the author.

Yessabah Limestone

Lithology and distribution

The Yessabah Limestone is regarded as earliest Permian in age (Campbell, 1962; Lindsay, 1967; Runnegar, 1979). It has been correlated with the Cedar Party Limestone, also a crinoidal limestone, which is exposed at the southern margin of the basin near Taree (Fig. 1) (Voisey, 1939a,b,c, 1958). In the study area the formation is almost continuously exposed and delineates the broad outline of the Parrabel Anticline (Fig. 3). The outcrop pattern is broken only occasionally by minor faulting. It ranges in thickness from 6 m to 460 m, and is thickest near Taits Creek and Yessabah. The limestone normally rests with sharp contact on the underlying Carboniferous clastic rocks but locally, especially in the Taits Creek area, it rests upon and grades laterally in a very short distance into polymict conglomerate, sandstone and siltstone (Lindsay, 1966, 1969; Northcott, 1973) that are probably braided-stream deposits. In upward succession, the Yessabah Limestone consists of three sedimentary units: (1) a basal calcareous wackestone; (2) a bioclastic crinoidal limestone; (3) a silicified coralline limestone (the Mount Pleasant Limestone Member).

Basal calcareous wackestone

Bright green calcareous wackestones occur at the base of the Yessabah Limestone and form up to 30% of the formation. They are well bedded and may be interbedded with thin units of crinoidal limestone. Where bedding is thin, crinkling or microfolding is often developed. The rocks are very consistent lithologically and consist of a variety of allochems and a little terrigenous material set in an abundant matrix, in association with some authigenic minerals. The unit fluctuates considerably in thickness, reaching a maximum of 75 m at Yessabah whilst locally at Moparrabah and the Taits Creek area it is entirely absent.

Allochems form 30% of the rock, and consist mainly of fragments of bryozoa, crinoids and brachiopods with lesser amounts of molluscan remains and foraminifera of the genus *Plectogyra*. Bryozoan fragments, which are usually fenestrate, are the most common allochems. Brachiopod fragments are usually small; commonly only spines are present. Most of the biogenic fragments provide little evidence of abrasion, and it is common to find articulated brachiopods and lengths of crinoid stem on bedding surfaces.

Terrigenous silt and fine sand form 10% of the rock, quartz forming more than half, the rest being feldspar and lithic fragments. Lithic fragments are mainly rounded fragments of devitrified volcanics, and rarely subangular fragments of mudstone. Over 60% of the rock consists of matrix, which is mainly micrite and finely divided organic material, with a small proportion of clay minerals. Authigenic quartz occurs sporadically throughout, commonly replacing brachiopod spines, micrite, and occasionally the cores of crinoid fragments.

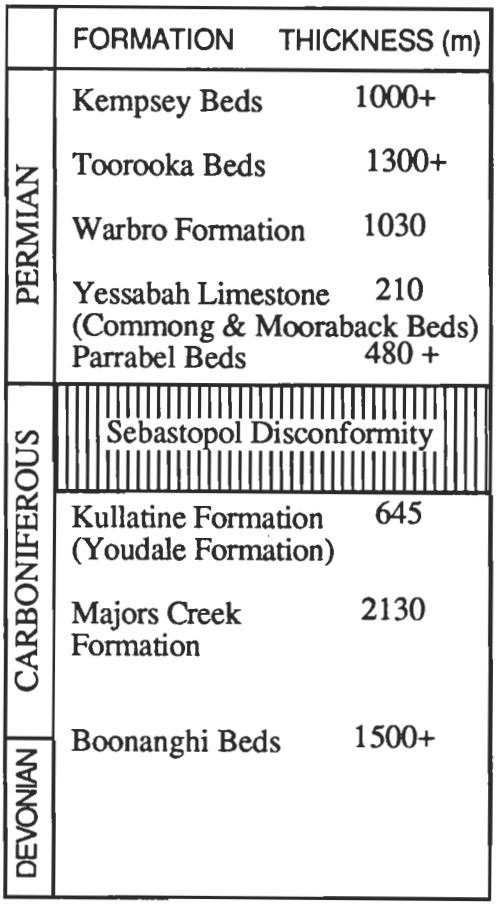

Figure 2. Simplified succession of the northern Manning–Macleay basin.

Crinoidal limestone

The main crinoidal limestone unit of the Yessabah Limestone is the most persistent and continuous of its lithological subdivisions. It is very constant in composition (Fig. 4b) and relatively constant in thickness. It consists of an alternation of two lithologies (Figs 5 and 10a). The first is a well washed (i.e. free of carbonate mud) and well sorted crinoidal grainstone (Fig. 6) that occurs in massive beds which at some localities have poorly developed cross-bed foresets. This alternates with a second lithology, a packstone, which contains a much smaller percentage of crinoidal debris. It is less well sorted than the crinoidal grainstone and contains a high proportion of angular fragments of fenestrate bryozoa (Fig. 7). Towards the base of the formation, the crinoidal sediment alternates with a third lithology, a calcareous wackestone (Fig. 8).

The crinoidal limestone was sampled and measured in two detailed stratigraphic sections: Taits Creek and Temagog Creek (Fig. 3). It consists of allochems, detrital quartz and diagenetic minerals, with a calcite matrix (Fig. 4a). The clastic grains are usually well rounded and well sorted, with an average maximum grain size of 4.9 mm. The allochems are mostly crinoid and bryozoan remains, with subordinate brachiopod, pelecypod and rare coral fragments and ooids. Crinoidal remains are the most abundant, and form 4–60% of the rock (Fig. 5).

Crinoidal material generally occurs as single well rounded fragments, mostly columnals up to 5 mm in diameter, although occasionally several columnals are found joined together, and rare cups have been described (Lindsay, 1967). The crinoid fragments are well sorted and generally free of of carbonate fines so they form a supporting framework.

Bryozoan fragments form up to 60% of the limestone, and are only exceeded in quantity by the crinoidal fragments. As would be expected, the proportions of crinoidal and bryozoan fragments are related in an inverse manner (Fig. 9a). The bryozoan fragments form two concentrations in the Taits Creek section. The lower concentration (57 m above the base of the section) represents a lithology rich in micrite, and the upper peak relates to the *Eurydesma* horizon (Fig. 5a). In the Temagog Creek section, the upper peak and the older of the two *Eurydesma* horizons are not present. The bryozoan fragments are usually highly angular (Fig. 7). The grain size varies with the proportion of bryozoan fragments: the larger the fragments, the higher the percentage. Brachiopod and pelecypod fragments occur in minor quantities, usually associated with the *Eurydesma* horizon, but random peaks with no apparent relationships are found in both sections.

Small numbers of ooids are scattered throughout the limestone. They vary in size from 0.1 to 1.0 mm, and occur mainly in coarse well washed crinoidal sediment. They generally have nuclei of microspar which may be replaced by euhedral dolomite rhombs.

The matrix consists of pseudospar and variable proportions of microspar. Microspar constitutes up to 53% of the matrix, and varies in proportion with the bryozoan fragments (Fig. 9b). Thin sections with a high proportion of crinoid fragments contain rare patches of microspar which is usually associated with localised concentrations of fine bryozoan fragments. Bryozoan fragments are considerably larger and more complete in sections with a high proportion of microspar. As a result the curve for micrite/microspar is similar to the curve of the 5 largest allochems (Fig. 5).

The Mount Pleasant Limestone Member

The Mount Pleasant Limestone Member is a silicified, predominantly coralline, bioclastic packstone, sporadically interbedded with calcareous mudstone and red chert. It lies at the top of the Yessabah Limestone and interfingers with the Warbro Beds (Lindsay, 1964, 1969). It is very variable in thickness and occurs only in the eastern (Yessabah) and northern (Willi Willi) limits of the study area, where it reaches its maximum development of 160 m and 300 m respectively. East and west of Willi Willi, the member grades laterally into cherty, black, laminated mudstones which pass rapidly into the sediments of the Warbro Beds. Thus, in the type section of the Yessabah Limestone, the Mount Pleasant Limestone is represented by these cherty black mudstone. At Yessabah the Mount Pleasant Limestone is well developed, but again interfingers rapidly along strike with normal Warbro Formation rocks.

The silicified limestone occurs in beds 1–2 m thick and consists mainly of interlocking fragments of coral, with subordinate amounts of crinoid, bryozoan, brachiopod

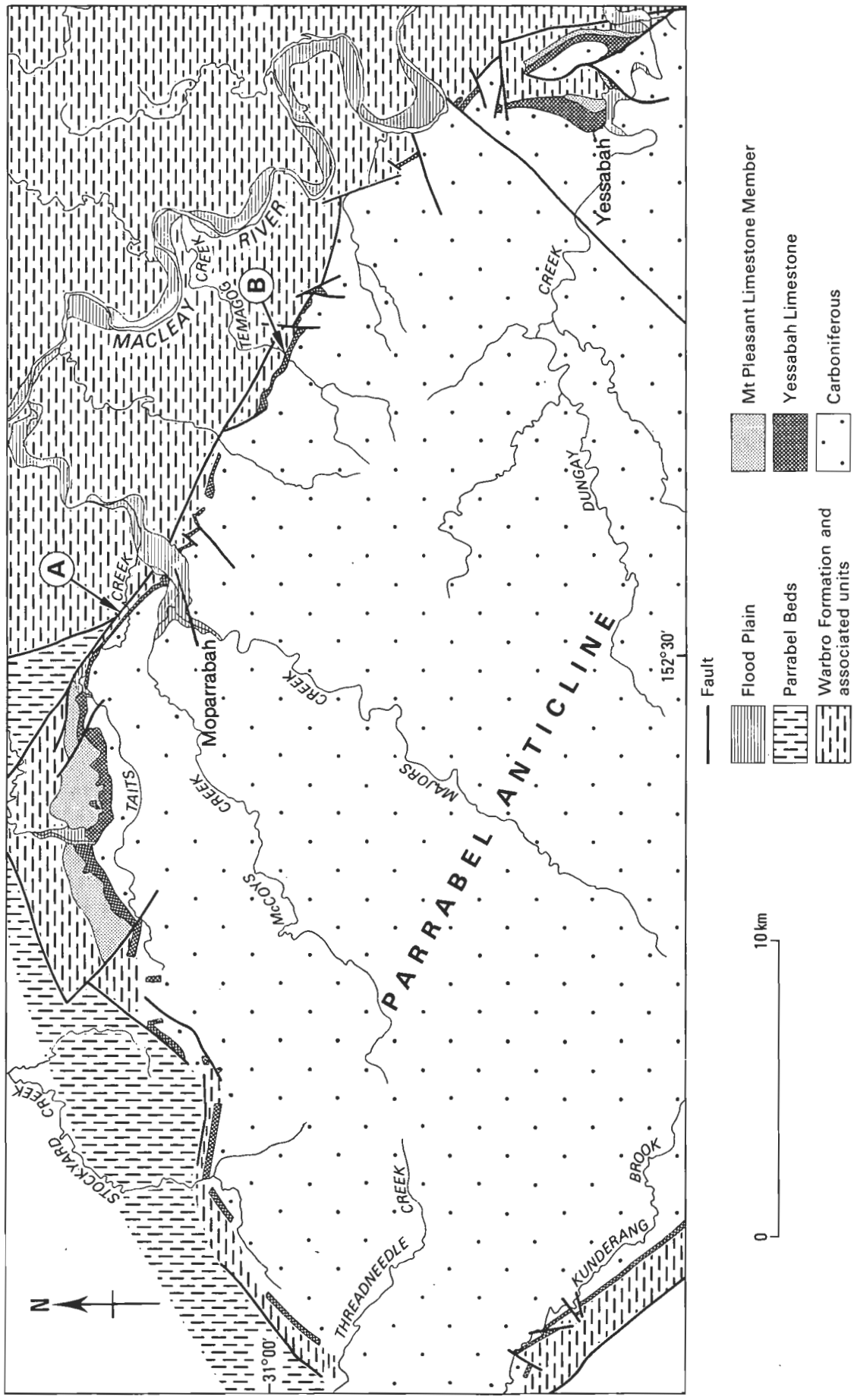

Figure 3. Map of the study area showing the distribution of the Yessabah Limestone and related units.
Locations of the detailed sections shown in Figure 5 are shown as (A) Taits Creek and (B) Temagog Creek.

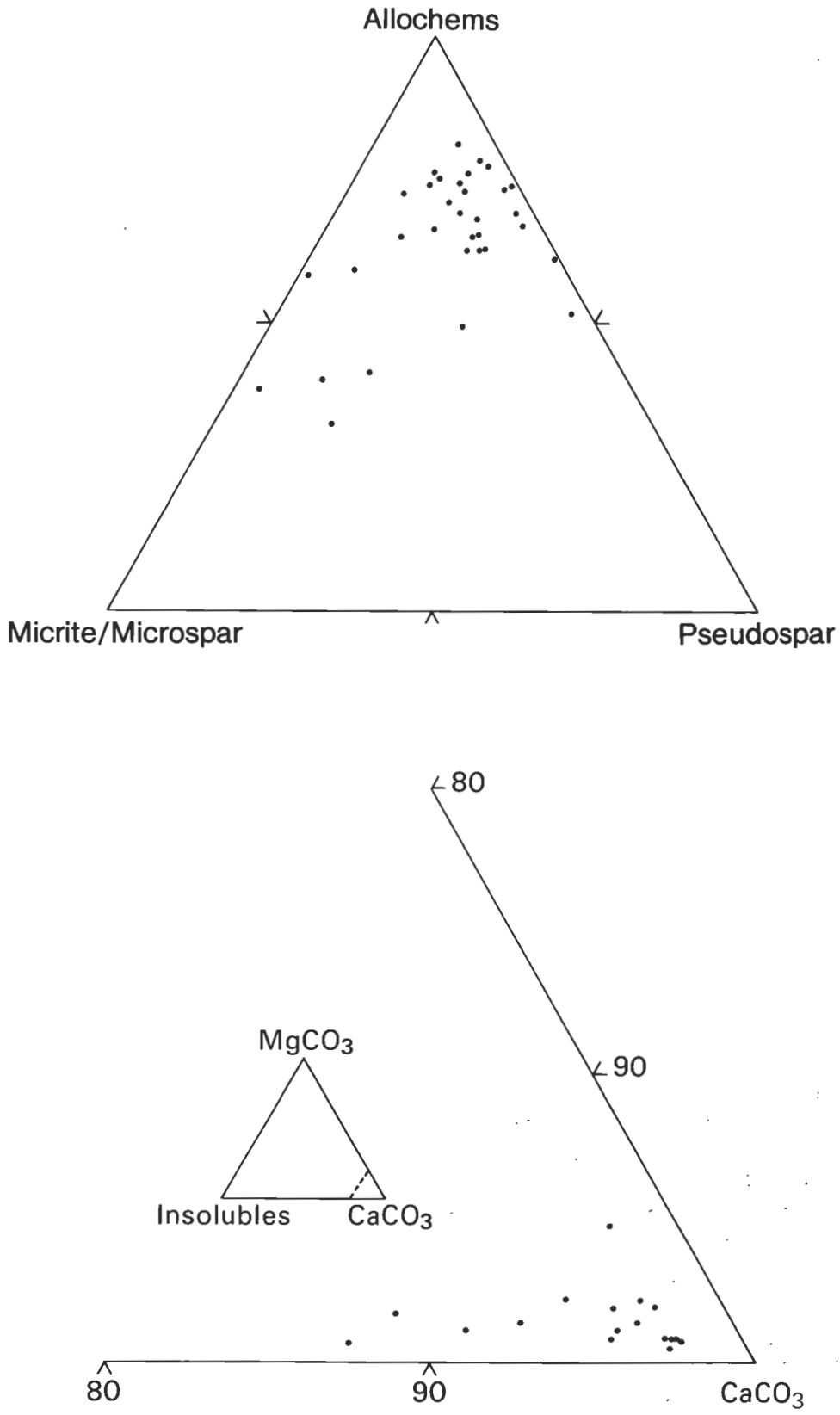

Figure 4. Ternary diagrams showing (upper) textural composition and (lower) chemical composition of the Yessabah Limestone.

and pelecypod fragments. Coralline fragments are usually completely replaced by silica, and appear as ghost outlines. The coral fragments are mostly of *Cladochonous* and show up more clearly in weathered hand specimens. Crinoidal fragments are subordinate to coralline fragments but occur in greater proportions towards the top of the formation. They are angular, seldom broken, and reach 3 mm in diameter.

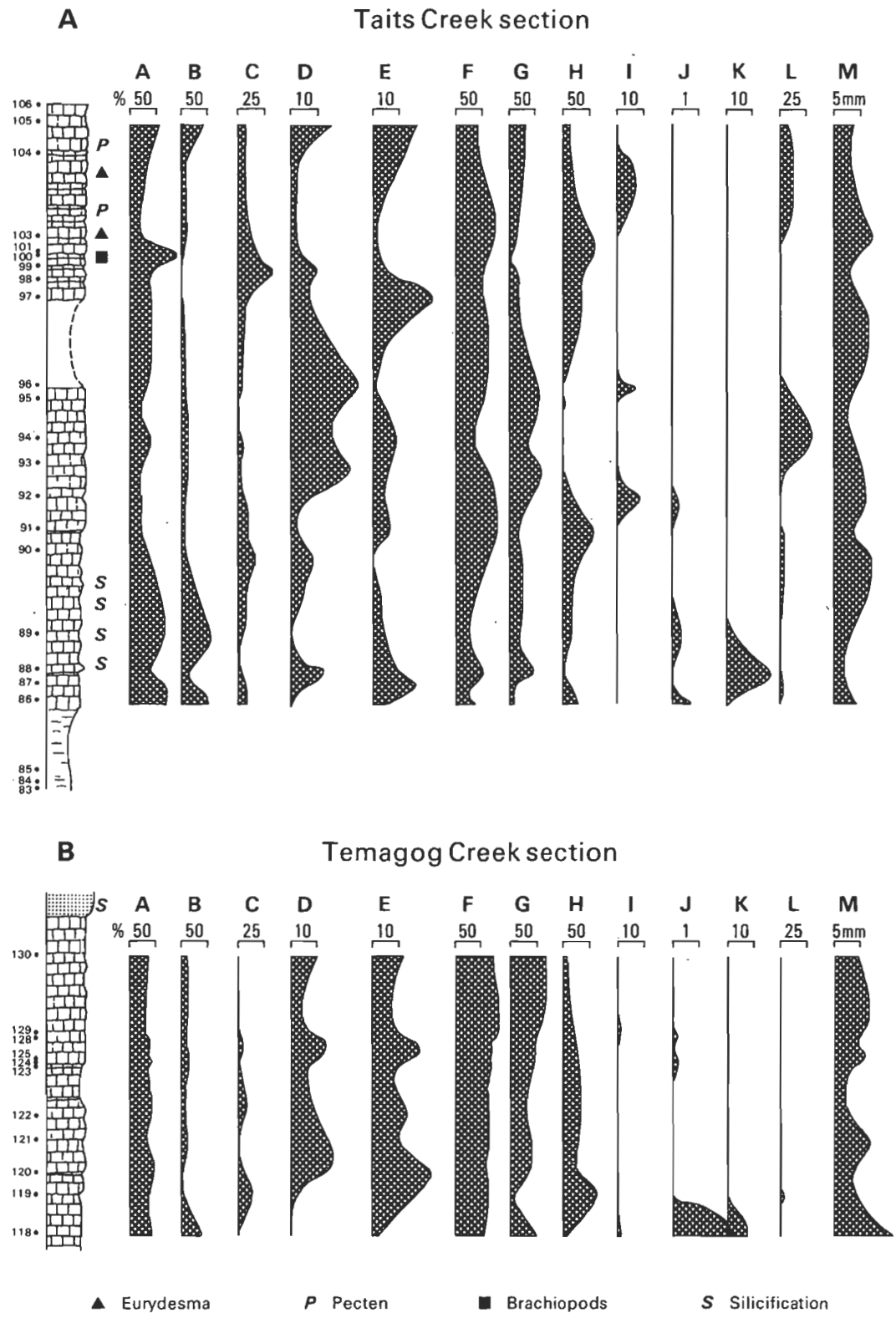

Figure 5. Composition of the Yessabah Limestone at (A) Taits Creek and (B) Temagog Creek.
The locations of the sections are shown on Figure 3.
A total matrix, B micrite/microspar, C pseudospar, D rim cement, E recrystallised calcite, F total allochems, G crinoids, H bryozoa, I brachiopods and pelecypods, J detrital quartz, K secondary quartz, L dolomite, M average of five largest allochems. Sample numbers and locations are shown to the left of the lithologic columns. Except for the mean of the five largest allochems, which is shown as mm, all variables are expressed as percentages.

Wackestone occurs in thin beds 5–15 cm thick interbedded with the silicified grainstone. In hand speci-

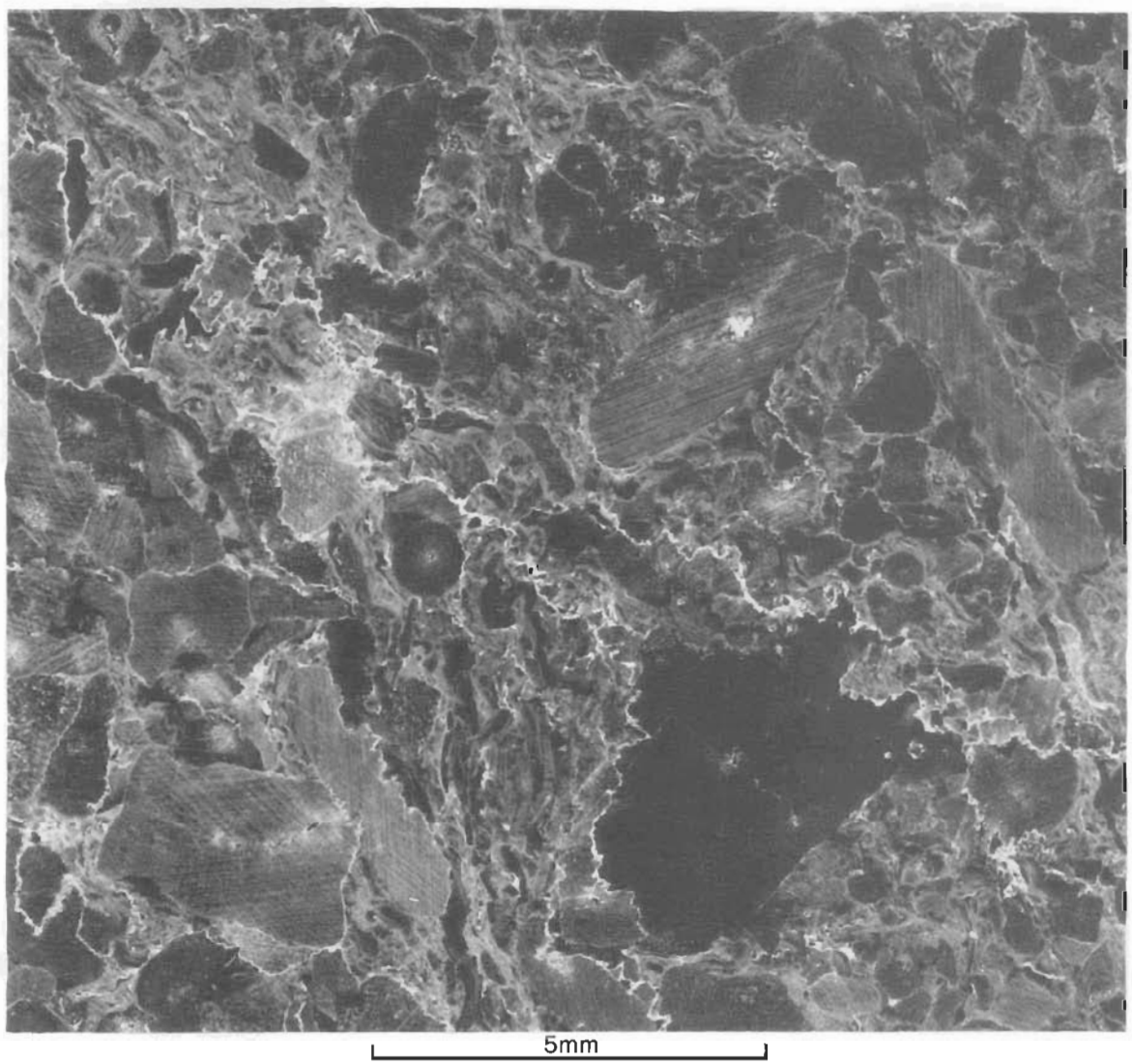

Figure 6. Typical thin section of a crinoidal grainstone from the main crinoidal limestone unit of the Yessabah Limestone.

men it is pale green or purple, the pale green wackestone commonly containing angular fragments of the red mudstone and some detrital quartz.

Allochems in the wackestone consist of spongy spicules, brachiopod spines, and finely divided fragments of brachiopods, bryozoan and pelecypods. Many of the fragments are replaced in part by silica. Detrital quartz forms less than 10% of the rock, and occurs as angular fragments with a maximum grain size of 0.1 mm. The thin wackestone interbeds are commonly finely laminated and may contain well preserved fossils. The bioclastic material shows almost no evidence of transport; large articulated crinoid stems are preserved along with articulated brachiopod valves, and occasionally both valves of a pectinid are found together. Where the latter are found with one valve in the plane of the bedding and the second normal to it, the valve in the bedding plane is flattened and the length of the valve normal to the bedding is reduced by 50 per cent. Small-scale crinkles occur in the calcareous mudstone in the lower parts of the formation. Some beds contained angular contorted chips of red mudstone in a green mudstone matrix. Beds of red chert are relatively rare and usually occur towards the top of the formation.

Associated formations

Warbro Formation

The Warbro Formation either conformably overlies the main crinoidal limestone unit of the Yessabah Limestone, or locally interfingers with, or grades laterally into, the Mount Pleasant Limestone Member (Lindsay, 1969). The unit consists largely of grey or black mudstone with interbedded grey lithic sandstone. The sandstone forms about 25% of the formation and occurs in thin beds up to 10 cm thick, separated from each other by 2–25 cm of mudstone. Some beds are graded; their lower contacts are sharp and their upper contacts are usually gradational. The sandstone beds appear to form the upper stages of a Bouma sequence and are probably turbidites. Unfortunately the upper contact of this formation is faulted. Two other units, the Toorooka

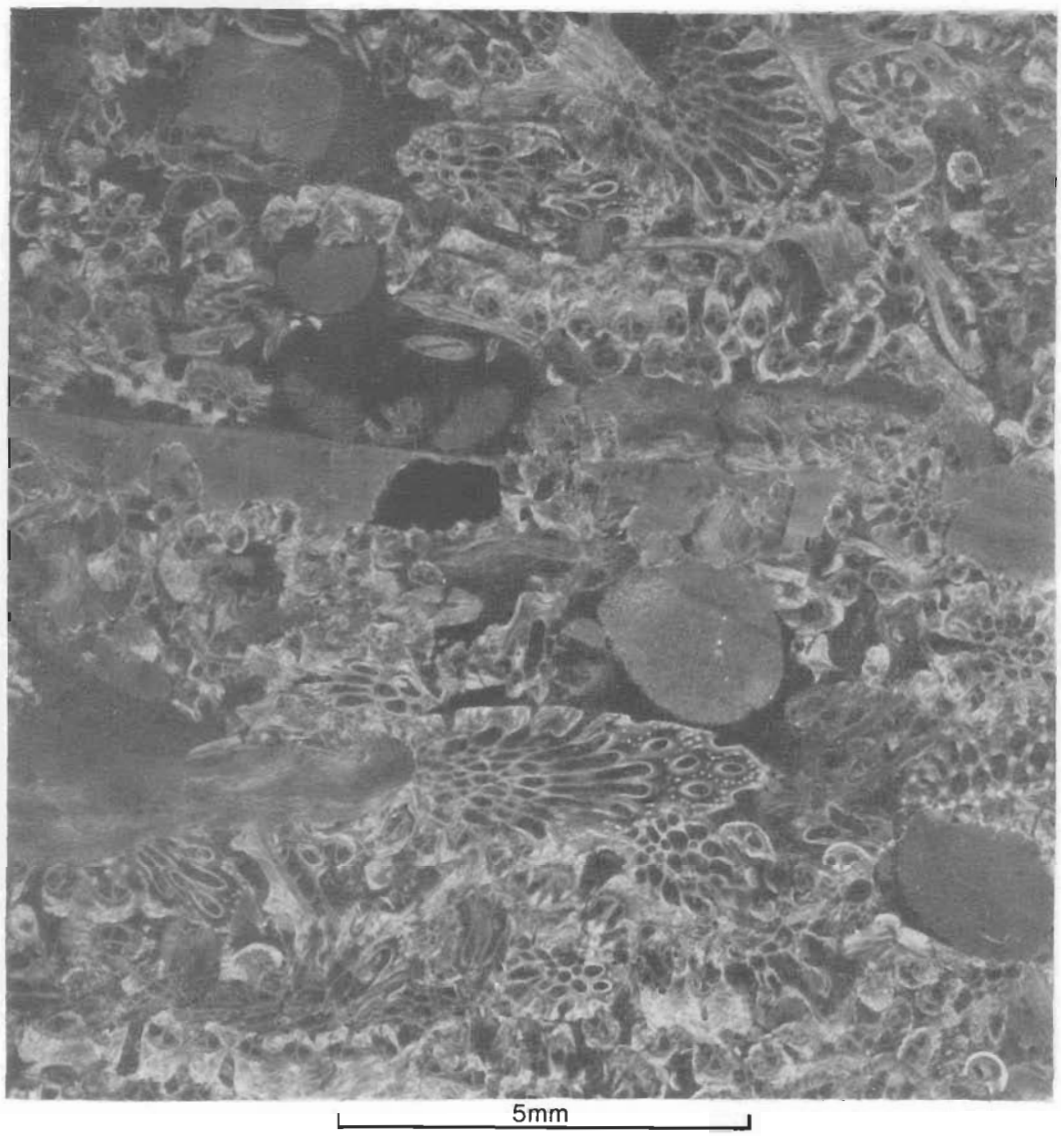

Figure 7. Thin section of a bryozoan-rich grainstone.

and Kempsey Beds, occur in isolated fault-bounded blocks adjacent to the Warbro Formation. Both consist of sedimentary rocks with similar facies associations, and all are probably genetically related.

Parrabel Beds

The Parrabel Beds consist of interbedded mudstone, diamictite and lithic sandstone containing a Lower Permian marine fauna (Lindsay, 1969; Bourke, 1971; Kinney & others, 1985). The relationship of the Parrabel Beds to the Warbro Beds and the Yessabah Limestone is unclear, as the unit is only exposed in a series of fault blocks along the northern margin of the study area. Originally Lindsay (1969) suggested that the unit overlies the Warbro Formation. As discussed below, it now seems more likely that it is somewhat younger and perhaps related to the Yessabah Limestone.

Diamictites are the most distinctive lithology of the Parrabel Beds. The beds are from 25 cm to more than 60 m thick, and generally consist of 90% matrix with uniformly dispersed clasts. Clasts are typically 2–5 cm in diameter, although locally they may be as large as 50 cm (Lindsay, 1969; Kinney & others, 1985). The composition of the clasts is varied, and includes silicic volcanics, sedimentary rock fragments and rarely granites. The matrix is black or green mudstone or a medium-grained bluish green lithic sandstone. Mudstone is the most common lithology (40%) of the Parrabel Beds. It is either blue-green, hard and cherty, or olive-green, soft and calcareous. Beds of lithic sandstone from 2.5 cm to 1.5 m thick occur interbedded with the mudstones and diamictites. The Parrabel Beds contain a calcareous unit, the Eastern Branch Member (Kinney & others, 1985), which is important in understanding the relationship of the formation to the Yessabah Limestone. The unit, which is well bedded and about 140 m thick, consists of siliciclastic siltstone interbedded with black calcareous siltstone, sandstone and limestone. The individual sandstone and limestone units are graded. Kinney & others (1985) suggest that it is a redeposited equivalent of the Yessabah Limestone.

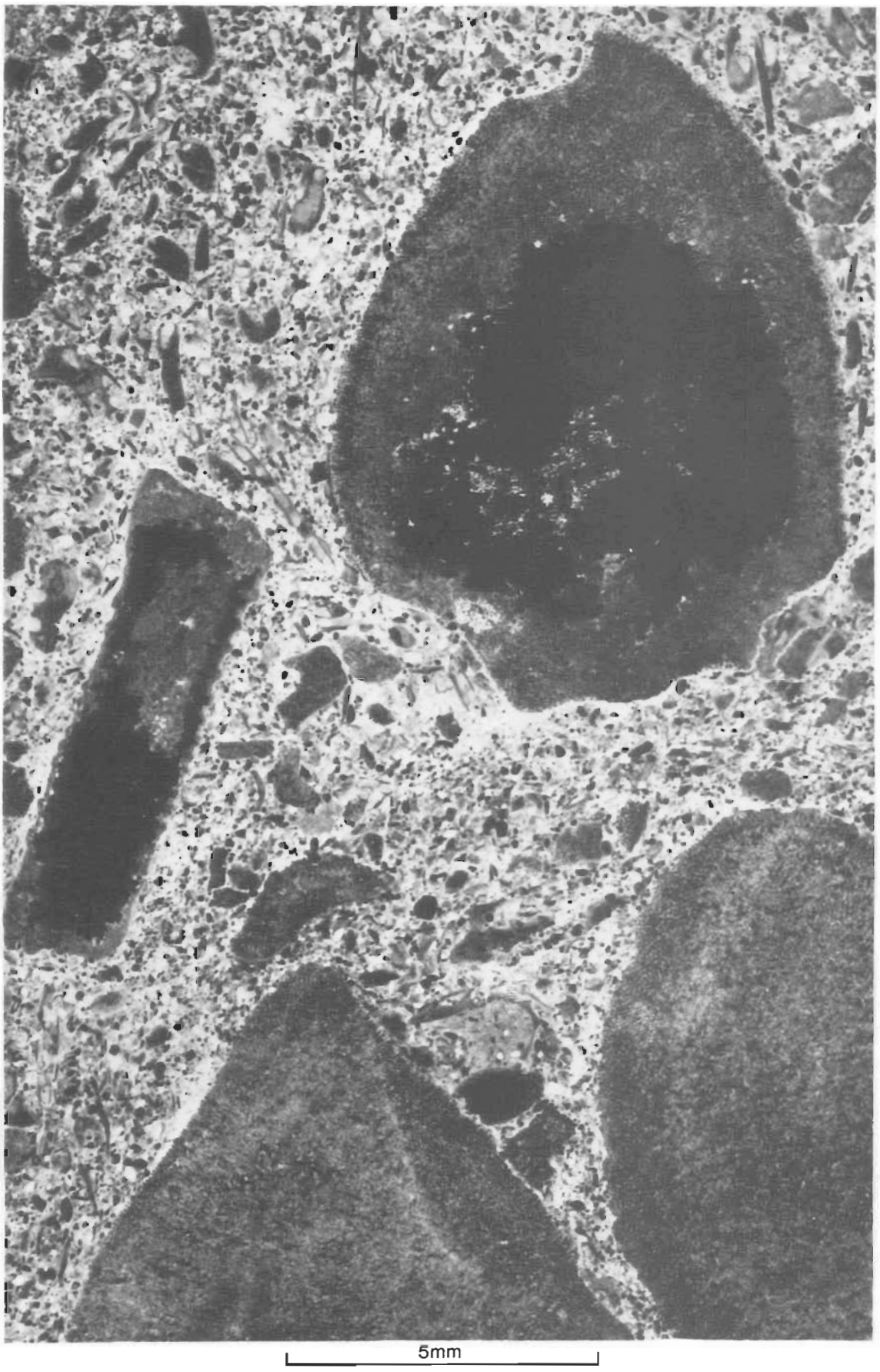

Figure 8. Thin section of a crinoidal wackestone containing exceptionally large crinoid fragments with cores replaced by silica.

Environmental interpretation

The detailed petrography of the Yessabah Limestone and associated units suggests that deposition occurred in an environment in which the water was gradually deepening with time. As the water depth increased, the composition and faunal associations of the resulting sediments evolved. The formation gradationally overlies braided-stream deposits, which suggests that the whole unit is transgressive.

The basal wackestone is usually thinly laminated and contains a very high percentage of micrite/microspar. The occurrence of articulated invertebrate remains is further evidence of feeble current activity. The unit is generally poorly exposed, and there are few sedimentary structures to help elucidate its origins, but it appears to have been deposited in a relatively shallow marine setting on a gently sloping carbonate ramp.

The transition from the basal wackestone to the main crinoidal limestone is gradational. The crinoidal limestone unit is very different from the basal unit. Lower in the formation, the crinoidal sediment alternates with variably laminated wackestone. The crinoidal grainstone appears to be the result of considerable reworking, winnowing and redistribution of the original material by comparatively strong currents, whereas the bryozoan packstones were deposited in a less energetic setting. Blyth Cain (1968) found that winnowing of crinoidal debris was a slow process and that to produce well sorted and 'clean-washed' crinoidal limestones would require prolonged reworking that would result in considerable abrasion of the crinoid particles, observations which are consistent with the texture of the massive, well washed, crinoidal grainstone units in the Yessabah Limestone.

The alternation of well washed crinoidal units with the less well sorted bryozoan-rich units might at first be attributed to variations in current velocity. However, it is more likely a response to the cyclical development of the benthic biota. Carozzi & Soderman (1962) have pointed out that colonisation of the sea floor by crinoids requires an undisturbed substrate. Once established, the dense growth of the crinoids screens out clastic sediments carried either by traction or in suspension. Ultimately, the crinoid association reaches a climax and collapses, allowing the recolonisation of the site by bryozoa, which again stabilise the substrate and prevent reworking of the fines by current activity. The cycle then begins again as crinoid larvae recolonise the stabilised substrate. The presence of ooids and the well sorted highly rounded nature of the crinoidal sediments suggests that the water at the time of deposition was relatively shallow, probably close to wave base, and that current activity was high. Variations in thickness of the main limestone unit associated with what appear to be large foresets indicate an initial seafloor relief of approximately 60 m, suggesting that these cross-bedded units were deposited as crinoidal banks.

The sediments of the Mount Pleasant Limestone Member reflect a much quieter environment than either of the two units discussed previously. The sediments consist either of massive coralline remains or of micrite with dispersed bioclastic material. The bioclastic material shows almost no evidence of transport; some bivalves are still articulated. The calcareous muds are often finely laminated, suggesting that current activity was minimal.

It appears that the currents active during the deposition of the Mount Pleasant Limestone Member were very weak. The currents appear to have been even weaker laterally from the limestone member, suggesting that the Mount Pleasant Limestone Member may have developed as a series of reef-like mounds. This is supported by the large thickness of the member where it is developed and the rapid rate at which it grades laterally into the black laminated muds. The black mudstones suggest that at least locally the reef mound provided an effective barrier to circulation, creating restricted marine environments shoreward from them.

The carbonates of the Yessabah Limestone were modified considerably by diagenesis in several stages (Lindsay, 1964). The main components of diagenesis were (a) compaction, (b) cementation and recrystallisation, (c) dolomitisation and (d) silicification (Fig. 5). Compaction began during deposition and was followed by cementation and recrystallisation. The movement of fluids resulted in the formation of stylolites leading to redistribution of calcite, dolomitisation and finally selective silicification.

Warbro Formation

The sedimentary rocks of the Warbro Beds form a typical distal turbidite association. The transition to this environment was gradational but over a relatively small interval. The gradually deepening water appears to have ultimately been unsuited to crinoids and eventually most other life forms. As the screening effect of the crinoids was reduced, clastic sediments were able to travel further and further basinward as weak turbidity flows. Locally these flows were diverted around the reef-like mounds of coralline debris.

Sequence model

Sequence stratigraphy has dramatically changed the way in which sedimentary basins are analysed (Sloss, 1988) by providing a way of subdividing an apparently complex sedimentary succession into packages (sequences) that correspond to chronostratigraphically-constrained, genetic depositional intervals (Vail & others, 1977a,b, 1984; Vail, 1987). Within one sequence, sediments can be related to a specific set of depositional processes that operated within well constrained time limits. The sediments contained within a sequence thus have predictable lithofacies associations and stratal patterns. Structural complexities make a regional environmental interpretation of the Yessabah Limestone and associated units difficult. However, when viewed in a sequence framework a reasonable model can be constructed from the surviving disparate elements.

The Yessabah Limestone rests on the Sebastopol Disconformity. The change in lithofacies across this boundary from Carboniferous to Permian rocks is abrupt. Korsch & Harrington (1981) and Harrington & Korsch (1985) attributed the disconformity to gentle tectonic uplift. However, the disconformity appears at both ends of the basin where the Late Carboniferous sedimentary rocks were deposited, in an environment that was rapidly shallowing upward. This suggests that we are looking at a depositional sequence boundary relating

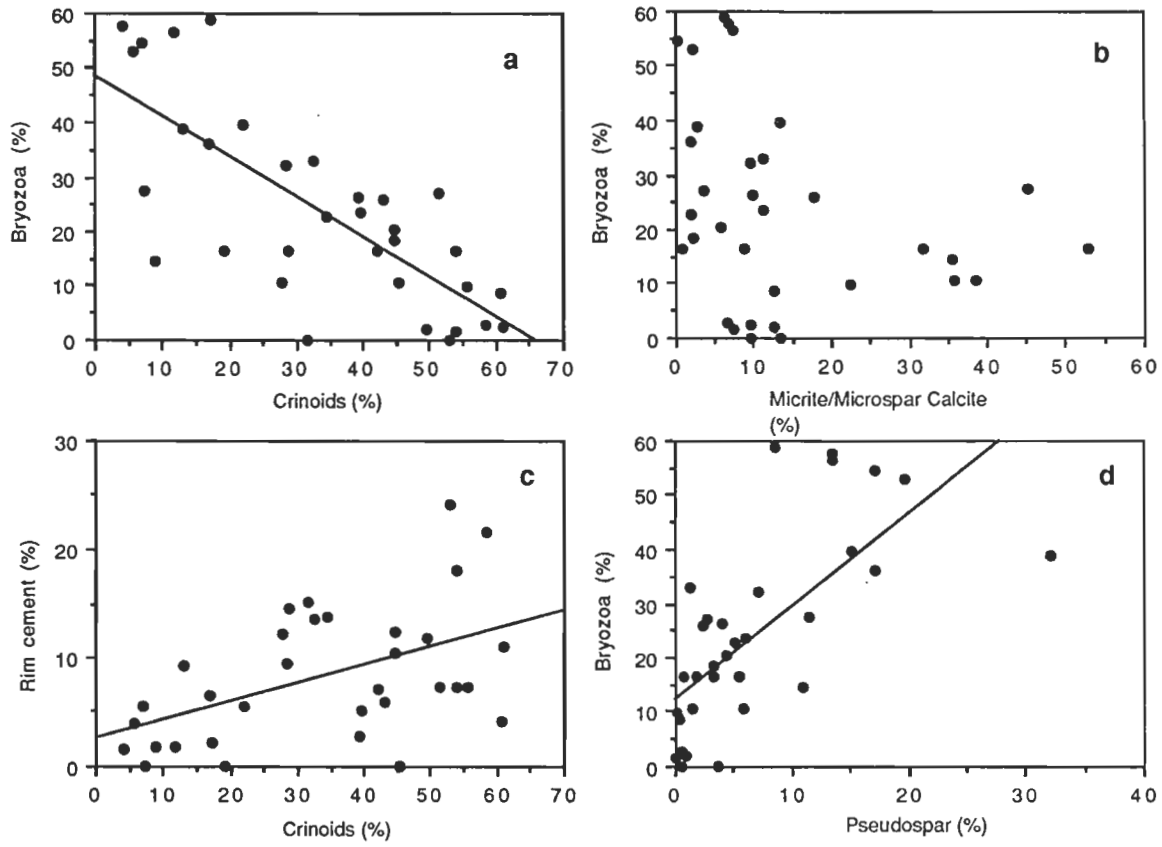

Figure 9. Relationship between major components of the Yessabah Limestone.
Straight lines are least-squares best fits.

to a major sea-level change rather than the results of a local tectonic event. Vail & others (1977b) suggested that there was a major fall in eustatic sea level towards the end of the Carboniferous, which is supported by data from the Australian continent (Roberts, 1983). The sediments above the boundary, including the Yessabah Limestone, appear to form part of a deepening-upward sequence. The earliest Permian sediments in the Manning–Macleay Basin were probably deposited during a major sea-level cycle which began with a fall in sea level at the end of the Carboniferous followed by a sea-level rise that continued into the earliest Permian.

Analysis of the late Palaeozoic forearc basin suggests initial rapid subsidence followed by equally rapid sedimentation into a basin with a pronounced shelf break (Lindsay, 1990). Spatial relationships among Carboniferous facies support this general picture. A major sea-level fall would thus result in the development of what van Wagoner & others (1987) define as a type-1 sequence boundary. In such a setting, the regional surface (lower sequence boundary) would be characterised by subareal exposure with subsequent erosion associated with stream rejuvenation and a basinward shift of facies. Because of the basinward shift, shallow marine or non-marine facies will directly overlie much deeper water rocks deposited as part of the previous sequence. Because subsidence was rapid, the ensuing rise of relative sea level should be considerably more dramatic than normal.

This framework has been applied to the apparently disparate elements of the Yessabah Limestone and associated formations to produce a coherent sequence and hence facies model (Fig. 10) . The Yessabah Limestone forms the transgressive systems tract on the shelf, marginal to the basin. Slightly earlier than the Yessabah Limestone, the lowstand systems tract containing the Parrabel Beds was deposited in the deep basin; the beds are mostly either pelagic mudstone or sedimentary rock deposited from mass movement. Further upslope from the Parrabel Beds, but still part of the lowstand systems tract, are the coarse braided-stream gravels (Mooraback and Commong Beds of Northcott, 1973) that occur beneath the Yessabah Limestone. These conglomerates formed as a result of the basinward shift of facies as sea level fell. Above the crinoidal limestone are the deeper water sediments of the Warbro Beds and the reef-like mounds of the Mount Pleasant Limestone Member. These were deposited as part of the transgressive systems tract as sea level continued to rise rapidly and deeper water sedimentation became the norm.

The depositional succession of sedimentation is as follows:

1. Sea-level fall. Large areas of the basin margin were exposed above sea level, resulting in rejuvenation of streams and the deposition of braided-stream gravels close to the new shoreline. The increased erosion onshore resulted in the offshore development of a major prograding lowstand systems tract preserved as the poorly known Parrabel Beds (Lindsay, 1964, 1969; Kinney & others, 1985). The lower part of this unit may well contain the remains of a fan system — certainly there is evidence of major mass movement. Similarly, canyons may have formed along the basin margin. Upward in the Parrabel Beds the abundance of diamictite

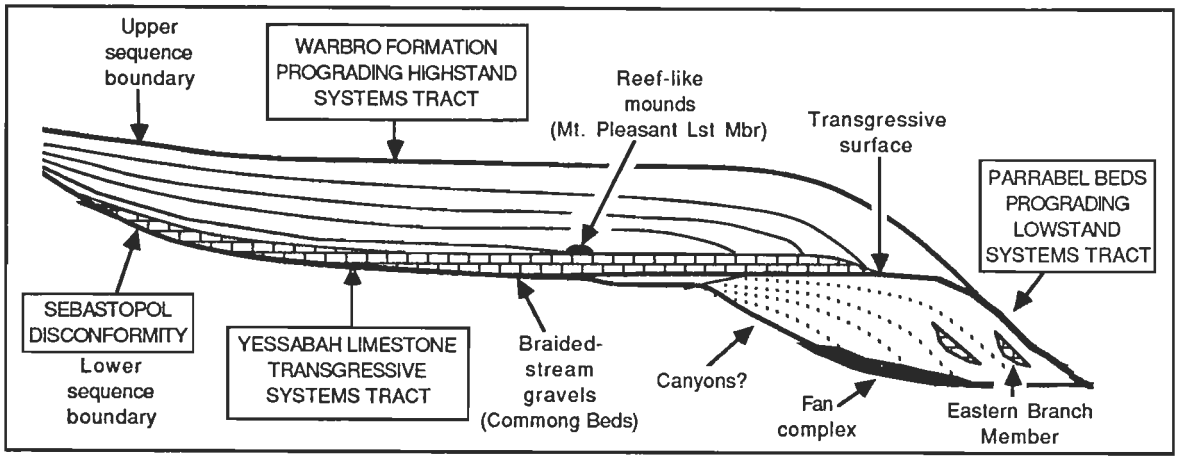

Figure 10. Schematic depositional sequence showing the relationship between the Yessabah Limestone and associated units.

should decrease in the lowstand wedge and prograding mudstones or shales should predominate. (Unfortunately, it was not possible to ascertain these relationships in the field.) As relative sea level reached the lowstand, conditions along the basin margin would have been stable for a period, allowing the growth of crinoids in the shallow water. The remains of these crinoids were carried into the deeper basin by turbidity currents to become part of the lowstand systems tract (Eastern Branch Member of the Parrabel Beds).

2. Sea-level rise. As sea level began to rise, the Yessabah Limestone was deposited as a transgressive system tract over the Parrabel Beds and the braided-stream gravels of the lowstand systems tract. The transgression thus resulted in the shallow marine carbonates of the Yessabah Limestone being deposited in conformity with shallow marine Carboniferous rocks in the north and deeper water Carboniferous turbidites in the south. As sea level continued to rise, its effects exaggerated by rapid basin subsidence, the deeper water sediments of the Warbro Formation were deposited as a highstand systems tract which prograded out over the Yessabah Limestone. Because the water was deepening rapidly the highstand systems tract is dominated by pelagic shales and distal turbidites. Locally, close to the shelf break, carbonate sedimentation persisted somewhat longer as reef-like structures dominated by corals developed, at times restricting circulation and producing anoxic conditions in adjacent clastic units.

Conclusions

The Yessabah Limestone is a transgressive unit deposited in a shallow water, high energy environment. The sea bed was dominated by prolific growths of crinoids and bryozoa. These generated large volumes of bioclastic material which were at times extensively reworked and accumulated as crinoidal banks. The crinoidal and associated units form integral parts of a single sequence deposited during a major sea-level cycle that began at the end of the Carboniferous and extended into earliest Permian. Initially, sea level fell rapidly, producing a major basinward shift of facies that resulted in the deposition of coarse braided-stream gravels onshore and the Parrabel Beds, as part of the lowstand systems tract offshore in the deep basin. As sea level again began to rise, the Yessabah Limestone was deposited over the transgressive surface as part of the transgressive systems tract. Sea level continued to rise, resulting in the deposition of the Mount Pleasant Limestone Member and the Warbro Formation as part of the highstand systems tract, which then prograded out over the crinoidal sediments of the Yessabah Limestone.

Acknowledgements

I wish to thank H.J. Harrington and R.J. Korsch for discussions on the regional geology and D. Feary, J. Kennard, B. McKelvey and I. Penn for reviewing the manuscript.

References

Bathurst, R.G.C., 1958 — Diagenetic fabric in some British Dinantian limestones. *Liverpool and Manchester Geological Journal*, 2, 11–36.

Bathurst, R.G.C., 1975 — Carbonate sediments and their diagenesis. Developments in Sedimentology No. 12. *Elsevier, New York*, 178–209, 517–543.

Blyth Cain, J.D., 1968 — Aspects of the depositional environment and palaeoecology of crinoidal limestones. *Scottish Journal of Geology*, 4, 191–208.

Bourke, D.J., 1971 — The structural and stratigraphic study of the Upper Kunderang Brook District. *B.Sc Honours thesis, University of New England, Armidale, New South Wales.*

Campbell, K.S.W., 1962 — Marine fossils from the Carboniferous glacial rocks of New South Wales. *Journal of Paleontology*, 36, 38–52.

Carne, J.E. & Jones, L.J., 1919 — The limestone deposits of New South Wales. *Mineral Resources of New South Wales*, no. 25.

Carozzi, A.V. & Soderman, J.G.W., 1962 — Petrography of Mississippian (Borden) crinoidal limestones at Stobo, Indiana. *Journal of Sedimentary Petrology*, 32, 397–414.

Cawood, P.A., 1976 — Cambro-Ordovician strata, northern New South Wales. *Search*, 7, 317–318.

Cawood, P.A., 1980 — The geological development of the New England Fold Belt in the Woolomin–Nemingha and Wisemans Arm regions. The evolution of the Palaeozoic fore-arc terrain. *Ph.D. thesis, University of Sydney*, 429 pp.

Cawood, P.A., 1982a — Tectonic reconstruction of the New England Fold belt in the early Permian: an example of development at an oblique-slip margin. *In* Flood, P.G. & Runnegar, B., New England geology. *Voisey Symposium*

Volume: Armidale, Australia. University of New England, New South Wales, 25–34.

Cawood, P.A., 1982b — Structural relations in the subduction complex of the Paleozoic New England Fold Belt, eastern Australia. *Journal of Geology*, 90, 381–392.

Harrington, H.J. & Korsch, R.J., 1985 — Tectonic model for the Devonian to middle Permian of the New England Orogen. *Australian Journal of Earth Sciences*, 32, 163–179.

Kinney, P.D., Leitch, E.C. & Vallance, T.G., 1985 — Thermal metamorphism near Willi Willi, New South Wales. *Australian Journal of Earth Sciences*, 32, 333–342.

Korsch, R.J. & Harrington, H.J., 1981 — Stratigraphic and structural synthesis of the New England Orogen. *Journal of the Geological Society of Australia*, 28, 205–226.

Leitch, E.C., 1975 — Plate tectonic history of the Palaeozoic history of the New England Fold Belt. *Bulletin of the Geological Society of America*, 86, 141–144.

Lennox, P.G. & Roberts, J., 1988 — The Hastings Block — a key to the tectonic development of the New England Orogen. *In* Kleeman, J.D., New England Orogen — tectonics and metallogenesis. Symposium proceedings. *University of New England, Armidale, New South Wales*, 68–77.

Lindsay, J.F., 1961 — The stratigraphy, sedimentation and palaeontology of a Permian and Carboniferous sequence at Willi Willi, near Kempsey, N.S.W. *B.Sc. Honours thesis, University of New England, Armidale, New South Wales*, 100 pp.

Lindsay, J.F., 1964 — Permian and Carboniferous sedimentation of the Macleay district, N.S.W. *M.Sc. thesis, University of New England, Armidale, New South Wales*, 300 pp.

Lindsay, J.F., 1966 — Carboniferous subaqueous mass-movement in the Manning–Macleay Basin, Kempsey, New South Wales. *Journal of Sedimentary Petrology*, 36, 719–732.

Lindsay, J.F., 1967 — A blastoid from the Lower Permian of the Manning–Macleay Basin, New South Wales. *Australian Journal of Science*, 29, 223.

Lindsay, J.F., 1969 — Stratigraphy and structure of the Palaeozoic sediments of the lower Macleay region, northeastern New South Wales. *Journal & Proceedings of the Royal Society of New South Wales*, 102, 41–55.

Lindsay, J.F., 1990 — Fore-arc basin dynamics and sedimentation controls, Tamworth Trough, eastern Australia. *BMR Journal of Australian Geology & Geophysics*, 11, 521–528.

Lucia, F.J., 1962 — Diagenesis of crinoidal sediments. *Journal of Sedimentary Petrology*, 32, 848–865.

Marsden, M.A.H., 1972 — The Devonian history of northeastern Australia. *Journal of the Geological Society of Australia*, 19, 124–162.

Moore, R.C., 1957 — Mississippian carbonate deposits of the Ozark region. *Society of Economic Palaeontologists, Mineralogists, Special Publication* no. 5, 101–111.

Northcott, I.W., 1973 — Biostratigraphy of the Carboniferous–Permian succession of the Parrabel Anticline, west of Kempsey, northern New South Wales. *B.Sc. Honours thesis, University of New England, Armidale, New South Wales*, 81 pp.

Orme, G.R. & Brown, W.W.M., 1963 — Diagenetic fabric in the Avonian limestones of Derbyshire and North Wales. *Proceedings of the Yorkshire Geological Society*, 34, 51–66.

Roberts, J., 1983 — Carboniferous sealevel changes derived from depositional patterns in Australia. *Compte Rendu*, 4, 43–64.

Runnegar, B, 1979 — Ecology of *Eurydesma* and the *Eurydesma* fauna, Permian of eastern Australia. *Alcheringa*, 3, 261–285.

Skupin, K, 1973 — Stratigraphy and microfacies in the crinoidal limestones (Trochiten Limestone, Triassic) of southwest Germany. *Sedimentary Geology*, 9, 1–19.

Sloss, L.L., 1988 — Forty years of sequence stratigraphy. *Geological Society of America, Bulletin*, 100, 1661–1665.

Stauffer, K.W., 1962 — Quantitative petrographic study of Paleozoic carbonate rocks, Caballo Mountains, New York. *Journal of Sedimentary Petrology*, 32, 357–396.

Swarzacher, W., 1963 — Orientation of crinoids by current action. *Journal of Sedimentary Petrology*, 33, 580–586.

Vail, P.R., 1987 — Seismic stratigraphy interpretation using sequence stratigraphy. Part 1: Seismic stratigraphy interpretation procedure. *In* Bally, A.W. (editor), Atlas of seismic stratigraphy. *American Association of Petroleum Geologists Studies in Geology* no. 27, 1, 1–10.

Vail, P.R., Hardenbol, J. & Todd, R.G., 1984 — Jurassic unconformities, chronostratigraphy, and sea-level changes from seismic stratigraphy and biostratigraphy. *In* Schlee, J.S. (editor), Interregional unconformities and hydrocarbon accumulations. *American Association of Petroleum Geologists Memoir* 36, 63–81.

Vail, P.R., Mitchum, R.M. jr. & Thompson, S., 1977a — Seismic stratigraphy and global changes of sea level. Part 3: Relative changes of sealevel from coastal onlap. *In* Payton, C.E. (editor), Seismic stratigraphy — applications to hydrocarbon exploration. *American Association of Petroleum Geologists Memoir* 26, 63–81.

Vail, P.R., Mitchum, R.M. jr. & Thompson, S., 1977b — Seismic stratigraphy and global changes of sea level. Part 4: Global cycles of relative changes of sea level. *In* Payton, C.E., Seismic stratigraphy — applications to hydrocarbon exploration. *American Association of Petroleum Geologists, Memoir* 26, 83–97.

van Wagoner, J.C., Mitchum, R.M., Posamentier, H.W. & Vail, P.R., 1987 — Seismic stratigraphy interpretation using sequence stratigraphy. Part 2: Key definitions of sequence stratigraphy. *In* Bally, A.W. (editor), Atlas of seismic stratigraphy. *American Association of Petroleum Geologists, Studies in Geology* no. 27, 1, 11–14.

Voisey, A.H., 1934 — A preliminary account of the geology of the middle north coast district of New South Wales. *Linnean Society of New South Wales, Proceedings*, 59, 334–347.

Voisey, A.H., 1936 — The Upper Palaeozoic rocks around Yessabah, near Kempsey, New South Wales. *Journal and Proceedings of the Royal Society of New South Wales*, 70, 183–204.

Voisey, A.H., 1938 — The Upper Palaeozoic rocks in the neighbourhood of Taree, New South Wales. *Linnean Society of New South Wales, Proceedings*, 64, 242–254.

Voisey, A.H., 1939a — The upper Palaeozoic rocks between Mount George and Wingham, N. S. Wales. *Linnean Society of New South Wales, Proceedings*, 64, 242–254.

Voisey, A.H., 1939b — The geology of the county of Buller. *Linnean Society of New South Wales, Proceedings*, 64, 385–393.

Voisey, A.H., 1939c — The Lorne Triassic Basin and associated rocks. *Linnean Society of New South Wales, Proceedings*, 64, 255–265.

Voisey, A.H., 1950 — The Permian rocks of the Manning–Macleay province, New South Wales. *Journal and Proceedings of the Royal Society of New South Wales*, 84, 64–67.

Voisey, A.H., 1958 — Further remarks on the sedimentary formations of New South Wales. *Journal and Proceedings of the Royal Society of New South Wales*, 91, 165–189.

Walkden, G.M. & Berry, J.R., 1984 — Syntaxial overgrowths in muddy crinoidal limestones: cathodoluminescence sheds new light on an old problem. *Sedimentology*, 31, 251–267.

Woolnough, W.F., 1911 — Preliminary note on the geology of the Kempsey district. *Royal Society of New South Wales Journal*, 45, 159–168.

BMR Journal of Australian Geology & Geophysics, 12, 161–190

Groundwater and surface water interaction at Lake George, New South Wales

G. Jacobson[1], J. Jankowski[2] & R.S. Abell[1]

Lake George is a fluctuating closed lake in the eastern highlands of Australia. Groundwater in the 932 km^2 catchment is mainly of low salinity, but high salinity groundwater is evident beneath the lake bed. Porewater analyses reveal a salinity profile in a clay aquitard 50 m thick, beneath the lake bed, that has the characteristics of diffusion but is also influenced by mixing with (a) lakewaters infiltrating downwards, and (b) groundwaters rising upwards under pressure. Hydrostatic balance is apparently achieved at a depth of 10 m below the lake bed; this coincides with the maximum porewater salinity of 40–42 000 mg/L total dissolved solids (TDS). Salt accumulates in lake-full periods and concentrates by evaporation of lake waters. A net loss of salt is evident in recessive phases of the lake. During drying and refilling episodes, the lake water surface becomes the water table and vice versa. Salt is concentrated in the capillary zone during dry periods and is also transmitted downwards by diffusion. In recessive phases there is infiltration of lake water which has a freshening effect on the top of the salinity profile, but also transmits some salt. The processes of salt accumulation and diffusion in the aquitard may have operated for much of the Quaternary. In the Lake George basin, five types of water are characterised: surface water in creeks and in the lake; groundwater in the catchment, and in sandy aquifers beneath the lake and bed; and porewater in the clay aquitard underlying the lake bed. Creek water and catchment groundwater is fresh to brackish and generally of the HCO_3–Cl or Cl–HCO_3 type with Na and Mg as major cations. The lake water is alkaline, of varying salinity up to 45 000 mg/L TDS, and of the Cl–Na type. Varying ionic concentrations in these waters are the result of evaporative concentration and precipitation of carbonate minerals. Beneath the lake bed are saline aquifer groundwaters (up to 48 000 mg/L TDS) and aquitard porewaters (up to 42 000 mg/L TDS); these are Cl–Na waters with appreciable Mg. Sulphate is also retained in the groundwater which evolves chemically through interaction with the aquifer matrix. Hydrochemical evolutionary pathways are different for groundwaters and for surface waters. In surface waters (creek and lake), dolomite and calcite saturation is achieved early but these waters are undersaturated with gypsum. In the groundwaters (catchment and lake bed), saturation with dolomite and calcite is achieved early but equilibrium relationships are more complex. Shallow groundwaters, down to 15 m beneath the lake bed, show evidence of mixing with infiltrating lake waters, and this has retarded mineral precipitation. The deeper, saline groundwaters are close to saturation with gypsum. Stable isotope data also indicate mixing down to 15 m below the lake bed between evaporated lake waters infiltrating downwards and saline groundwaters under upwards pressure. Chlorine-36 determinations indicate that younger groundwaters at 10–50 m below the lake bed overlie groundwaters at 100 m that are tens of thousands of years old.

'These are much deeper waters than I had thought'

A. Conan Doyle

The Reigate Squires, *in* Memoirs of Sherlock Holmes, 1888

Introduction

In much of Australia, the antiquity of the landscape has led to deep weathering and the availability of salt which has increasingly been released as a result of climatic and anthropogenic change. Thus, problems of land and stream salinity are developing on a large scale in many catchments. The interaction of groundwater and surface water is an important factor in the transport and accumulation of salt (Macumber, 1983) but the processes are not fully understood. Terminal lake basins are sites of salt accumulation, both natural and human-induced. Lake George is an example of a temperate zone, fluctuating closed lake with varying salinity. It can be considered as a natural analogue for a wastewater disposal basin, and its groundwater system may throw light on the prospects for long term hydrogeological safety of such basins.

The Lake George drainage basin is an elongate, north–south basin of 932 km^2 within the Southern Tablelands of New South Wales (Fig. 1). The lake itself is at latitude 35°05'S and longitude 149°25'E, about 40 km northeast of Canberra and about 100 km inland. The lake is closed and fluctuating, containing water for 85–90% of the time; the fluctuations, documented since 1820, have a period of about a decade (Fig. 2), with a maximum lake depth of 7 m. BMR has monitored lake levels and salinity on a monthly basis since 1958 (Jacobson & Schuett, 1979).

The decade of the 1980s was generally dry in southeast Australia, and Lake George was mostly dry. This enabled the investigation of the geology beneath the lake bed (Abell, 1985), with the drilling of several stratigraphic holes, undertaken in conjunction with geological mapping of the catchment (Abell, in press). In 1987 several additional holes were drilled in the lake bed, to establish the nature of the groundwater regime and ascertain its relationship to that of the catchment. Piezometer nests were established at two sites in the lake bed, 353 and 355 (Fig. 3), to depths of 10 m, 55 m and 100 m at each site. A shallow (2 m) piezometer was installed at site 351. Drillholes were cored at two other locations, 352 and 354, to allow the extraction of porewaters for determination of chemistry and porosity. The selected transect is considered to be representative of conditions under the lake bed.

The interaction of groundwater and surface water at Lake George has been the subject of speculation. A considerable loss of dissolved salt has been observed during recessive phases of the lake (Jacobson & Schuett, 1979) and attributed to wind deflation of precipitated salts. Transfer of salts from surface water to groundwater during seiches has been suggested as a possible cause (Torgersen, 1984). Bowler (1986) suggested that the porewaters may act as a storage system for salt transferred from surface waters. This report outlines the hydrogeology of the Lake George basin and clarifies the processes involved in the interaction of the groundwater and surface water systems.

[1]Groundwater Program, Bureau of Mineral Resources, GPO Box 378, Canberra ACT 2601
[2]Centre for Groundwater Management and Hydrogeology, University of New South Wales, Kensington, NSW 2033

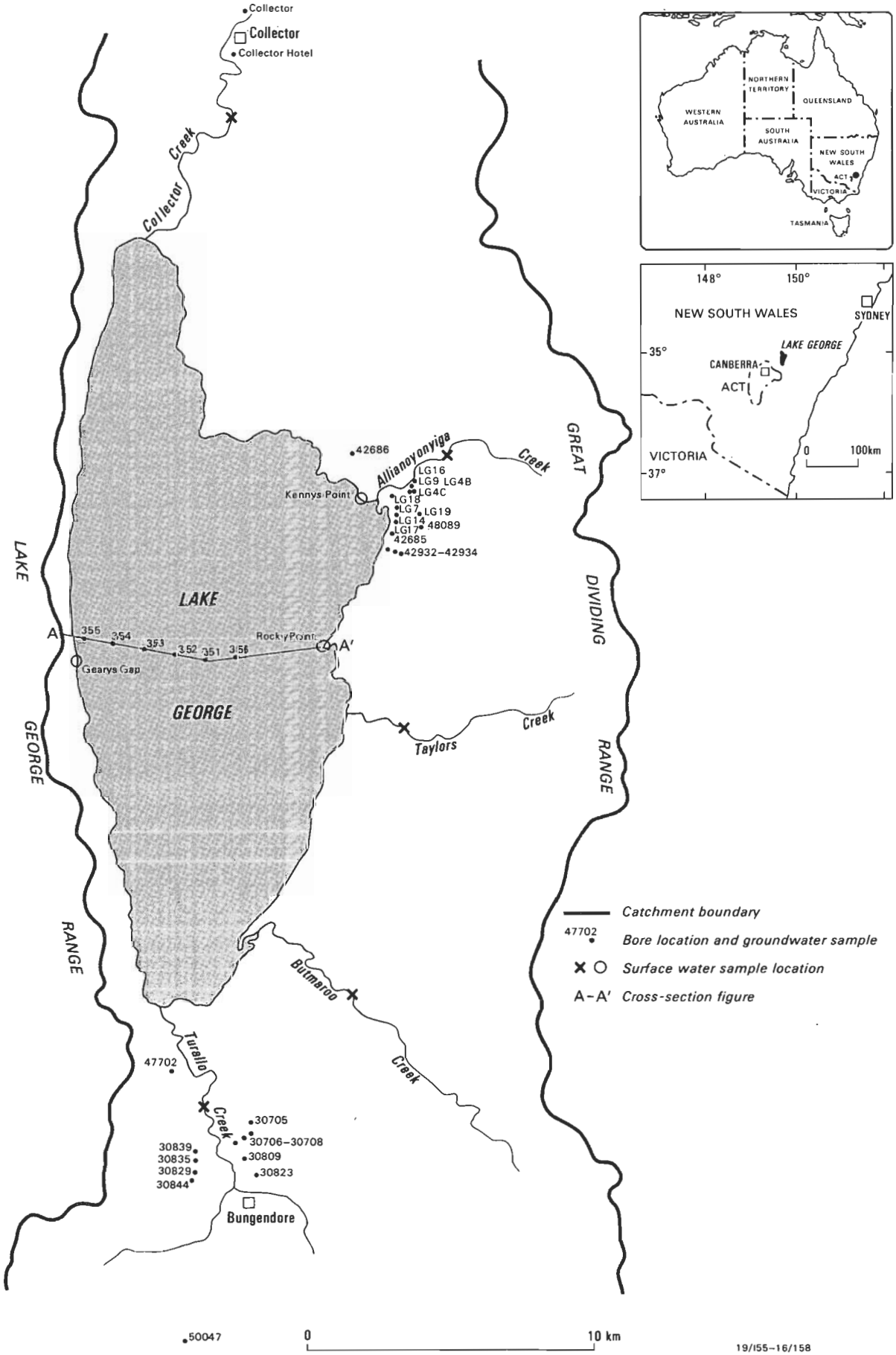

Figure 1. Location map.

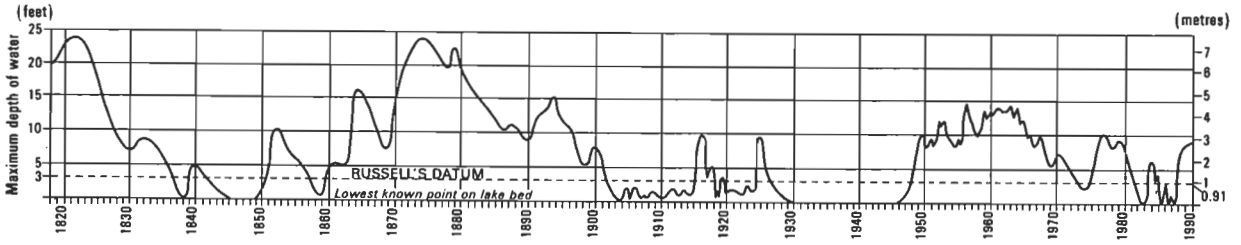

Figure 2. Fluctuations in water level, Lake George, 1819–1990.

Geology and physiography

The geology of the catchment is shown in Figure 4. The pre-Cainozoic, bedrock geology comprises marine sedimentary rocks of Middle to Upper Ordovician age, which are overlain unconformably by late Silurian volcanic rocks and intruded by Siluro-Devonian granite. The sequence was folded, faulted and weakly metamorphosed by a series of Palaeozoic earth movements which gave a meridional trend to the geological structure. After Permian time the region remained sufficiently stable for an ancient landscape to develop by the Late Cretaceous.

In the mid-Tertiary, the Lake George basin originated by faulting, possibly by the rejuvenation of late Palaeozoic faults (Abell, 1985). The Cainozoic sediments were deposited in a normal fault-angle basin. Sedimentary events have been dated from Quaternary and Tertiary pollen (Truswell, 1984; Singh & Geissler, 1985) and from a palaeomagnetic profile dating back at least to the Pliocene (Singh & others, 1981; Mason, 1987).

Beneath Lake George, drilling has revealed the existence of more than 150 m of fluvio-lacustrine sediments. This has enabled the Cainozoic sequence in the basin to be divided into three lithostratigraphic units: the Geary's Gap Formation, the Ondyong Point Formation, and the Bungendore Formation (Fig. 5). The Gearys Gap Formation consists of deeply weathered fluvial sand and gravel. These early Tertiary sediments were deposited unconformably on Palaeozoic bedrock, and are associated with a prior drainage system which was incised into bedrock and flowed northwest. Palaeochannels can be traced under the lake bed (Abell, 1985). The Ondyong Point Formation consists of fluvial sand and lacustrine clay and silt deposited disconformably on deeply weathered sediments. The Bungendore Formation comprises lacustrine clay and silt; it is conformable on the Ondyong Point Formation and separated from it by a laterally persistent layer of sand and silt. The latter two units represent deposition in a closed drainage basin and their lithofacies is largely a function of climatic change.

A complex clay-mineral assemblage has been identified in the Cainozoic sequence (Abell & others, 1985). Calcite and dolomite also occur in small quantities throughout the sediments. Gypsum occurs in the upper part of the Bungendore Formation and at its lower boundary with the Ondyong Point Formation. Traces of halite occur in both the Bungendore Formation and Ondyong Point Formation. These minerals are considered to be authigenic.

Quaternary sediments in the basin include colluvial deposits on the flanks of hills and along the Lake George escarpment, and lacustrine strandline and aeolian deposits around the lake margins. Ancient strandlines up to 37 m above the lake bed testify to very large fluctuations of water level in late Quaternary time. Above this elevation the lake overflowed through Gearys Gap into the Yass River drainage system; this last happened between 27 000 and 21 000 years B.P. (Coventry, 1976).

The Lake George basin now represents a base level of internal drainage. The basin margin is defined by the topographically subdued watershed of the Great Divide in the east, and by the Lake George Range in the west. At its northern and southern limits, the basin margin comprises subdued topography with low saddles, a complex of natural and artificial drainage lines, and swampy lagoonal areas. Within the basin, topographic relief commonly ranges from 680 to 900 m above sea level. The floor of the lake is at an elevation of about 674 m.

Streams in the basin occupy wide open valleys in their upper reaches. They converge towards Lake George by meandering across flat alluvial plains and embayments. Evidence of faultline rejuvenation disrupting the headwater system of the Yass River is indicated by elevated river gravels, the remnant of a broad valley at Gearys Gap, and the barbed drainage of creeks flowing to the northern end of Lake George (Taylor, 1907; Ollier, 1978; Abell, 1985).

The pre-European landscape of the basin consisted of wooded, eucalypt-covered terrain, relics of which still remain. Fragmentary charcoal in lake-bed sediments, and plant microfossil evidence for the expansion of eucalypts, suggest increased fire frequencies, possibly due to human activity, in the last 130 000 years (Singh & Geissler, 1985). The largely erosional present-day landscape reflects the impact of European settlement over the last 200 years. Extensive clearing of vegetation for grazing and cultivation has led to land degradation, including erosion gullying, particularly in areas blanketed by colluvial and alluvial slope deposits. The expansion of Canberra has demanded building materials, and sand and gravel are extracted from strandline and aeolian deposits around the northern and southern margins of Lake George. This has led to the deterioration of natural vegetation and landforms associated with these deposits.

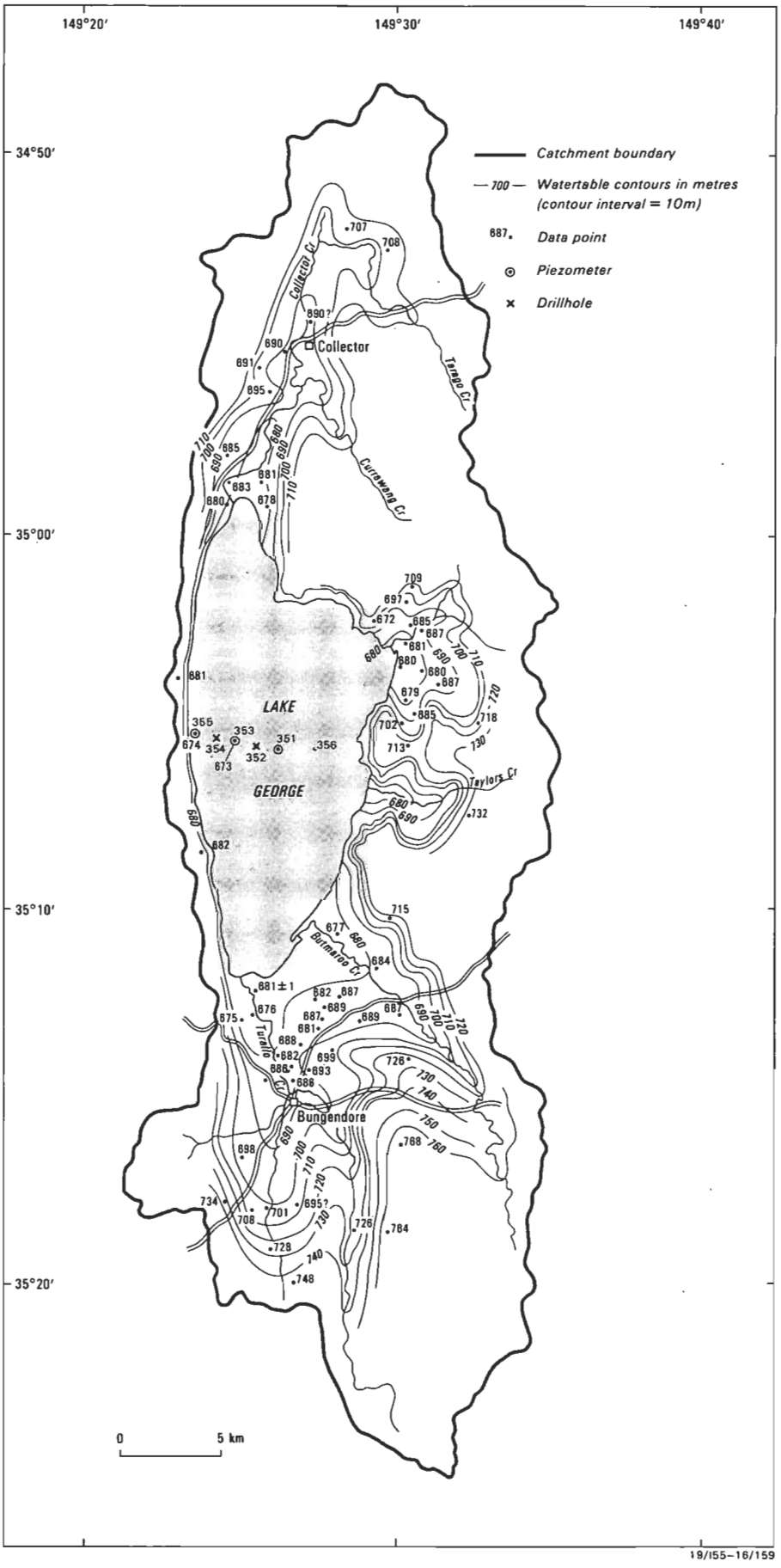

Figure 3. Potentiometry of the Lake George catchment.

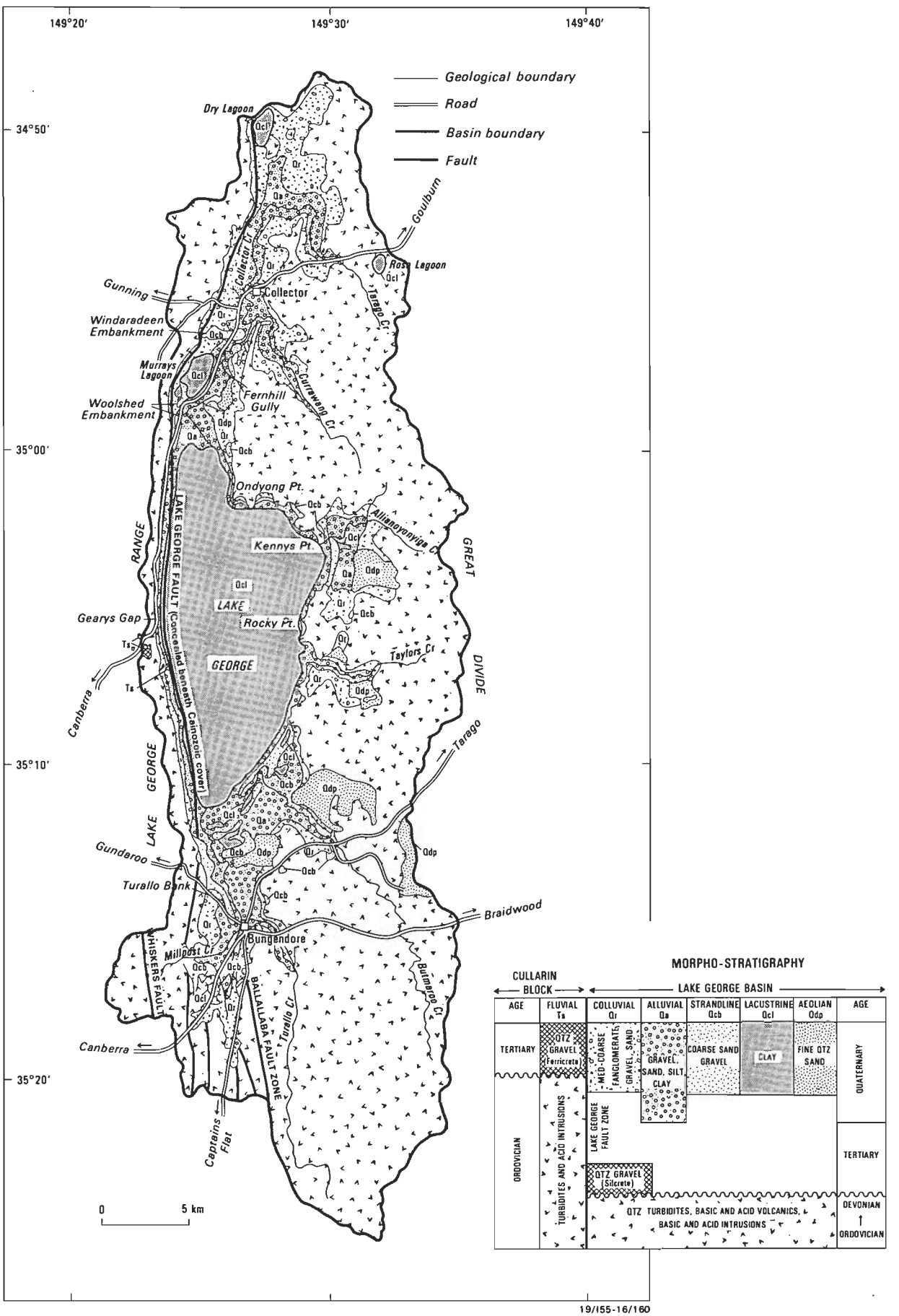

Figure 4. Geology of the Lake George catchment.

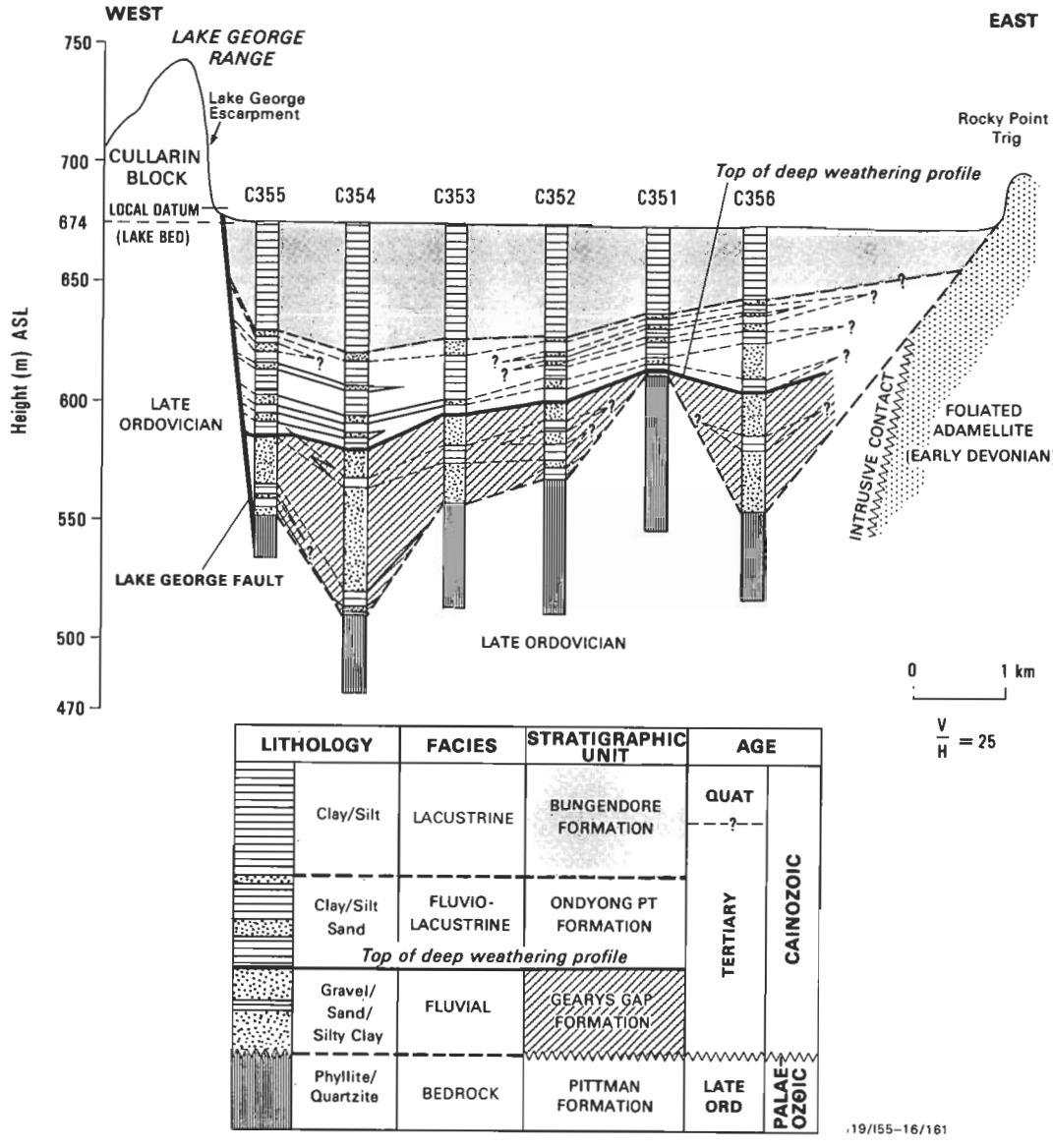

Figure 5. Cross-section of Lake George showing stratigraphy.

Climate and hydrology

The present warm temperate, continental climate over the Lake George basin is typified by hot summers and cold winters. Average monthly temperatures at lake level are: January, maximum 27°C, average 20°C, minimum 12.5°C; July, maximum 10.5°C; average 5°C, minimum −0.5°C. The effect of altitude in the catchment is to moderate the summer and lower the winter temperatures. The annual precipitation is variable: the range over a century of records is 390 mm to 1120 mm. Mean annual precipitation is estimated as 750 mm, based on records from two rain gauges in the catchment at Bungendore and Collector. Precipitation is distributed fairly evenly throughout the year with a maximum in October. Evaporation is about 1200 mm annually and occurs mainly between October and April.

Lake George constitutes about 16% of the total area of the drainage basin. Several creeks and watercourses converge towards the lake: Collector Creek from the north, Allianoyonyiga, Taylor and Butmaroo Creeks from the east and Turallo Creek from the south (Fig. 3). About 50×10^6 m^3/year enters the lake from surface runoff.

Lake George is a shallow body of water which shows marked fluctuations in level and salinity. The lake hydrograph is one of the oldest and most continuous water level records in Australia (Russell, 1886). In historical times, changes in the regional climatic pattern have caused the lake to dry out. Over the last ten years, Lake George has dried out for a nine month period in 1982–83, and annually in 1986, 1987 and 1988. Over the last 170 years, the hydrographic record (Fig. 2) shows that the water depth in Lake George has rarely passed 6 m and has not exceeded 7.5 m. Commonly its depth is 1.5–4.5 m and its area 130–160 km^2.

Monitoring during lake-full periods shows that the lake

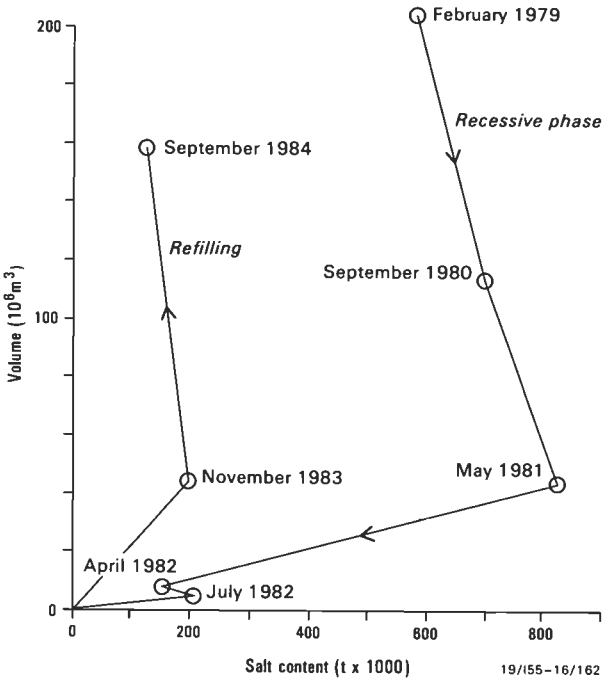

Figure 6. Loss of dissolved salt in recessive phase, 1982.

level fluctuations are a response to seasonal and long-term variations in rainfall, evaporation and inflow of streams (Jacobson & Schuett, 1979). The lake water balance shows marked seasonal characteristics. In general, increases in water volume between May and October correspond with large inflows of water and low evaporation, whereas decreases in water volume between November and April correspond with lesser inflows and high evaporation. The longer term fluctuations with a periodicity of about a decade (Fig. 2) reflect climate variability in southeast Australia, and the dry phases of Lake George correspond with economically significant, severe droughts in this region. The drying out of Lake George in 1982–83 corresponded with the major El Niño Southern Oscillation event of the century. Salinity of the lake water also fluctuates; it increases as the lake level and water volume decrease. Salinity ranges from about 400 mg/L total dissolved solids (TDS) when the lake level is 4 m and water volume is about 450 x 10^6 m^3, up to 40 000–45 000 mg/L when the lake level is less than 1 m, and water volume less than 40 × 10^6 m^3.

In recessive phases of the lake, such as the drying-out in 1982, a net loss of dissolved salt is observed. Thus the total dissolved salt content increased during lake recession from 600 000 t in 1979 to about 800 000 t in early 1981 (Fig. 6). This was rapidly lost during drying out when the lake level fell below a critical depth of 1 m. On refilling in 1983 the total salt content rose to 200 000 t at a lake level of 1 m.

The lake and the groundwater system are hydraulically connected when the lake fills (Fig. 7). When the lake is dry, the watertable is about 0.5 m below the surface and playa-like conditions develop. Lake water levels are subject to diurnal fluctuations, which may be up to 10 cm, as a result of seiches. The seiches are induced by northerly or southerly winds spreading thin sheets of water across the lake bed (Burton, 1972). This water movement gives visible diurnal changes in water level and area, leading to increased water losses by evaporation or infiltration.

Hydrogeology

Figure 8 illustrates the dual hydrological cycle for the Lake George Basin. In the wet cycle, the lake is filled and maintained mainly by surface runoff; shallow aquifers are recharged, mainly in the winter months when rainfall exceeds evaporation (Burton, 1977). In the dry cycle, groundwater flow towards and beneath the lake discharges through capillary evaporation from the dry lake bed.

Figure 3 shows potentiometry in the catchment based on information from water bores. Groundwater flows towards Lake George in fractured rock and alluvial aquifers from the north, east and south. On the west side, the topographic divide is close to the lake; this probably coincides with the groundwater divide although potentiometric information is sparse in this area. Groundwater in sand and gravel aquifers beneath the lake bed (Gearys Gap, Ondyong Point Formation) is confined by a clay aquitard (Bungendore Formation). Recharge to the lake-bed aquifers occurs mainly in alluvial embayments at the lake margin (Fig. 9). Hydraulic continuity is assumed in this study although these aquifers are in fact shoestring sands, and considered on a detailed scale may not be continuous. The alluvial aquifers are used for water supply at the town of Bungendore and the Woodlawn mine. Throughout the catchment, fractured bedrock aquifers are used for dispersed farm and livestock water supplies.

In the alluvial aquifers north and south of the lake, the groundwater is fresh, containing 150–500 mg/L TDS. To the east, the alluvial aquifers contain 800–1500 mg/L TDS. Fractured rock aquifers in the catchment vary in salinity from 250 to 2000 mg/L TDS; this variation is ascribed to dissolution of salts in the weathered mantle and varying residence time of groundwater (Evans, 1987).

Beneath the lake bed, investigation drillholes show that 50 m of clay overlies thin sand and gravel aquifers (Fig. 9) which in turn overlie bedrock at depths of up to 160 m.

Groundwater pressures have been measured in lake boreholes. Fluctuations in groundwater level reflect the marked seasonal climatic variation in the catchment (Fig. 10) and are dampened with increasing depth. These groundwaters are saline (10 000–48 000 mg/L TDS; Fig. 11), and are therefore of variable density. To allow comparison, the measured heads have been converted to equivalent freshwater heads. Upwards movement of groundwater beneath the lake bed is inferred from the head distribution, and the lake thus appears to be a zone of regional groundwater discharge. The groundwater pressure is generated by the catchment topography which is up to 200 m above Lake George.

The salinity configuration of the groundwater beneath the lake (Fig. 11) appears to be unstable, in that denser

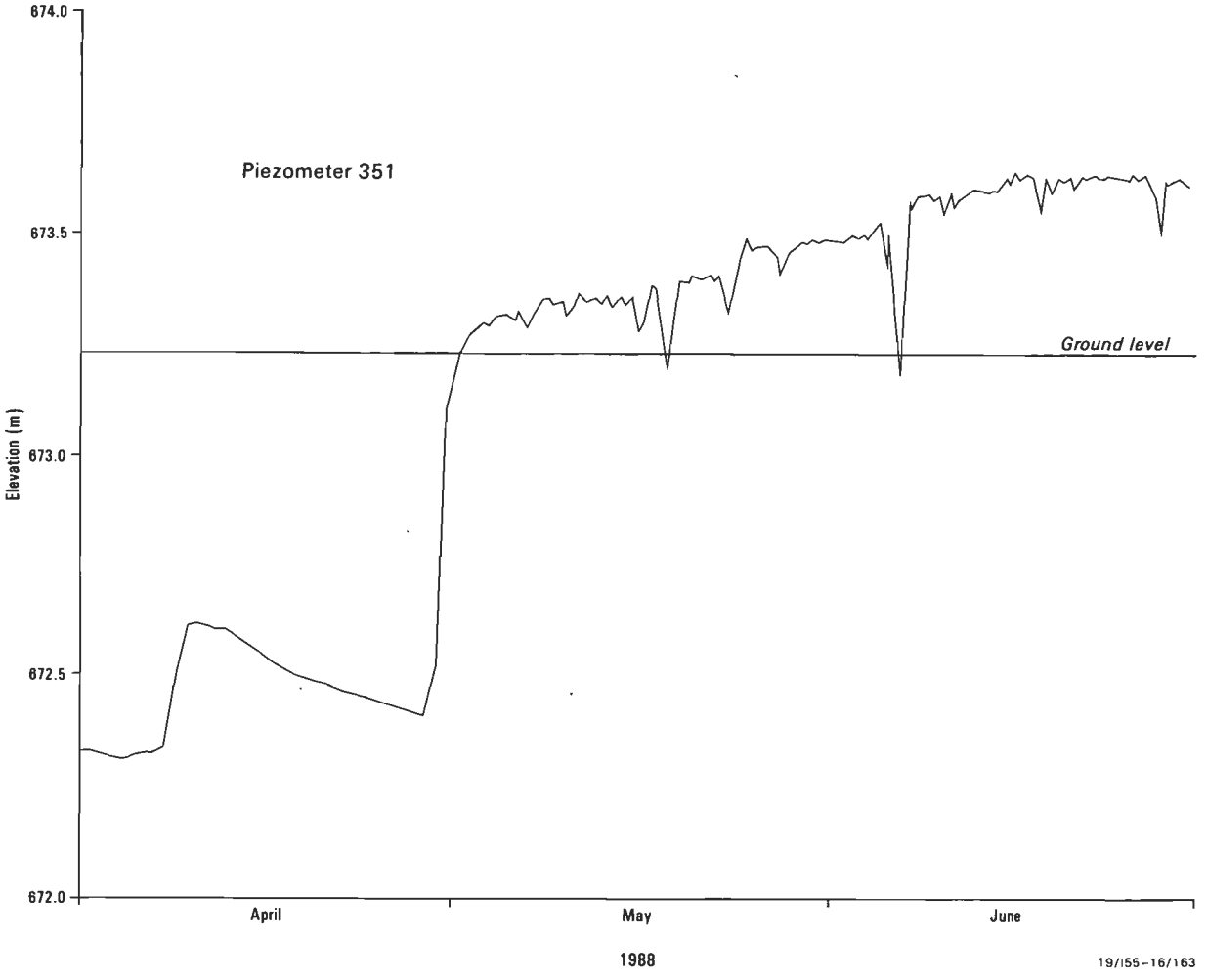

Figure 7. Lake George hydrograph, 1988, showing effects of lake filling.

water (>40 000mg/L TDS) overlies less dense water (10 000 mg/L TDS). In this situation, whether flow of fluid actually occurs depends on the magnitude and direction of the pressure gradient. J.S. Hanor (Louisiana State University) and W.R Evans (BMR) (personal communication, 1989) have analysed a similar case involving one-dimensional vertical fluid flow through the Geera Clay aquitard in the Murray Basin, southeast Australia. Their analysis was based on Darcy's Law, from which it can be shown that for such a density-layered system to be in hydrostatic equilibrium

$$dP/dz = \sigma g$$

where dP/dz is the pressure gradient, σ is fluid density, and g is the gravitational constant. For fluid flow to occur, there must be an imbalance of the pressure gradient, so that

$$dP/dz > \sigma g$$

for upwards flow, or

$$dP/dz < \sigma g$$

for downwards flow.

In order to analyse the Lake George situation, groundwater pressures in piezometers were calculated as

$$P = \sigma g L$$

where L is the vertical length of the fluid column in the piezometer. From this, the pressure driving fluid flow was calculated to be about 7500 Pa/m in the top 10 m of the profile and about 10 000 Pa/m from 10 to 100 m (Fig. 12). The pressure resisting fluid flow, due to fluid density, σg, was calculated as decreasing vertically downwards from just over 10 000 Pa/m near the surface to 9840 Pa/m at a depth of 100 m. Comparing the magnitudes of the two opposing gradients (Fig. 12), it appears that upwards flow occurs in the lower part of the section. There is hydrostatic balance at a depth of about 10 m below the lake bed, and above that level a lessening of the pressure gradient implies that downwards flow occurs.

The salinity of pore waters in the aquitard (Bungendore Formation) is shown in Figures 13 and 14. Salinity increases downwards to a maximum of 32 000 mg/L at 7 m and 12 m in bore 352, and to maxima of 42 000 mg/L at 4.5 m and 40 000 mg/L at 12.5 m in bore 354. Beneath these maxima, salinity decreases downwards, almost linearly, to 10 000 mg/L at 53 m in

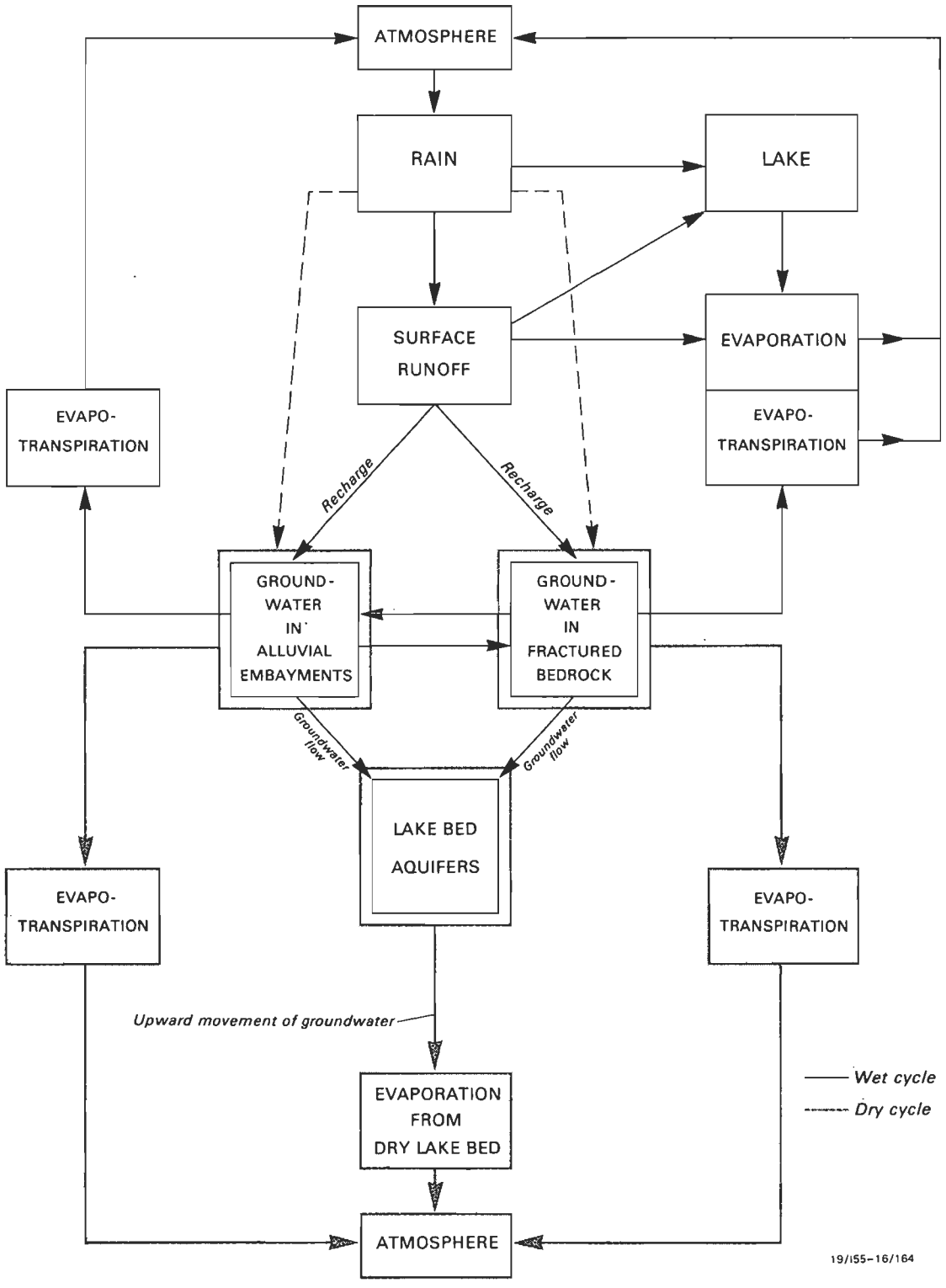

Figure 8. Hydrological cycle for the Lake George basin, showing wet and dry cycles.

352 and 18 000 mg/L at 52 m in 354. The nearly linear trend in salinity suggests diffusive transport of salt downwards. The lower salinity in the upper part of the section suggests dilution by superimposed freshwater and displacement of the diffusive profile downwards.

To estimate the diffusive flux of solute Fick's first law can be applied. According to this,

$$J = - D^{\circ} (\varphi/\theta^2) \nabla C$$

where J is solute flux (kg/m^2s), D° is the diffusion coefficient in free solution (m^2/s), φ is porosity (m^3/m^3), θ is the resistivity formation factor, which is an index of tortuosity (m/m) and ∇C is the concentration gradient ($kg/m^3/m$). The diffusion coefficient was taken as 1.25×10^{-9} m^2/sec for NaCl in the appropriate concentration

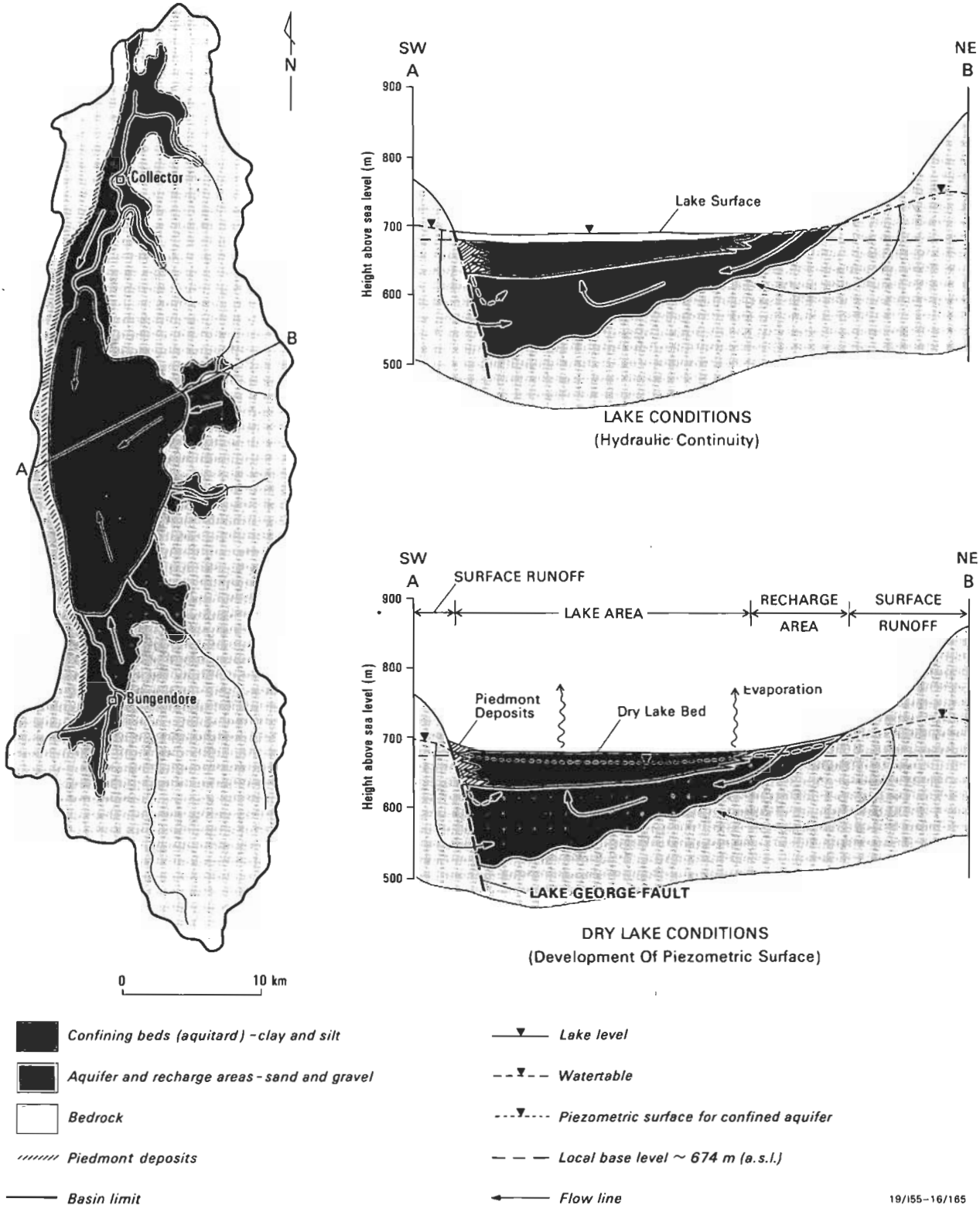

Figure 9. Hydrogeology of the Lake George basin.

range at 18°C; average porosity was estimated as 0.55 based on measurements in core samples (Figs 13, 14); the formation factor was estimated as 3.5 based on published experimental results for sediments of similar porosity (Manheim & Waterman, 1974); and the concentration gradient was calculated as 0.172 kg/m^3/m from

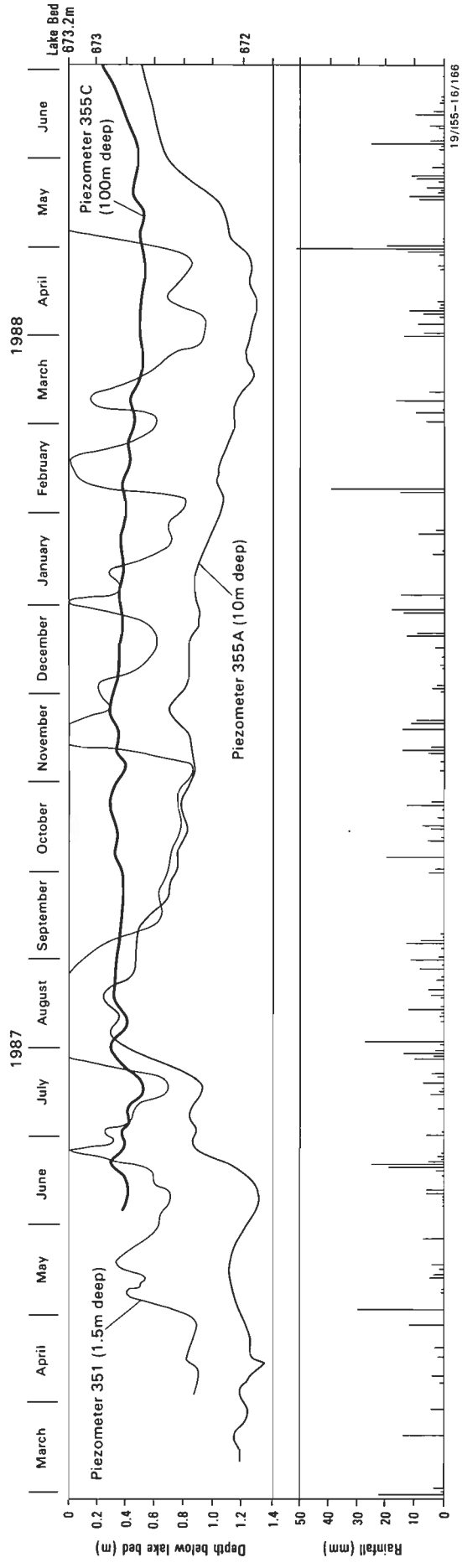

Figure 10. Fluctuations in measured potentiometric level, Lake George groundwaters.

data obtained for Na in bore 352 (Fig. 13). Substituting in the above equation, we obtain

$J = -(1.25 \times 10^{-9})\ (0.55/12.25)\ (0.172)\ kg/m^2s$

$= -3.05 \times 10^{-4}\ kg/m^2year$

Thus the flux of dissolved NaCl downwards through the aquitard is about 0.3 g/m^2year.

The total mass of dissolved salt in the aquitard can be calculated as the product of porewater volume and salinity (Figs 13, 14) for sites 352 and 354. For 5 m sections of the aquitard, Figure 15 shows the salt distribution with depth. For a 54 m deep section in bore 352, the total salt accumulated is 549 kg for a 1 m^2 cross-sectional area, and for a 52 m deep section in bore 354 the total salt accumulated is 764 kg for a 1 m^2 cross-sectional area. Thus the average salt accumulation beneath Lake George is about 0.65 t per 53 m section per m^2 area. The total salt accumulation for the 53 m aquitard section is the product of lake area and salt accumulation, i.e. $15\,000 \times 10^4 \times 0.65$ t = 97.5×10^6 t. This compares with the mobile salt mass in the lake water (Fig. 6) of about 800 000 t.

Considering a 1 m^2 column of the aquitard, we find that 0.65 t of salt has accumulated, and that the present-day diffusion rate is 0.3 g/year. This implies that salt accumulated and diffused over a period of (650 000/0.3) years, i.e. about 2×10^6 years. Porosity was probably greater in the past and there was probably an increased concentration gradient during arid periods, suggesting a somewhat greater diffusion rate at times. Nevertheless, these processes have operated in the aquitard for a considerable part of Quaternary time.

Hydrochemistry

Chemical analyses of selected samples of Lake George catchment waters are shown in Table 1. This data base has been developed over 20 years from analyses by BMR supplemented by selected analyses from files of the New South Wales Department of Water Resources. In the present investigation, lake-bed piezometers have been sampled and analysed for major ions, stable isotopes and radioisotopes.

Major ion concentrations

The hydrochemistry of surface waters is considered in terms of two groups: creek runoff water and lake water. Five creeks flow into Lake George intermittently (Fig. 3). Salinity of their water ranges from 100 to 2500 mg/L TDS, and varies with time and the amount of stream flow. The freshest creek water, from 100 to 300 mg/L TDS, is of the HCO_3–Cl–Na–Mg type, creek water with 300 to 1500 mg/L TDS is generally Cl–HCO_3–Mg–Na–Ca water, and more saline creek water is Cl–Na water.

The lake water varies in salinity inversely with lake stage and water volume. Figure 16 shows compositional changes as the lake level falls. The fresher lake water is of the Cl–Na type with appreciable Mg and HCO_3. The brackish and saline lake waters are also Cl–Na waters but have greater concentrations of Cl, Na and SO_4. With increasing lake salinity the Ca concentration in lake waters increases very slowly; the HCO_3 concentration

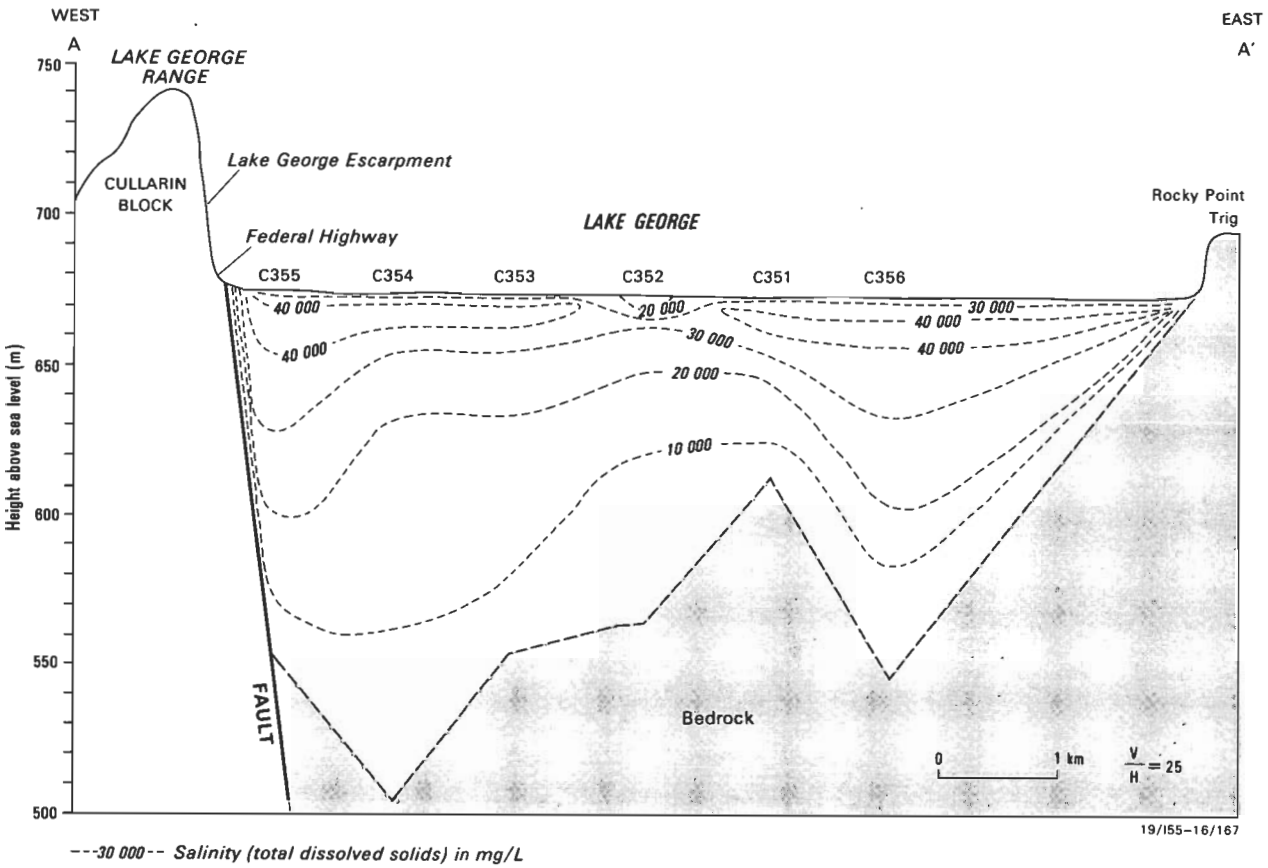

Figure 11. Distribution of salinity in lake-bed groundwaters.

increases initially then decreases in the more saline waters. With increasing salinity, the lake waters become more alkaline, with pH about 9, and contain CO_3 (Table 1).

The hydrochemistry of the groundwaters is considered in terms of three groups: catchment borewater, groundwater beneath the lake bed, and porewater in the aquitard. The catchment bores, in alluvial and fractured rock aquifers, generally contain groundwater with 150–2000 mg/L TDS. The fresher catchment groundwater, less then 200 mg/L, is of the HCO_3–Na–Mg–Ca type; it becomes the HCO_3–Cl–Na–Mg–Ca type in the salinity range 200–400 mg/L TDS, and the Cl–HCO_3–Na–Mg–Ca type above 400 mg/L TDS. Groundwaters beneath the lake bed are brackish Cl–Na waters with appreciable SO_4 and Mg (Table 1).

The porewaters are alkaline and Cl–Na rich with appreciable SO_4 and Mg. Salinity trends are paralleled by Na and Cl concentrations, but the Mg and SO_4 concentrations show different characteristics in the two investigated sections (Figs 13, 14).

The major ion composition of surface waters and groundwaters is shown in a Piper trilinear diagram (Fig. 17). Distinctive evolutionary trends are evident. With increasing salinity, the surface waters trend towards the Cl and Na corners, reflecting the process of evaporative concentration. Groundwaters follow a more complicated pathway and trend eventually towards the SO_4 and Mg corners. Groundwaters from beneath the lake bed are distinctively grouped on Figure 17; they plot along the Cl–SO_4 side of the anion diagram, close to the Cl corner, and along the Na–Mg side of the cation diagram, close to the Na corner. Samples from 50 and 100 m plot close to the evolutionary pathway of the catchment groundwaters, but samples from 1 and 10 m plot closer to the evolutionary pathway of the surface waters. This suggests mixing of surface waters and groundwaters beneath the lake bed and explains the high SO_4 concentrations in the waters at 10 m depth (Figs 13, 14). Sulphate is concentrated by the infiltration of lake waters and the upwards flow of groundwater, but is not taken up in precipitation as the mixed waters are undersaturated with gypsum.

Figure 18 shows relationships of the major ions Na, Mg, and Ca, with increased salinity. Surface waters and groundwaters again reveal distinctive evolutionary trends. In the lake waters, Na concentration increases along a line with 45° slope (Fig. 18a), indicating that evaporative concentration is the main process. In the catchment and lake-bed groundwaters, Na concentration also increases more or less linearly towards a maximum at a depth of 10 m beneath the lake bed. The concentration line is displaced relative to that of the lake waters, and probably represents the acquisition of Na by dissolution of stored salts in the weathered zone, and subsequently of aquifer matrix. Creek runoff waters are grouped with the catchment groundwaters in this plot, and the scatter of points reflects the variability of catchment conditions.

In the lake waters, Mg concentration increases with increasing salinity along a line with slope 45° (Fig. 18b), indicating that evaporative concentration is the main process. In the catchment groundwaters and creek runoff

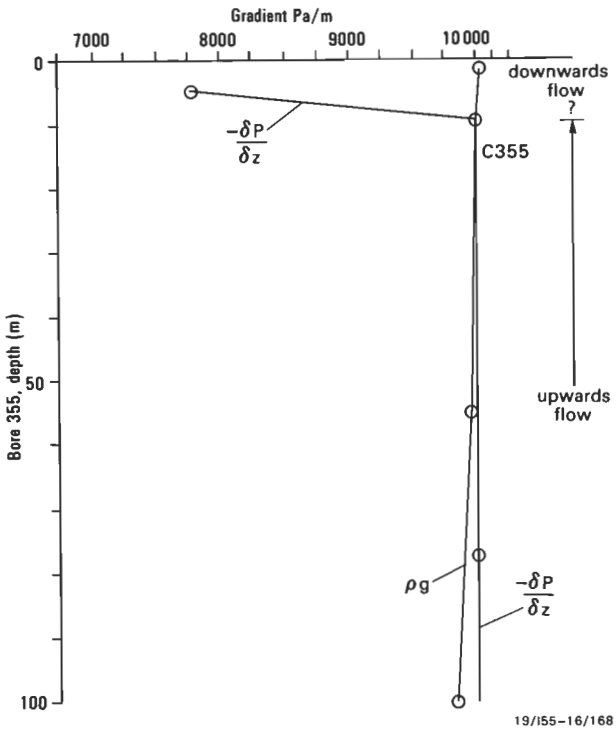

Figure 12. Comparison of pressure gradients affecting fluid flow.

waters, the Mg concentration trend is also linear but the line is displaced above that of the lake waters. Dissolution of chlorite in aquifer matrix is probably the main contributor of Mg to the groundwater system (Evans, 1987). The linear trend continues to the more saline lake bed groundwaters where the scatter of points on the plot suggests some mixing with surface waters.

The plot of Ca concentration versus salinity (Fig. 18c) is completely different. In the surface waters, Ca concentration increases until salinity reaches about 1000 mg/L TDS, probably as a result of dissolution. It then decreases slightly with further increase in salinity. This is probably due to precipitation of calcite and dolomite. In the catchment groundwaters, Ca concentration increases with increased salinity, as a result of dissolution of aquifer matrix. In the saline lake-bed groundwaters the Ca concentration again decreases, and the scatter on the plot suggests some mixing of these saline groundwaters with lake waters.

Figure 19 shows relationships of Cl, SO_4 and alkalinity concentrations with increasing salinity. The Cl concentration (Fig. 19a) increases with salinity in fresher surface waters and catchment groundwaters; the Cl is probably derived from stored salts in the weathered zone (Evans, 1987). Brackish and saline lake waters show an increase in Cl concentration with salinity, along a line with slope 45°, suggesting evaporative concentration. The SO_4 concentration (Fig. 19b) increases as salinity increases in both surface waters and groundwaters. Lake waters increase in SO_4 concentration relative to TDS along a 45° slope line, indicating evaporative concentration. In lake-bed groundwaters the SO_4 concentration increases markedly relative to TDS. This reflects both dissolution of sulphide in the aquifer matrix, and downwards diffusion of salts concentrated in shallow groundwater under dry lake conditions. The alkalinity (Fig. 19c) generally increases with salinity in fresher surface waters and groundwaters. Both trends flatten off at about 1000 mg/L TDS due to precipitation of carbonate minerals. In the lake waters, increasing salinity beyond 1000 mg/L TDS parallels increased alkalinity; this probably reflects equilibrium with atmospheric CO_2, with decreasing Ca (Fig. 18).

Ionic ratios and correlations

Figure 20 shows changes in certain ionic ratios with increased salinity of surface waters and groundwaters. These changes indicate distinct evolutionary processes in these waters. Thus the Mg/Ca ratio (Fig. 20a) increases more rapidly relative to TDS in lake waters than in lake-bed groundwaters. This might reflect several concurrent processes. The concentration of Mg by evaporation in the lake waters is enhanced by the reduction of Ca due to equilibrium with atmospheric CO_2, and dolomitisation of calcite in the aquifers reduces the Mg concentration and counteracts the effect of ion exchange, in which Ca is adsorbed preferentially to Mg. In lake waters the Ca/alkalinity ratio (Fig. 20b) initially increases, then decreases with increased salinity beyond 1000 mg/L TDS; in the lake-bed groundwaters, the ratio increases until 10 000 mg/L TDS, then decreases. The latter effect is due to mixing with lake waters that contribute alkalinity. The Ca/SO_4 ratio (Fig. 20c) increases in regional groundwaters until about 1000 mg/L TDS, then decreases. The initial increase reflects dissolution of aquifer matrix, releasing Ca; the subsequent decrease reflects the taking up of Ca in precipitation of carbonate minerals whereas SO_4 remains in solution. In surface waters the Ca/SO_4 ratio decreases throughout with increased salinity. Some Ca is taken up in precipitation, whereas SO_4 concentrations increase with evaporation.

The ionic ratios are different for lake-bed groundwaters at different depths. The deeper groundwaters continue regional groundwater trends, and the shallower groundwaters show the influence of mixing with lake waters.

Figure 21 shows the relationship between alkalinity ($HCO_3 + CO_3$) and total hardness (Ca + Mg). This ratio is close to unity for the fresher catchment groundwaters. In the more saline groundwaters the ratio is close to 0.5, indicating that precipitation of carbonate minerals takes place. In the fresher surface waters the alkalinity/hardness ratio is close to unity but with increased salinity it decreases as carbonate minerals precipitate.

Solution chemistry

Saturation indices are defined as the logarithms of the ion activity product divided by the equilibrium constant. In this study, the saturation indices and CO_2 partial pressures of the ionic components have been calculated using an unpublished BMR computer program 'ACTIVITY' written by J.S. Hanor, and based on Pitzer's equations (Pitzer, 1973) as developed by Harvie & Weare (1980) and Harvie & others (1984).

Figure 22 shows saturation indices for dolomite, calcite, and gypsum, plotted against salinity. Saturation for dolomite ($SI_D = 0$) is achieved at low salinities in catchment groundwaters and in creek waters (Fig. 22a). Saturation indices for dolomite increase in creek and

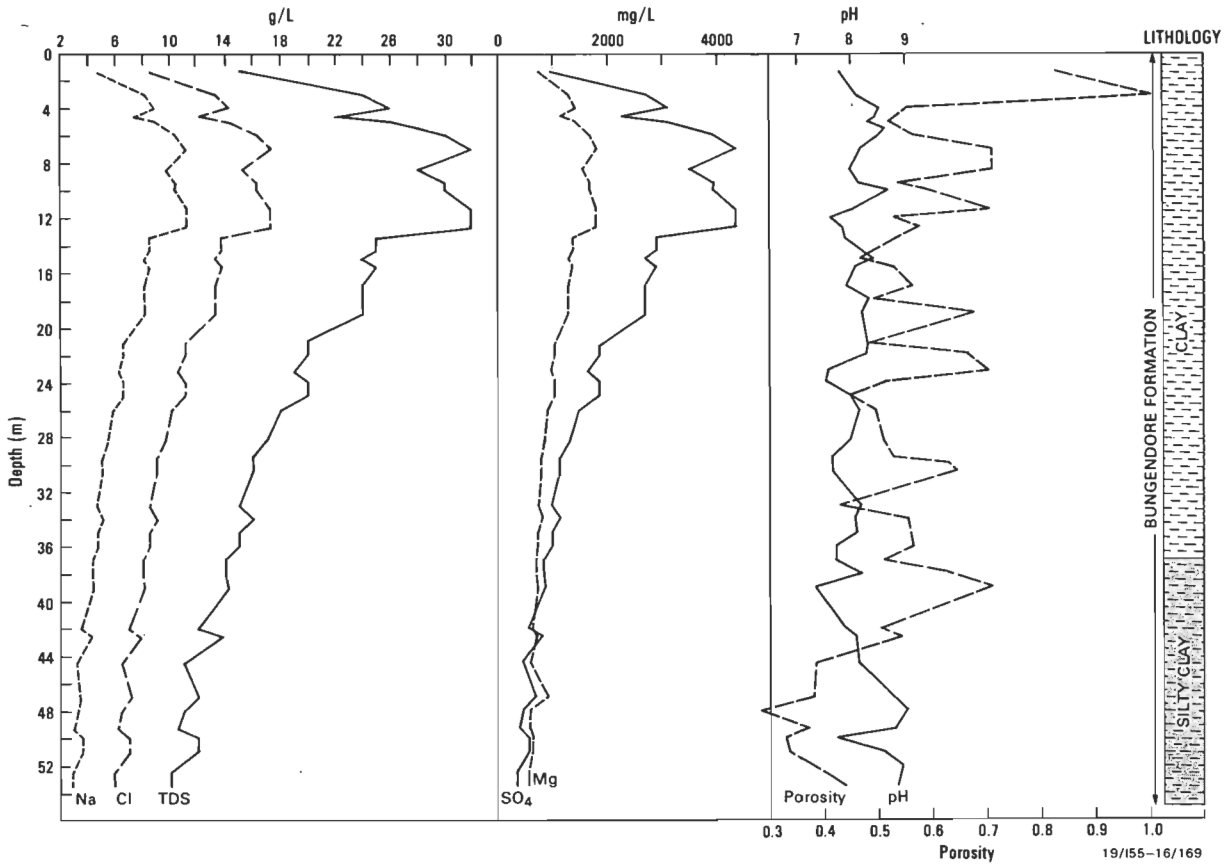

Figure 13. Pore-water chemistry and porosity, bore 352.

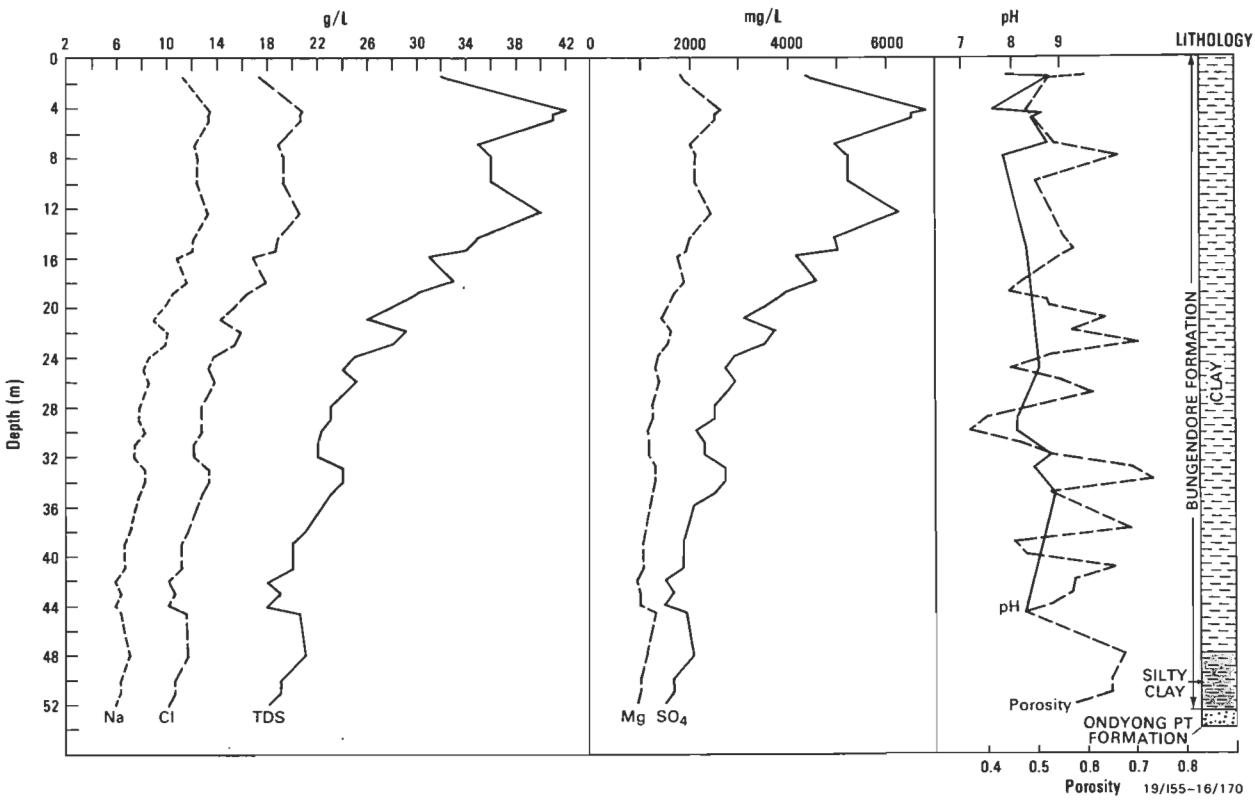

Figure 14. Pore-water chemistry and porosity, bore 354.

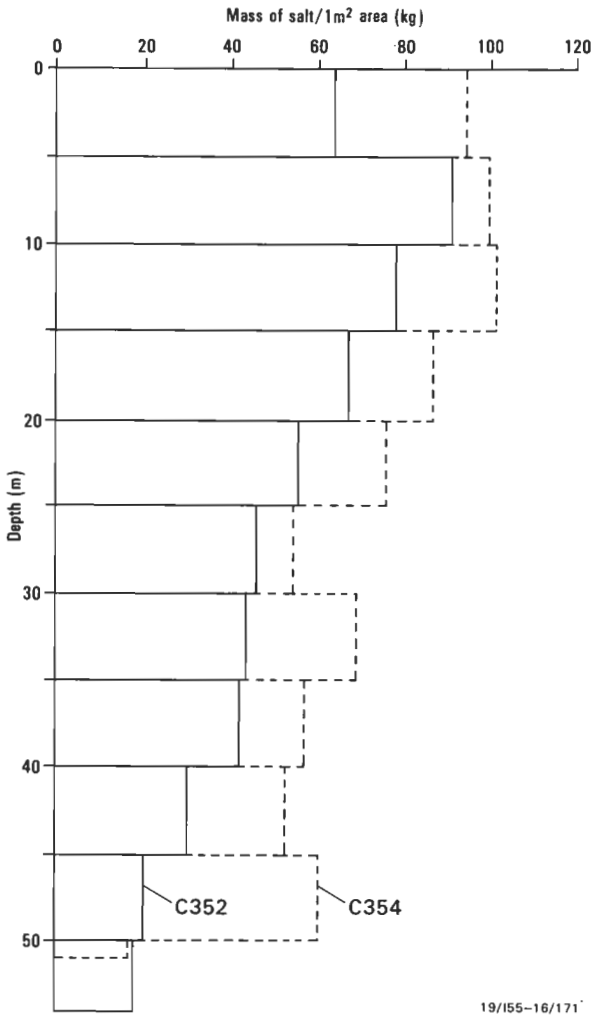

Figure 15. Salt accumulation in the aquitard beneath Lake George.

lake waters with increasing salinity. In the catchment groundwaters, saturation indices for dolomite also increase with increasing salinity. The saturation indices decrease then increase again in the saline groundwaters beneath the lake bed.

Similar trends are observed for saturation indices for calcite (Fig. 22b), except that brackish regional groundwaters are in equilibrium for calcite, i.e. $SI_C = 0$. The sample from 2 m below the lake bed has a low saturation index for both dolomite and calcite, compared with samples from 10 m depth and from lake waters. This is probably due to mixing between the lake waters and groundwaters. Two waters that are individually saturated for calcite at different CO_2 partial pressures can mix to produce a solution that is undersaturated for calcite (Bögli, 1971). At Lake George, there is mixing of two waters at different P_{CO_2}: surface waters with high P_{CO_2} and groundwaters with less P_{CO_2}, both of which are saturated for calcite and dolomite. This produces a mixed water that is not, in fact, undersaturated, but is somewhat less saturated than the two initial waters.

Saturation indices for dolomite and calcite derived from aquitard pore waters tend to be grouped separately on the diagrams (Fig. 22). They plot between the saline lake waters and equivalent aquifer waters, reflecting the dual influence of infiltrating lake water and upwards flow of groundwater.

Saturation indices for gypsum (Fig. 22c) show different trends for surface waters and groundwaters. With increasing salinity, saturation indices increase in surface waters up to a constant level at about 1000 mg/L TDS. Saturation indices for groundwaters increase with increasing salinity, and the most saline aquitard pore waters at 10 m below the lake bed are in equilibrium with gypsum. These are mixed waters and their saturation indices for gypsum are the average of two initial waters, i.e. the lake water and deeper groundwaters.

Figure 23 shows the relationship between saturation indices for dolomite and calcite and the calculated partial pressure of CO_2 for surface waters and groundwaters. For the surface waters, the plots of saturation indices show trends towards supersaturation with decreasing P_{CO_2}. As P_{CO_2} decreases towards its atmospheric value, $10^{-3.5}$, the trend line flattens. For the groundwaters there is a general trend towards supersaturation from catchment through lake-bed groundwaters, but a wide scatter of P_{CO_2} values. For lake-bed groundwaters, the degree of saturation for dolomite and calcite increases with increasing P_{CO_2} in bore 355, and with decreasing P_{CO_2} in bore 353. This relationship for lake-bed groundwaters is controlled by dissolution and precipitation reactions and mixing. The position of aquitard pore waters on these diagrams is closer to that of surface waters than of aquifer groundwaters.

Ion transfer

Ion transfer calculations trace the amount of substance (moles) gained as a result of dissolution, and lost as a result of precipitation of minerals and ion exchange, during the evolution of the lake waters and lake-bed groundwaters. These calculations are similar to those for evaporation budgets based on chloride concentration factors for continental brines (Eugster, 1970). In this study, ion transfer has been related to chloride concentration factors and compared with actual chemical analyses of Lake George groundwaters in the early phase of solute concentration (cf. Jankowski & Jacobson, 1990). Chloride is considered to be a conservative element up to the halite precipitation stage; halite only occurs as surface encrustation after long dry periods in Lake George. Tables 2 and 3 show ion transfer calculations for lake-bed groundwaters and lake waters in relation to the chloride concentration factors. For these calculations the inflow waters are taken as the freshest catchment groundwaters (Table 2) and creek waters (Table 3). The calculated gains from dissolution or losses from precipitation are plotted for individual ions against the concentration factor in Figures 24 and 25.

For lake-bed groundwaters (Fig. 24), alkalinity values decrease markedly relative to chloride as a result of precipitation of carbonate minerals. In the most saline groundwaters, the calculated loss is about 1450 mmol/L taken up in precipitation. Values of Ca, Mg, and Na decrease more slowly with calculated losses of 200, 350 and 250–350 mmol/L for these three ions. Ca and Mg are probably taken up in precipitation of carbonate minerals, and Na in ion exchange with clays. However, data from the two boreholes 353 and 355 show different

Table 1. Chemical analyses of surface waters and groundwaters.

Sample	*Depth*	*Lake stage*	*TDS mg/L*	*Na mg/L*	*K mg/L*	*Ca mg/L*	*Mg mg/L*	*HCO_3 mg/L*	*CO_3 mg/L*	*SO_4 mg/L*	*Cl mg/L*	*pH*	*Chemical types*[1]
Creek waters													
Allianoy Cr	—	1.16	100	6	6	2	2	20	0	1	7	6.1	HCO_3-Cl-Na-Mg
Butmaroo Cr	—	1.16	190	42	1	15	19	117	0	10	65	7.6	HCO_3-Cl-Na-Mg
Butmaroo Cr	—	3.17	205	37	2	14	15	101	0	43	40	7.4	HCO_3-Cl-SO_4-Na-Mg-Ca
Collector Cr	—	4.14	217	40	0	14	11	29	0	77	50	6.9	SO_4-Cl-Na-Mg-Ca
Taylors Cr	—	1.16	310	62	2	15	26	68	0	10	148	7.3	Cl-HCO_3-Na-Mg
Butmaroo Cr	—	4.12	405	49	3	38	35	276	0	3	112	7.3	HCO_3-Cl-Mg-Na-Ca
Collector Cr	—	3.76	406	57	1	38	39	148	0	33	157	7.5	Cl-HCO_3-Mg-Na-Ca
Turallo Cr	—	4.12	640	116	3	52	53	287	0	43	225	7.4	Cl-HCO_3-Na-Mg-Ca
Collector Cr	—	1.16	645	80	1	70	73	268	0	61	238	8.0	Cl-HCO_3-Mg-Ca-Na
Collector Cr	—	1.77	1190	101	2	86	122	244	0	111	440	8.0	Cl-HCO_3-Mg-Na-Ca
Catchment bores — groundwaters													
Bore 47702	76.0	1.61	156	34	1	13	9	135	0	15	18	6.8	HCO_3-Na-Mg-Ca
Bore 30823	35.0	1.69	203	45	1	13	16	134	0	11	51	7.3	HCO_3-Cl-Na-Mg
Bore LG4B	39.5	3.00	207	36	1	17	17	115	0	5	70	7.4	Cl-HCO_3-Na-Mg-Ca
Bore 30844	65.0	1.61	217	40	0	17	23	199	0	11	27	8.0	HCO_3-Mg-Na
Bore 30839	50.0	1.71	225	39	1	20	23	195	0	11	35	7.9	HCO_3-Cl-Mg-Na-Ca
Bore 30829	62.0	1.69	245	48	1	19	14	189	0	46	24	7.8	HCO_3-SO_4-Na-Mg-Ca
Collector Hotel	40.0	4.14	250	43	0	20	19	138	0	10	65	6.8	HCO_3-Cl-Na-Mg-Ca
Bore 30707	22.0	3.06	252	45	3	21	17	73	0	34	97	6.6	Cl-HCO_3 - Na-Mg-Ca
Bore 50047	64.0	2.41	279	51	2	10	34	173	0	10	87	7.2	HCO_3-Cl-Mg-Na
Bore 30844	65.0	1.05	283	54	1	12	26	250	0	17	40	7.3	HCO_3-Cl-Na-Mg-Ca
Bore 30708	28.0	3.06	298	71	3	19	17	134	0	26	99	6.9	Cl-HCO_3-Na-Mg
Bore 30706	30.0	3.06	314	66	2	24	22	131	0	22	113	7.7	Cl-HCO_3-Na-Mg-Ca
Bore 30844	65.0	2.35	338	54	5	50	17	582	0	14	113	7.9	HCO_3-Cl-Na-Ca-Mg
Bore LG7	40.0	3.00	380	83	7	24	27	195	0	40	105	8.2	HCO_3-Cl-Na-Mg
Bore 30835	57.0	1.69	421	89	1	35	35	343	0	13	80	8.4	HCO_3-Cl-Na-Mg-Ca
Bore 30809	56.0	1.51	531	134	3	22	36	211	0	31	201	8.0	Cl-HCO_3-Na-Mg
Collector	40.0	1.47	610	122	1	41	46	115	0	22	319	8.2	Cl-Na-Mg
Bore 30844	65.0	1.61	658	137	2	49	50	433	0	41	166	8.1	HCO_3-Cl-Na-Mg
Bore LG 9	39.5	3.00	695	106	1	58	60	283	0	23	265	6.7	Cl-HCO_3-Mg-Ng-Ca
Bore LG 18	38.0	3.00	822	83	1	58	60	256	0	14	250	6.5	Cl-HCO_3-Mg-Na-Ca
Bore 42933	43.0	2.76	824	83	2	58	61	239	0	31	250	6.6	Cl-HCO_3-Mg-Na-Ca
Bore LG4C	39.5	3.00	824	134	1	75	82	335	0	25	365	7.3	Cl-HCO_3-Mg-Na-Ca
Bore 42686	40.0	1.51	848	146	2	51	93	250	0	28	406	8.1	Cl-HCO_3-Mg-Na
Bore 42686	40.0	2.36	906	153	2	81	76	342	0	31	395	7.2	Cl-HCO_3-Na-Mg-Ca
Bore 30705	23.0	3.06	955	283	3	33	43	400	0	58	339	7.7	Cl-HCO_3-Na-Mg
Bore 42685	57.0	2.71	993	181	2	84	84	283	0	23	265	6.9	Cl-HCO_3-Na-Mg-Ca
Bore LG 14	56.5	3.00	993	181	2	83	84	354	0	36	432	6.9	Cl-HCO_3-Na-Mg-Ca
Bore LG 16	39.5	3.00	1220	138	2	97	73	366	0	20	375	6.7	Cl-HCO_3-Na-Mg-Ca
Bore 48089	44.0	3.08	1354	188	3	100	80	364	0	17	490	6.9	Cl-HCO_3-Na-Mg-Ca
Bore LG 17	56.5	3.00	1526	190	2	94	85	359	0	12	505	7.0	Cl-HCO_3-Na-Mg-Ca
Bore 42932	57.0	2.76	1556	190	2	94	84	395	0	19	505	7.0	Cl-HCO_3-Na-Mg-Ca
Bore 42934	47.0	2.73	1956	250	2	119	105	383	0	25	715	6.9	Cl-HCO_3-Na-Mg-Ca
Bore LG 19	45.5	3.00	2060	250	2	119	107	388	0	26	715	6.8	Cl-HCO_3-Na-Mg-Ca
Lake bed aquifers — groundwaters													
Bore 351	1	—	34766	11800	33	160	1100	726	0	3100	18210	7.4	Cl-Na
Bore 353	10	—	40602	13000	15	330	1570	732	0	4750	20570	7.3	Cl-Na
	10	—	40680	13000	0	280	1400	760	0	4900	20720	7.5	Cl-Na
	50	—	14640	4220	7	420	640	547	0	730	8350	7.4	Cl-Na-Mg
	100	—	9391	2640	4	390	400	240	0	285	5552	6.8	Cl-Na
Bore 355	10	—	45877	13550	29	465	2180	1273	0	10200	18816	7.3	Cl-SO_4-Na-Mg
	10	—	46511	14400	18	500	1825	832	0	8180	21172	7.5	Cl-SO_4-Na
	10	—	46995	14300	17	485	1820	859	0	8300	21643	7.3	Cl-SO_4-Na
	10	—	47038	13700	7	410	1930	1284	0	11200	19140	7.4	Cl-SO_4-Na-Mg
	10	—	48354	14000	19	540	2020	1014	0	11600	19619	7.7	Cl-SO_4-Na-Mg
	50	—	27596	8400	0	540	1000	511	0	2420	14980	7.5	Cl-Na
	50	—	28495	8380	9	600	1170	533	0	2880	15060	7.5	Cl-Na
	50	—	29329	8720	8	610	1230	521	0	3060	15431	7.8	Cl-Na
	50	—	30261	8700	5	660	1300	509	0	2720	16621	7.2	Cl-Na
	100	—	12147	3870	5	245	406	302	0	630	6840	7.5	Cl-Na
Lake bed aquitard — porewaters													
Bore 352	9.7	—	30220	8970	46	320	1280	760	0	4970	13880	8.16	Cl-SO_4-Na-Mg
	15	—	25850	7370	47	400	1270	530	0	2970	13260	8.42	Cl-Na-Mg
	30	—	17900	5585	50	375	785	153	0	1040	9940	8.38	Cl-Na
	47	—	12800	3430	30	465	890	82	0	690	7180	7.60	Cl-Na-Mg
Bore 354	15.5	—	38800	12030	42	509	1930	765	0	5000	18560	8.30	Cl-Na- Mg
	30	—	25300	8180	38	465	1140	389	0	2090	12660	8.10	Cl-Na
	44.6	—	21950	6340	29	600	1310	328	0	1890	11460	8.25	Cl-Na-Mg
Lake waters													
Gearys Gap	—	4.05	1350	433	5	23	25	220	0	79	615	8.1	Cl- Na
Kennys Point	—	3.17	1627	553	5	9	36	251	0	92	781	8.0	Cl- Na
Kennys Point	—	3.17	1730	585	6	22	38	263	0	97	830	7.8	Cl- Na
Gearys Gap	—	2.69	2018	670	6	53	42	279	11	114	977	8.5	Cl- Na
Lake George	—	1.16	2415	840	7	29	49	311	0	148	1176	8.0	Cl- Na
Gearys Gap	—	1.74	5640	1960	9	32	126	650	50	315	2775	8.7	Cl- Na
Kennys Point	—	1.46	7163	2504	13	22	152	930	33	325	3535	8.9	Cl- Na
Rocky Point	—	1.00	7810	2650	30	50	160	703	38	450	4050	8.7	Cl- Na
Lake George	—	1.18	9540	3350	17	31	202	845	75	545	4800	8.8	Cl- Na
Gearys Gap	—	1.46	9893	3506	17	18	205	1085	66	470	4995	8.9	Cl- Na
Lake George	—	0.30	12817	4850	26	101	200	1712	0	1480	5740	7.8	Cl- Na
Rocky Point	—	0.59	28831	10500	23	24	585	551	381	1660	15386	9.3	Cl-Na
Kennys Point	—	0.83	38900	13700	40	35	740	1515	450	2391	20160	8.9	Cl-Na
Rocky Point	—	0.60	42081	14950	34	25	1000	812	361	2700	22603	9.0	Cl-Na
Gearys Gap	—	0.83	44800	15900	47	35	860	1565	595	2823	23005	8.9	Cl-Na

[1]Classification after Szczukariew & Priklonski (Alekin, 1970)

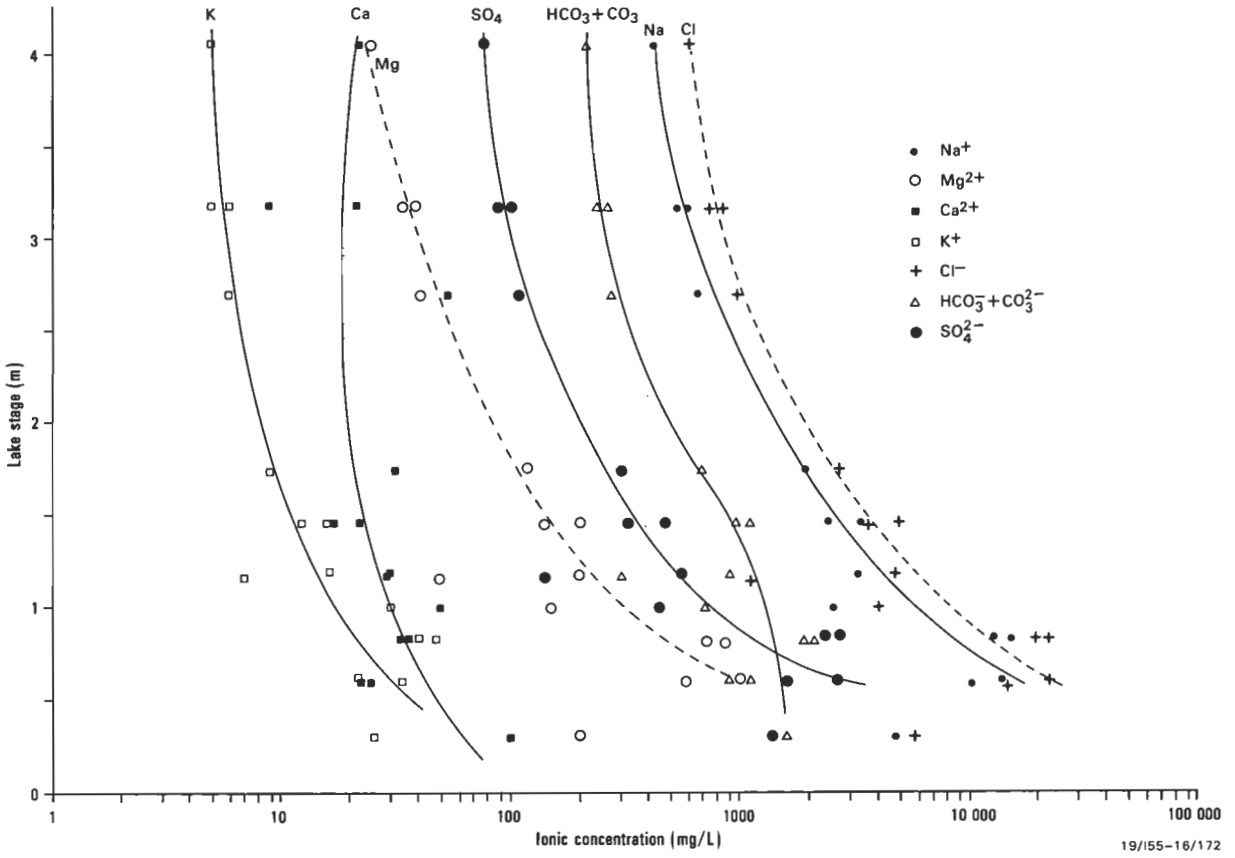

Figure 16. Compositional changes of major ions with varying lake stage and salinity.

values for losses of Mg and Na. Low values for losses of K are possibly due to this ion being partly taken up in ion exchange for clays. Apparent excessive losses of alkalinity compared with the cations are because its derivation is partly atmospheric. The SO_4 ion shows losses of 25 mmol/L in bore 355, but gains of 50 mmol/L in bore 353. These slight differences reflect the closeness to equilibrium with gypsum.

In the lake waters (Fig. 25), all ions are lost relative to chloride. Alkalinity is taken up in the precipitation of carbonate minerals, and the calculated loss is up to 800 mmol/L. When compared with the equivalent value for the groundwaters, this suggests that alkalinity is renewed by rainwater. The Ca and Mg values decrease as a result of precipitation of carbonate minerals; calculated losses are 180 and 200 mmol/L respectively. The losses of Na, K and SO_4 are up to 100 mmol/L. Na and K are possibly taken up in ion exchange with clays. The reason for SO_4 losses is not clear, as according to thermodynamic calculations, gypsum is not precipitated.

Stable isotope chemistry

Lake George groundwater samples were analysed for oxygen-18 and deuterium, the stable isotopes of water (Table 4).

The amounts of D and ^{18}O in Canberra rainfall (40 km from Lake George) vary; $\delta^{18}O$ and δD values range from −2.27 to −13.02 °/oo and from −7.6 to −94.1 °/oo respectively (C.J. Barnes, CSIRO Division of Water Resources, personal communication, 1989). The $\delta^{18}O$ — δD relationship for Canberra rainfall is shown in Figure 26. The stable isotope data plot on a line, the Local Meteoric Water Line:

$$\delta D = 8.52\ \delta^{18}O + 15.23$$

This line is close to the World Meteoric Water Line (Craig, 1961) but has a slightly greater slope and higher intercept. The greater slope probably indicates rapid evaporation of fresh water from light rainfall (Dansgaard, 1964). The higher intercept probably reflects some modification of continental air masses over the Eastern Highlands by interaction of humid air from the Pacific Ocean (cf. Gat & Carmi, 1970).

The isotopic contents of Lake George groundwaters range from +0.05 °/oo at 2 m depth to −5.48 °/oo at 100 m depth for $\delta^{18}O$ and from −0.4 °/oo at 2 m depth to −32.9 °/oo at 100 m depth for δD. All samples are enriched in ^{18}O and plot to the right of the Local Meteoric Water Line for Canberra. This suggests that these groundwaters have been affected by evaporation during or since recharge. The regression relationships between δD and $\delta^{18}O$ for groundwater samples at various depths are given in Figure 26. Although the regression lines are based on a limited number of samples, the low slope for samples from 50 and 100 m (3.0 and 4.3 respectively) implies that a high degree of evaporation has taken place in the time since recharge. These slopes are typical of evaporation into relatively dry air (cf. Gat, 1971), suggesting that recharge of these waters took place under semi-arid conditions. For 10 m deep samples, the slope is 7.3, suggesting that these waters are affected by surface evaporation (Fontes & Gonfiantini, 1967).

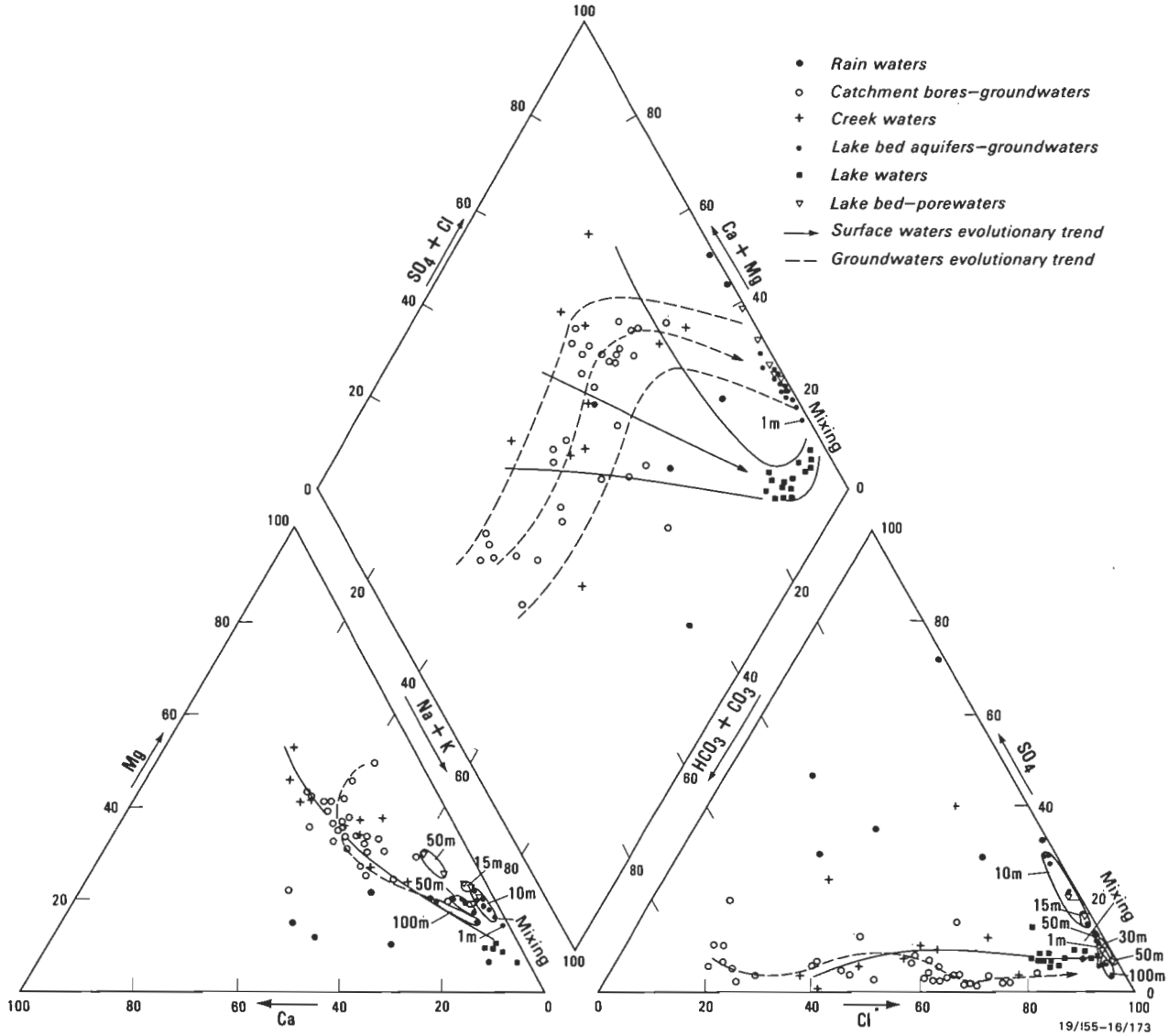

Figure 17. Trilinear diagram showing major ion hydrochemistry.

The deuterium-excess value has been calculated for groundwater samples from different depths. The deuterium-excess value, d, is given by Dansgaard (1964):

$$d = \delta D - 8\,\delta^{18}O$$

For samples at 2 m and 10 m, low values of deuterium-excess have been derived, averaging −0.8 and +0.8 respectively. Low values of deuterium-excess are elsewhere associated with extensive evaporation before infiltration (Rozanski, 1985), and this is probably the case for the shallow groundwater at Lake George. For samples from 50 m and 100 m, the average values of deuterium-excess are 2 and 9 respectively. These values indicate that relatively little evaporation occurred during the recharge process. A linear relationship between samples from 2 and 10 m suggests some mixing of evaporated surface waters and groundwaters (cf. Frape & Fritz, 1982).

Tritium and chlorine-36 determinations

Selected Lake George groundwater samples were analysed for the radioisotopes tritium and chlorine-36. Results are shown in Table 4. Significant activity of tritium (3 T.U.) was observed in groundwater at 2 m below the lake-bed, indicating that the water is probably modern (cf. Calf, 1988). A sample from a depth of 10 m contained 0.3 T.U., suggesting an age of 25–50 years. Two other samples with little or no tritium are considered more than 50 years old.

Chlorine-36 is a naturally occurring radioactive isotope with a half-life of about 301 000 years. The high solubility of the chloride ion in water makes it a useful isotope for the study of the origin and age of groundwaters. Recent Australian studies of groundwater using chlorine-36 include those of Bentley & others (1986) in the Great Artesian Basin and Davie & others (1989) in the Murray Basin. These studies indicate that processes which can affect the chlorine-36 signal include radioactive decay, subsurface production, dissolution of ancient salt evaporites, evaporation and ion filtration,

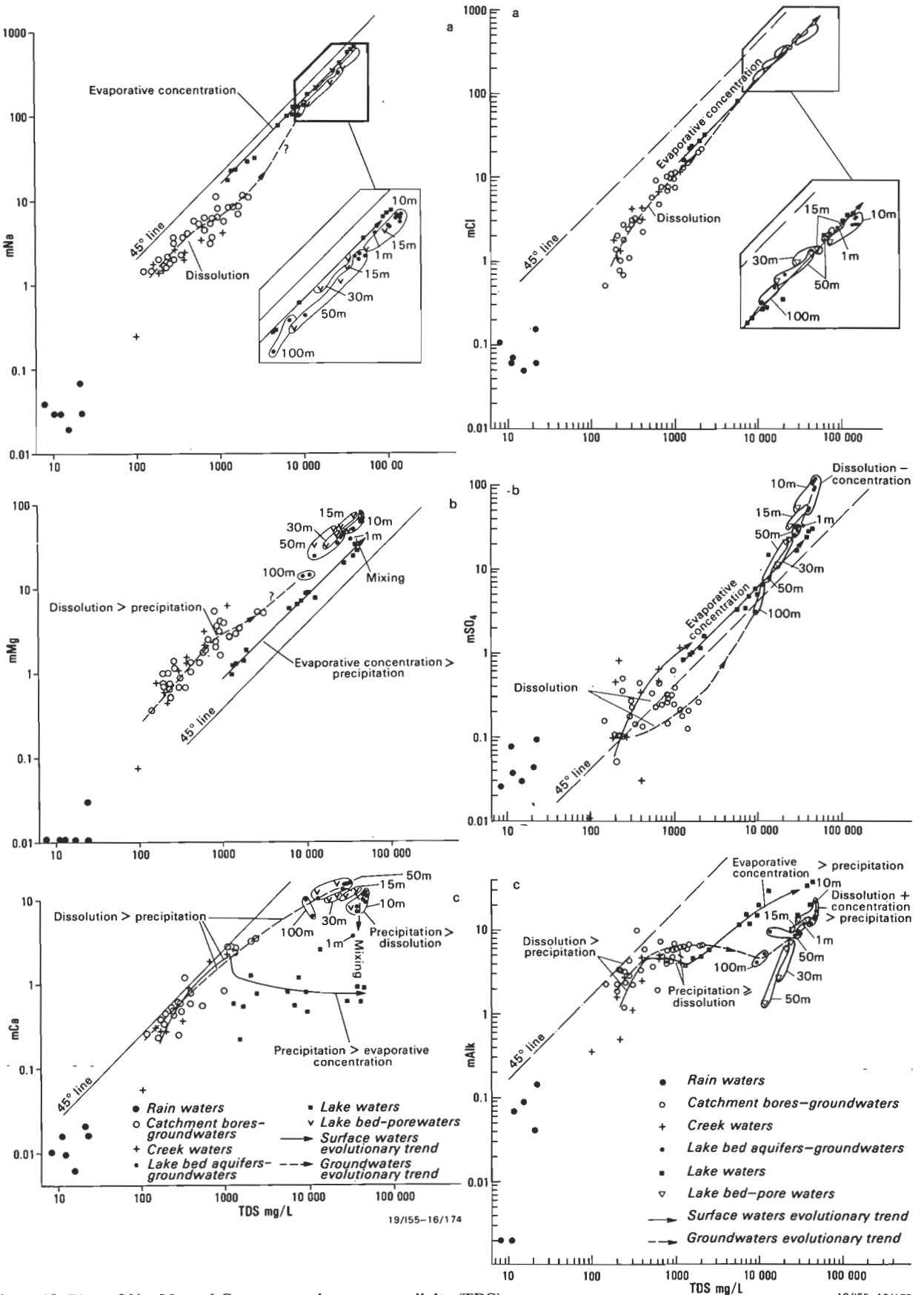

Figure 18. Plots of Na, Mg and Ca concentrations versus salinity (TDS).

mixing of two water bodies, and the addition of modern salt from atmospheric precipitation.

Figure 19. Plots of Cl, SO^4 and alkalinity concentrations versus salinity (TDS).

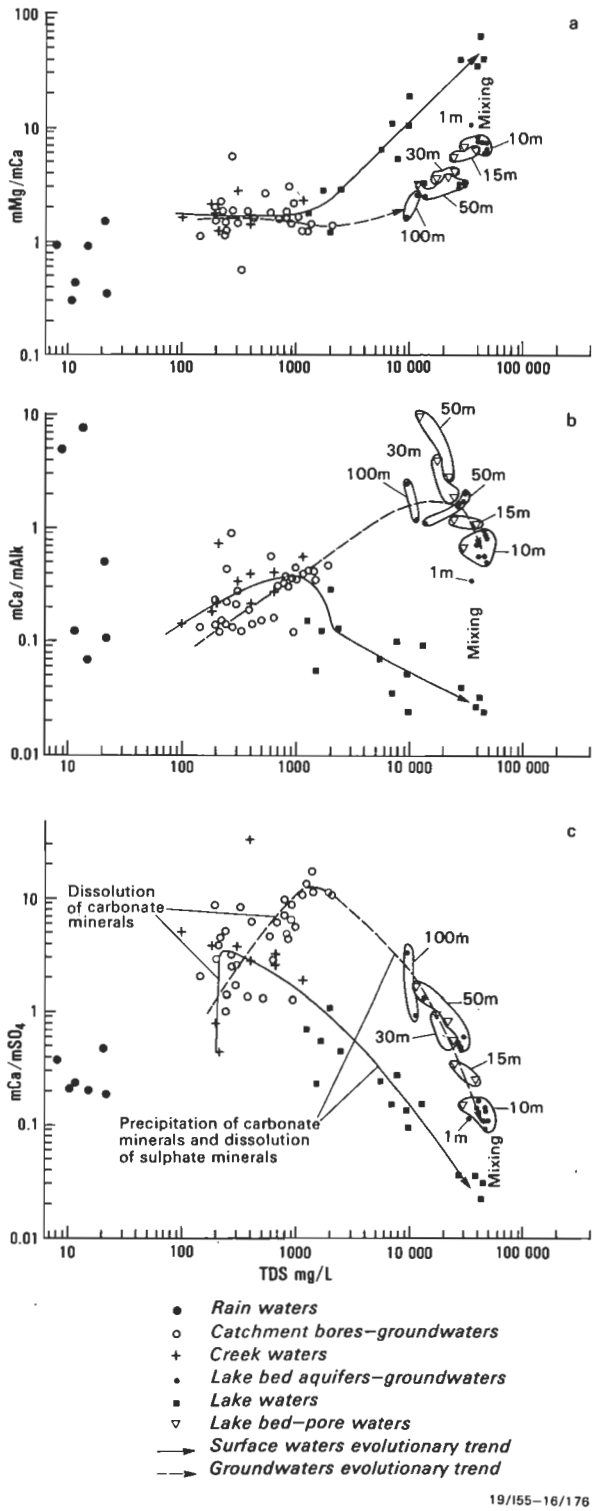

Figure 20. Plots of the ionic ratios Mg/Ca, Ca/Alkalinity and Ca/SO_4 versus salinity (TDS).

Six samples of Lake George groundwaters were analysed for chlorine-36, from two bores at 10, 50 and 100 m. A plot of $^{36}Cl/Cl$ versus $^{36}Cl/L$ is shown in Figure 27. For bore 353, diplacement of the point to the left from 10 to 50 m suggests the addition of low salinity waters, containing very little ^{36}Cl (cf. Phillips & others, 1983). From 50 to 100 m, the displacement to the left and downwards suggests decay of ^{36}Cl. For bore 355 from 10 m to 100 m, displacement of the point to the left suggests the addition of low salinity waters. There are evidently some differences in age between samples at 100 m in the two boreholes, and this may result from leakage of low salinity groundwaters from fractured rock aquifers at the lake margin into bore 355.

Figure 28 shows the relationship between ^{36}Cl and Cl concentrations in the groundwater. These contents are affected differently by various environmental processes, and this can be demonstrated with reference to a line from the origin of the plot. On this plot, relatively high concentrations of both ^{36}Cl and Cl are observed at 10 m depth where modern lake waters infiltrate. The linear relationship of the concentrations from 10 m to 100 m suggests that the dominant process is dilution.

Owing to the mixing of the waters in this system, it is not possible to derive rigorous ^{36}Cl ages from this data. The input value of the $^{36}Cl/Cl$ ratio is about 130×10^{-15} as suggested by the determined values for Lake George samples at 10 and 50 m. The standard radiometric decay equation (Bentley & others, 1986) suggests that the deeper groundwaters at 100 m are probably several tens of thousands of years old. The sample at 100 m in bore 355 is possibly more than 100 000 years old.

Discussion: hydrological processes

Hydrological processes in the Lake George basin are illustrated in Figure 29. In wet lake-full periods (Fig. 29a), salt enters the lake from creeks draining the catchment. Dilute surface water infiltrates the lake bed and balances the upwards movement of groundwater. A zone of hydrostatic balance between surface water and groundwater is evident at about 10 m below the lake bed. During drying-out phases (Fig. 29b) the lake water becomes saline through evaporation. In dry periods, conditions are playa-like; capillary-zone evaporation concentrates salt and generates saline waters in the 10 m zone below the lake bed. Salt diffuses downwards through the aquitard despite the upwards movement of groundwater. Thus salt accumulates in the wet periods and is concentrated in the dry periods, and there is some dilution in the wet periods. The low overall accumulation rate suggests that there is some recycling of salt between the surface water and groundwater systems, and some loss of efflorescent salt from the lake bed by wind action. The mechanisms for recycling may be diffusional transfer of dissolved ions from saline lake-bed porewaters to more dilute lake waters during refilling phases (cf. Lerman & Brunskill, 1971), and the transfer of ions from saline lake waters to shallow groundwaters during drying phases (cf. Lerman & Jones, 1973).

These cyclical processes might have been operating within the basin for 2×10^6 years, i.e. during the last stages of lacustrine sedimentation. The double peak of the salinity profile may indicate two periods of maximum aridity. The displacement of the salinity profile downwards may have occurred between 27 000 and 21 000 years B.P., when the 37 m deep lake overflowed through Gearys Gap (Coventry, 1976). Authigenic gypsum and halite (indicating arid periods) in the sequence of generally freshwater, lacustrine and fluvial

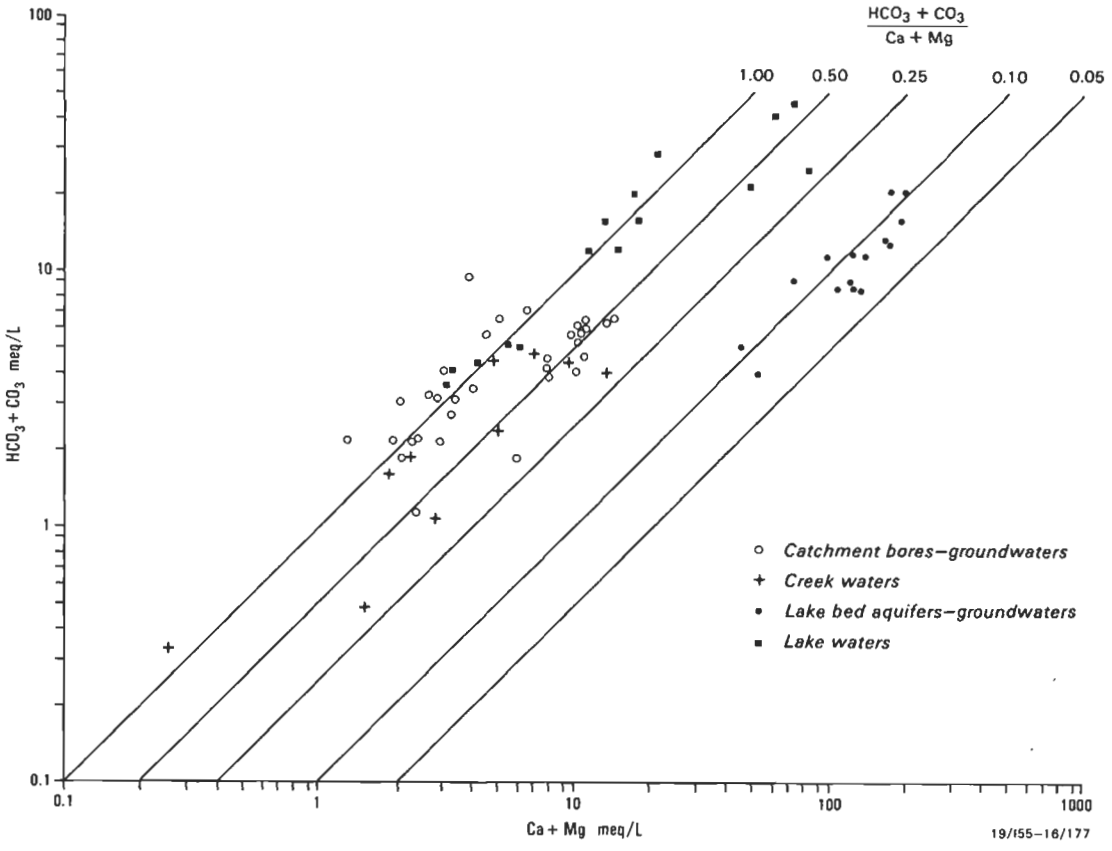

Figure 21. Plot of alkalinity ($HCO_3 + CO_3$) versus hardness (Ca + Mg).

sediments indicate older and larger climatic and hydrological fluctuations. Several different processes have contributed to the present day hydrochemistry of Lake George surface waters and groundwaters. The most important is mixing between lake waters and groundwaters in a zone of up to 15 m below the lake bed. The creek and lake waters evolve by evaporative concentration, dissolution and mineral precipitation. The regional and deeper lake-bed groundwaters evolve by dissolution and mineral precipitation in the flow system.

Figure 30 shows possible pathways of chemical evolution of Lake George waters. The fresher lake waters, up to 3000 mg/L TDS, are Cl–Na rich, and this suggests dissolution of halite crusts after dry periods. With increasing salinity, mainly because of evaporation, concentrations of all ions increase but their proportions change. The molar alkalinity concentration is greater than the molar Ca concentration throughout the change in salinity, although the ratio of molar alkalinity to molar Mg changes (Fig. 30). The ionic sequence for lake-waters up to about 10 000 mg/L TDS is $Na > Mg > Ca > K$ and $Cl > HCO_3 + CO_3 > SO_4$. In more saline lake waters the sequence becomes $Na > Mg > Ca > K$ and $Cl > SO_4 > HCO_3 + CO_3$. These changes are caused by evaporative concentration coinciding with precipitation of carbonate minerals which takes up alkalinity. The alkalinity concentration actually increases because of renewal by rainwater in lake-full conditions.

The chemistry of the shallow lake-bed groundwaters is affected mainly by mixing with lake waters, and dissolution and precipitation reactions. Deeper lake-bed and catchment groundwaters evolve through dissolution and precipitation of minerals, mainly carbonate, in the groundwater flow system. All groundwaters beneath the lake bed have the same ionic sequence, $Na > Mg > Ca > K$ and $Cl > SO_4 > HCO_3$. In these waters molar alkalinity is close to equilibrium with molar Ca. In the shallower groundwaters, the molar SO_4 concentration is greater than molar Mg, and in the deeper groundwaters molar Mg is greater than molar SO_4. Thus Lake George waters can be considered in terms of four hydrochemical types, evolving through changing molar ratios of Mg, SO_4, Ca and alkalinity (Fig. 30).

The evolutionary pathway for surface waters is simpler than that for groundwaters, reflecting mainly the evaporation of surface waters and their infiltration as Cl–Na waters. The pathway for groundwaters reflects the more complex processes pertaining to the groundwater system, especially the effects of interaction with the aquifer matrix.

Conclusions

1. The hydrological regime of Lake George is one of cyclical wet and dry conditions. Salt is transported into the lake from the catchment in wet periods. The lake salinity is inverse to water volume. In dry periods the lake acts as a playa, with capillary-zone evaporation.
2. Sand aquifers beneath the lake bed have upwards pressures directed through a clay aquitard. There is hydrostatic balance at a depth of 10–12 m beneath

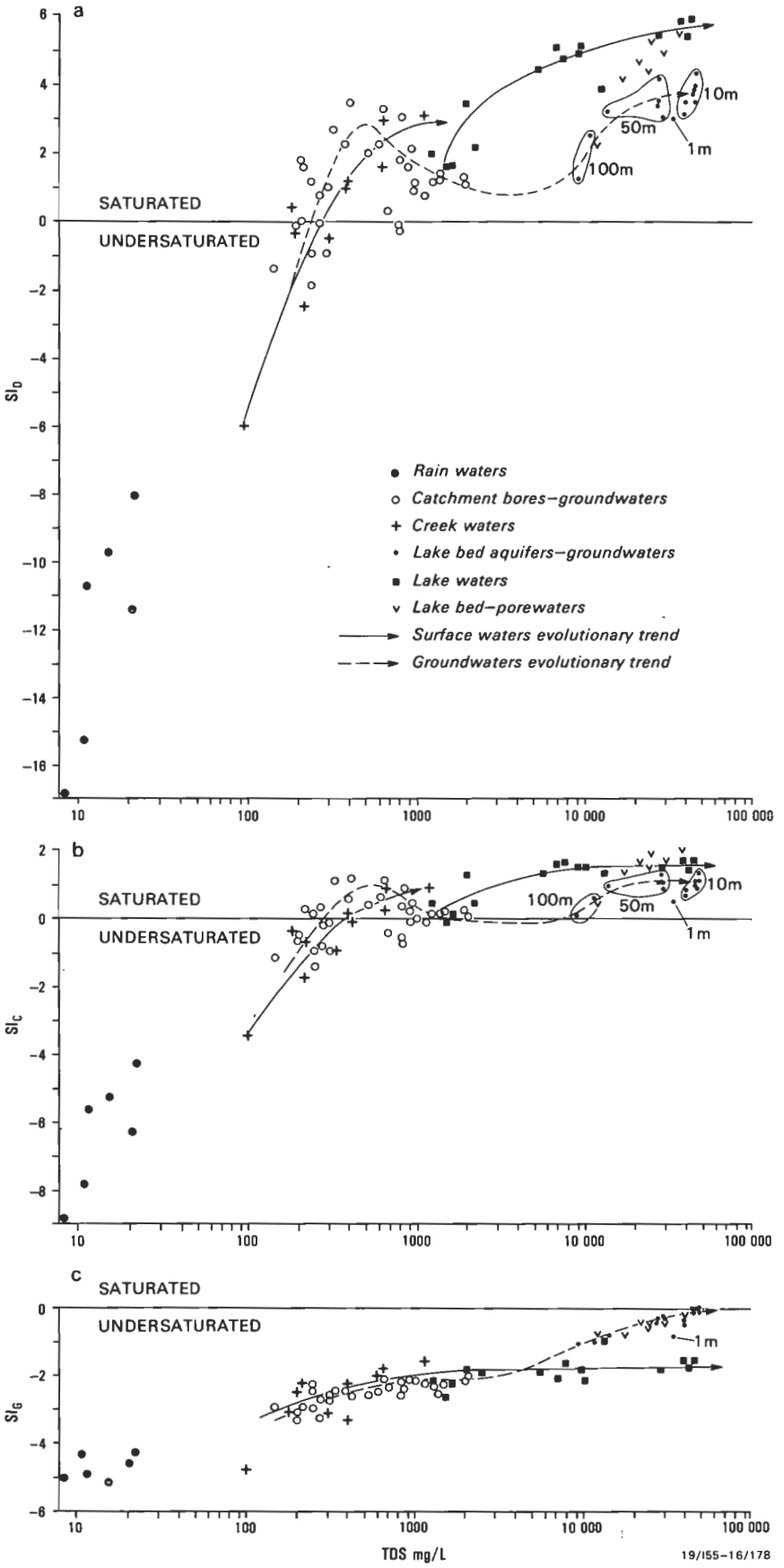

Figure 22. Saturation indices for dolomite, calcite and gypsum, as a function of salinity.

Table 2. Ion transfer calculations for Lake George, lake-bed groundwaters.

Sample	*C.F.*[1]	*Cl* mmol/L	*Na* mmol/L	*K* mmol/L	*Ca* mmol/L	*Mg* mmol/L	*Alkalinity* mmol/L	SO_4 mmol/L
Inflow waters	1	1.22	1.93	0.03	0.42	0.85	2.90	0.17
34766	421.02	0	—299.30	−11.79	−172.84	−312.61	−1209.06	−39.30
40602	475.57	0	−352.38	−13.89	−191.51	−339.63	−1367.15	−31.40
40680	479.05	0	−359.10	−14.30	−194.21	−349.59	−1376.79	−30.43
14640	193.05	0	−189.03	−5.61	−70.60	−137.76	−550.89	−25.22
9391	128.36	0	−132.90	−3.75	−44.18	−92.65	−368.31	−18.85
45877	435.02	0	−250.20	−12.31	−171.11	−280.08	−1240.70	+32.24
46511	489.49	0	−318.35	−14.22	−193.11	−340.98	−1405.88	+1.95
46995	500.39	0	−343.73	−14.58	−198.06	−350.45	−1437.05	+1.34
47038	442.52	0	−258.44	−13.10	−175.63	−269.73	−1262.27	+41.37
48354	453.59	0	−266.46	−13.12	−177.04	−302.44	−1298.79	+43.65
27596	346.34	0	−303.06	−10.38	−131.99	−253.25	−996.02	−33.69
28495	348.19	0	−307.50	−10.22	−131.27	−247.82	−1001.01	−29.21
29329	356.76	0	−309.25	−10.50	−134.62	−252.64	−1026.06	−28.79
30261	384.28	0	−363.23	−11.40	−144.93	−273.15	−1106.07	−37.01
12147	158.14	0	−136.87	−4.61	−60.31	−117.72	−453.66	−20.32

[1] Concentration factor, based on chloride
Positive value indicates gain of ions
Negative value indicates loss of ions

the lake bed and this coincides with maximum groundwater salinity.

3. A nearly linear salinity profile in the aquitard suggests that salt has diffused downwards over a long period of time. The salinity profile has been displaced downwards by the superimposition of fresh water.
4. Major-ion hydrochemistry indicates that the lake waters evolve by evaporative concentration and precipitation of carbonate minerals. Regional groundwaters evolve by dissolution, and there is mixing with infiltrating lake waters in the 10–12 m beneath the lake bed.
5. All waters in the catchment are saturated for dolomite and calcite, but undersaturated for gypsum. The mixing of lake waters with groundwater is reflected in a lesser degree of saturation.
6. Ion transfer calculations demonstrate substantial loss of HCO_3 from both lake waters and groundwater as a result of mineral precipitation. Losses of Mg, Ca, Na and K are also evident. Sulphate is lost in lake waters but gained in parts of the groundwater system through dissolution.
7. Stable isotope and tritium data confirm the effect of mixing lake waters with groundwaters in the top 12 m.
8. Chlorine-36 determinations suggest that groundwater 100 m beneath the lake bed is tens of thousands of years old.
9. Lake George is a natural analogue for a wastewater disposal basin with a thick clay aquitard; its net salt accumulation has occurred over a period of 1–2 million years.

Acknowledgements

We thank Jeff Hanor (Louisiana State University) and Ray Evans (BMR) for access to unpublished work on the Geera Clay, Keith Fifield and Raoul Davie (Australian National University) for chlorine-36 determinations of groundwater samples, Jon Olley (CSIRO Division of Water Resources) for stable isotope determinations, and Chris Barnes (CSIRO Division of Water Resources) for unpublished data on the stable isotope composition of Canberra rainfall. Graeme Calf (Australian Nuclear Science and Technology Organisation) undertook tritium determinations. The New South Wales Department of Water Resources provided water bore data for the Lake George catchment. BMR staff who provided technical assistance included Andre Zoska, Bill Keeley, Knut Reine and Greg Sparksman. We thank Ray Evans and two anonymous referees for comments on the manuscript.

Table 3. Ion transfer calculations for Lake George, lake waters.

Sample	*C.F.*[1]	*Cl* mmol/L	*Na* mmol/L	*K* mmol/L	*Ca* mmol/L	*Mg* mmol/L	*Alkalinity* mmol/L	SO_4 mmol/L
Inflow waters	1	1.05	1.23	0.08	0.30	0.43	1.30	0.19
1350	16.47	0	−1.47	−1.14	−4.36	−5.97	−17.81	−2.26
1627	20.92	0	−1.73	−1.48	−6.04	−7.41	−23.09	−2.96
1730	22.23	0	−1.95	−1.55	−6.11	−7.89	−24.60	−3.16
2018	26.17	0	−3.11	−1.85	−6.51	−9.40	−29.27	−3.72
2415	31.50	0	−2.28	−2.24	−8.71	−11.38	−35.86	−4.36
5640	74.33	0	−6.35	−5.47	−21.46	−26.42	−85.17	−10.65
7163	94.69	0	−7.78	−6.93	−27.80	−34.00	−107.33	−14.36
7810	108.48	0	−18.43	−7.56	−31.23	−39.54	−128.90	−15.64
9540	128.57	0	−12.74	−9.43	−37.72	−46.35	−152.09	−18.42
9893	133.80	0	−12.39	−9.83	−39.61	−48.45	−155.09	−20.18
12817	153.75	0	−21.48	−11.13	−43.51	−57.14	−171.85	−13.40
28831	412.13	0	−51.19	−31.03	−122.79	−151.14	−520.57	−59.95
38900	540.01	0	−69.59	−40.41	−160.80	−199.13	−669.90	−76.30
42081	605.44	0	−95.87	−45.59	−180.65	−216.25	−767.96	−85.34
44800	616.21	0	−67.82	−46.08	−183.62	−226.59	−765.78	−86.08

[1] Concentration factor, based on chloride
Negative value indicates loss of ions

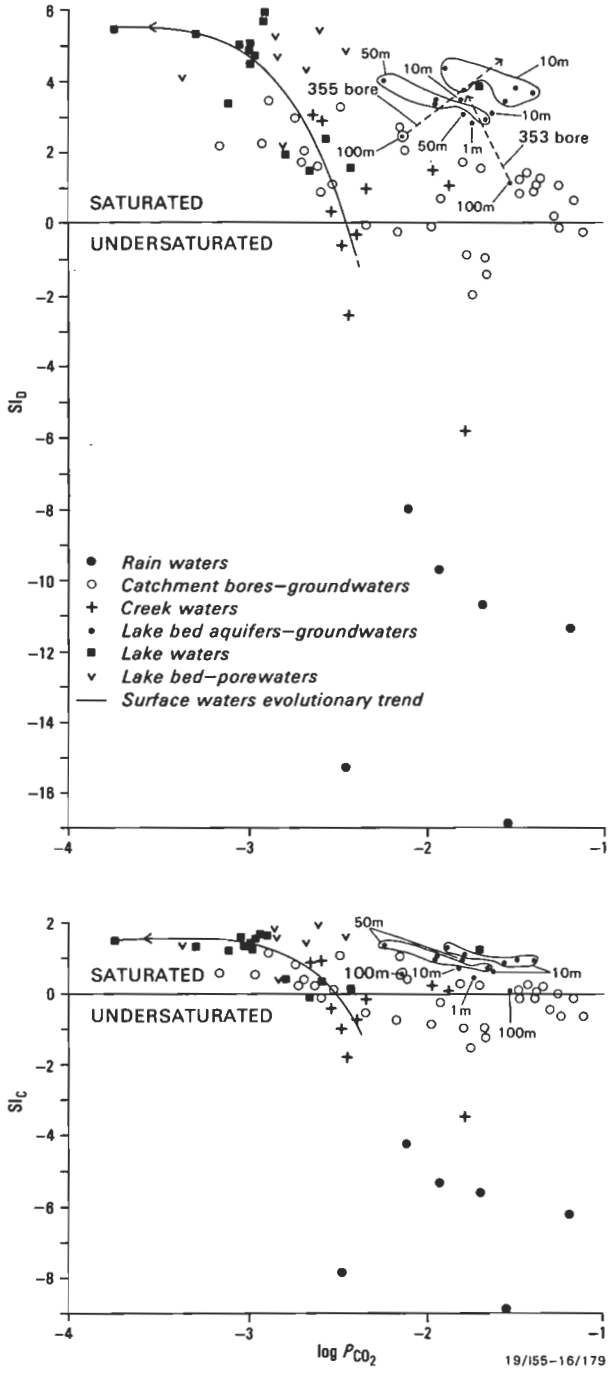

Figure 23. Relationship between partial pressures of CO_2 and saturation indices.

Table 4. Isotope data for Lake George groundwaters.

Location	Depth (m)	D (‰ SMOW)	^{18}O (‰ SMOW)	^{36}Cl ($^{36}Cl/Cl$ × ‰ 10^{-15})	^{3}H (T.U.)
355	10	−26.3	−3.32	124(± 9%)	0.3±0.3
355	10	−27.4	−3.69		
355	50	−16.8	−2.33	132(± 17%)	0.0±0.3
355	50	−14.6	−1.98		
355	100	−32.9	−5.48	113(± 11%)	0.1±0.3
353	10	−13.2	−1.70	122(± 12%)	
353	10	−15.2	−1.88		
353	50	−16.6	−2.44	121(± 7%)	
353	100	−28.7	−4.51	80(± 8%)	3.0±0.4
351	2	−0.4	+0.05		
352[1]	15	−14.79	−2.52		
352[1]	30	−13.01	−1.51		
352[1]	47	−16.83	−2.67		
354[1]	15.5	−13.80	−1.55		
354[1]	30	−11.75	−0.59		
354[1]	44.6	−15.94	−2.13		

[1]Pore waters

References

Abell, R.S., 1985 — Geology of the Lake George Basin, N.S.W. *Bureau of Mineral Resources, Australia, Record* 1985/4.

Abell, R.S., in press — The geology of the Canberra 1:100 000 sheet area, New South Wales and Australia Capital Territory. *Bureau of Mineral Resources, Australia, Bulletin* 233.

Abell, R.S., Fitzsimmons, J.L. & Slezak, T.I., 1985 — Mineralogy and major element analysis of Cainozoic sediments at Lake George, New South Wales. *Bureau of Mineral Resources, Australia, Record* 1985/20.

Alekin, O.A., 1970 — Osnovy Hydrokhimii (Principles of Hydrochemistry). *Hydrometeorologicheskoe Izdat., Leningrad.*

Bentley, H.W., Phillips, F.M., Davis, S.N., Habermehl, M.A., Airey, P.L., Calf, G.E., Elmore, D., Gove, H.E. & Torgersen, T., 1986 — Chlorine-36 dating of very old groundwater. I, The Great Artesian Basin, Australia. *Water Resources Research*, 22, 1991–2001.

Bögli, A., 1971 — Corrosion by mixing of karst waters. *Transactions, Cave Research Group, Great Britain*, 13, 109–114.

Bowler, J.M., 1986 — Spatial variability and hydrologic evolution of Australian lake basins: analogue for Pleistocene hydrologic change and evaporite formation. *Palaeogeography, Palaeoclimatology, Palaeoecology*, 54, 21–41.

Burton, G.M., 1972 — Lake George, N.S.W. Notes for sedimentologists excursion, November 1970. *Bureau of Mineral Resources, Australia, Record* 1972/79.

Burton, G.M., 1977 — Recharge conditions and the siting of bores in fractured-rock aquifers of the A.C.T. *Bureau of Mineral Resources, Australia, Report* 173.

Calf, G.E., 1988 — Tritium activity in Australian rainwater 1962–1986. *Australian Nuclear Science and Technology Organisation, Report* ANSTO/E680.

Coventry, R.J., 1976 — Abandoned shorelines and the late Quaternary history of Lake George, New South Wales. *Journal of the Geological Society of Australia*, 23, 249–273.

Craig, H., 1961 — Isotopic variations in meteoric waters. *Science*, 133, 1702–1703.

Dansgaard, W., 1964 — Stable isotopes in precipitation. *Tellus*, 16, 436–468.

Davie, R.F., Kellett, J.R., Fifield, L.K., Calf, G.E., Evans, W.R., Bird, J.R., Topham, S. & Ophel, T.R., 1989 — Chlorine-36 measurements in the Murray Basin: preliminary results from the Victorian and South Australian Mallee region. *BMR Journal of Australian Geology & Geophysics*, 11, 261–272.

Eugster, H.P., 1970 — Chemistry and origin of the brines of Lake Magadi, Kenya. *Mineralogical Society of America, Special Paper* 3, 213–235.

Evans, W.R., 1987 — Hydrogeology of the Australian Capital Territory and environs. *Bureau of Mineral Resources, Australia, Report* 263.

Fontes, J.C. & Gonfiantini, R., 1967 — Comportement isotopique au cours de l'evaporation de deux Bassins Sahariens. *Earth and Planetary Science Letters*, 3, 258–266.

Frape, S.K. & Fritz, P., 1982 — The chemistry and isotopic composition of saline groundwaters from the Sudbury Basin, Ontario. *Canadian Journal of Earth Sciences*, 19, 645–661.

Gat, J.R., 1971 — Comments on the stable isotope method in regional groundwater investigations. *Water Resources Research*, 7, 980–993.

Gat, J.R. & Carmi, I., 1970 — Evolution of the isotopic composition of atmospheric waters in the Mediterranean Sea area. *Journal of Geophysical Research*, 75, 3039–3048.

Harvie, C.E., Møller, N. & Weare, J.H., 1984 — The prediction

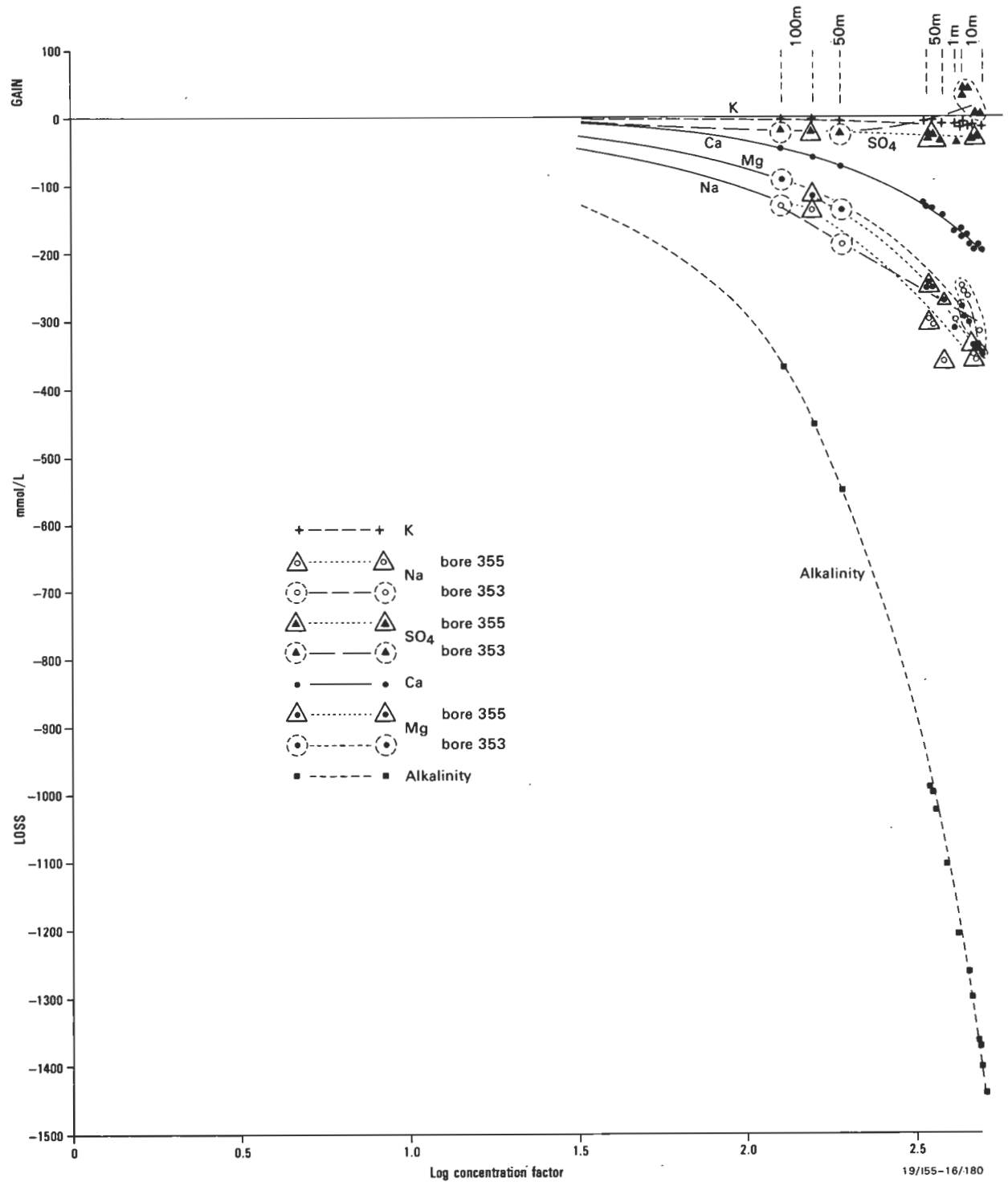

Figure 24. Ion transfer as a function of chloride concentration factor, lake-bed groundwaters.

of mineral solubilities in natural waters: the Na–K–Mg–Ca–H–Cl–SO_4–OH–HCO_3–CO_3–CO_2–H_2O system to high ionic strengths at 25°C. *Geochimica et Cosmochimica Acta*, 48, 723–751.

Harvie, C.E. & Weare, J.H., 1980 — The prediction of mineral solubilities in natural waters: the Na–K–Mg–Ca–Cl–SO_4–H_2O system from zero to high concentration at 25°C. *Geochimica et Cosmochimica Acta*, 44, 981–997.

Jacobson, G. & Schuett, A.W., 1979 — Water levels, balance, and chemistry of Lake George, New South Wales. *BMR Journal of Australian Geology & Geophysics*, 4, 25–32.

Jankowski, J. & Jacobson, G., 1990 — Hydrochemical processes in groundwater-discharge playas, central Australia. *Hydrological Processes*, 4, 59–70.

Lerman, A. & Brunskill, G.J., 1971 — Migration of major constituents from lake sediments into lake water and its bearing on lake water composition. *Limnology and Oceanography*, 16, 880–890.

Lerman, A. & Jones, B.F., 1973 — Transient and steady-state salt transport between sediments and brine in closed lakes. *Limnology and Oceanography*, 18, 72–85.

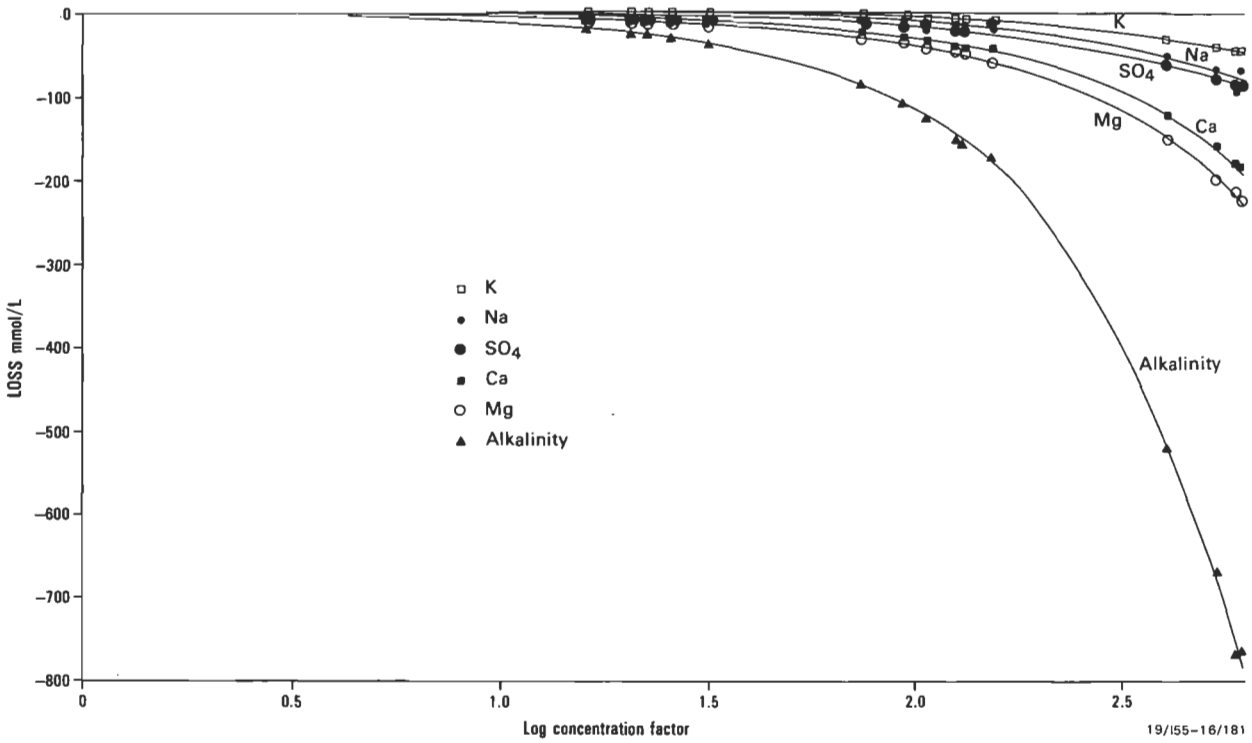

Figure 25. Ion transfer as a function of chloride concentration factor, lake waters.

Macumber, P.G., 1983 — Interactions between groundwater and surface systems in Northern Victoria. *Ph.D. thesis, University of Melbourne*, 506 pp.

Manheim, F.T. & Waterman, L.S., 1974 — Diffusimetry (diffusion constant estimation) on sediment cores by resistivity probe. *In* C.C. von der Borch, J.G. Sclater, S. Gartner, R. Hekinian & D.A. Johnson, *Initial Reports of the Deep Sea Drilling Project*, 22, 663–669.

Mason, J.M., 1987 — Palaeomagnetics and a soupcon of palynology for Lake George, N.S.W. *Abstracts, Conference on Cenozoic of the Australian Region, Warrnambool, Victoria, 1987* (unpublished.)

Ollier, C.D., 1978 — Tectonics and geomorphology of the Eastern Highlands. *In* Davies, J.L. & Williams, M.A.J. (editors), Landform evolution in Australasia. *Australian National University Press, Canberra*, 5–47.

Phillips, F.M., Smith, G.I., Bentley, H.W., Elmore, D. & Gove, H.E., 1983 — Chlorine-36 dating of saline sediments: preliminary results from Searles Lake, California. *Science*, 222, 925–927.

Pitzer, K.S., 1973 — Thermodynamics of electrolytes I: Theoretical basis and general equations. *Journal of Physical Chemistry*, 77, 268–277.

Rozanski, K., 1985 — Deuterium and oxygen-18 in European groundwaters – links to atmospheric circulation in the past. *Chemical Geology*, 52, 349–363.

Russell, H.C., 1886 — Notes upon floods in Lake George. *Journal and Proceedings, Royal Society of New South Wales*, 20, 241–260.

Singh, G. & Geissler, E.A., 1985 — Late Cainozoic history of vegetation, fire, lake levels and climate, at Lake George, New South Wales, Australia. *Philosophical Transactions, Royal Society of London, B*, 311, 379–447.

Singh, G., Opdyke, N.D. & Bowler, J.M., 1981 — Late Cainozoic stratigraphy, palaeomagnetic chronology and vegetational history from Lake George, N.S.W. *Journal of the Geological Society of Australia*, 28, 435–452.

Taylor, T.G., 1907 — The Lake George Senkungsfeld, a study of the evolution of Lakes George and Bathurst. *Linnaean Society of New South Wales, Proceedings*, 32, 325–345.

Torgersen, T., 1984 — Wind effects on water and salt loss in playa lakes. *Journal of Hydrology*, 74, 137–149.

Truswell, E.M., 1984 — Lake George: preliminary palynology of deep sediments. *BMR Research Newsletter*, 1, 12–13.

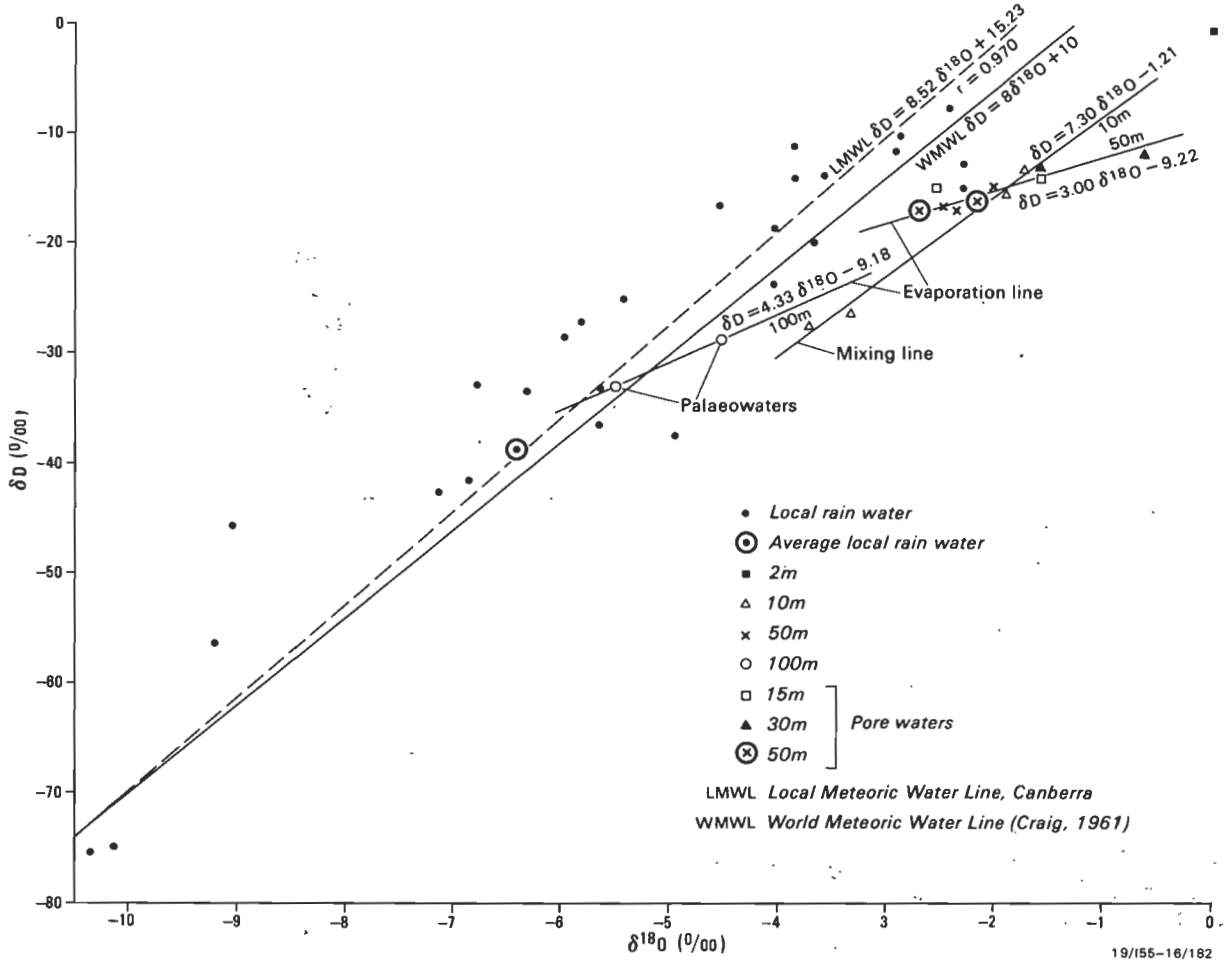

Figure 26. Relationships between stable isotope contents of rainwater and groundwater.

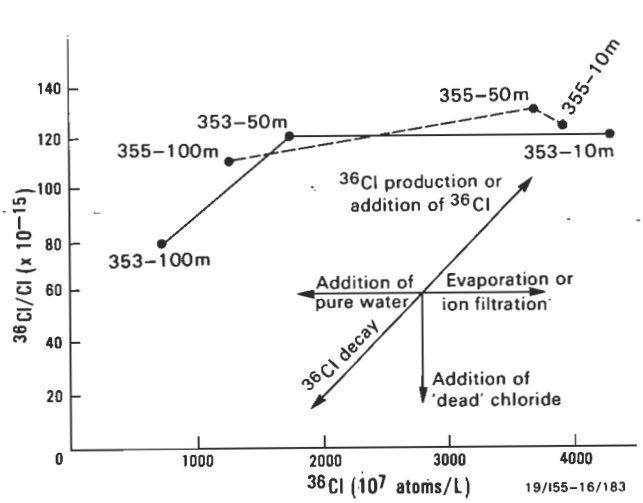

Figure 27. Relationship between $^{36}Cl/Cl$ ratio and ^{36}Cl concentration in lake-bed groundwaters.

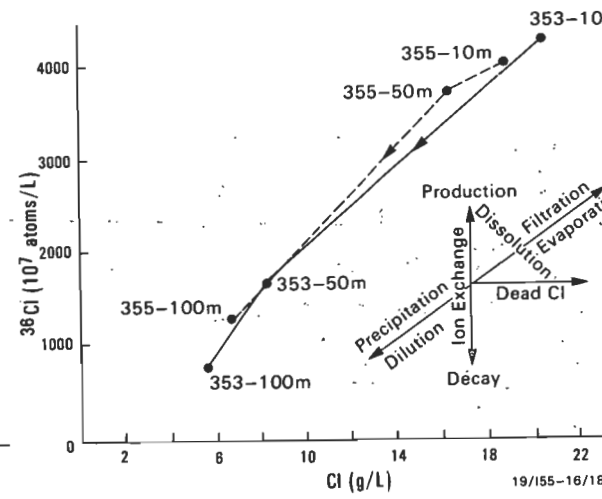

Figure 28. Relationship between ^{36}Cl and Cl concentrations in lake-bed groundwaters.

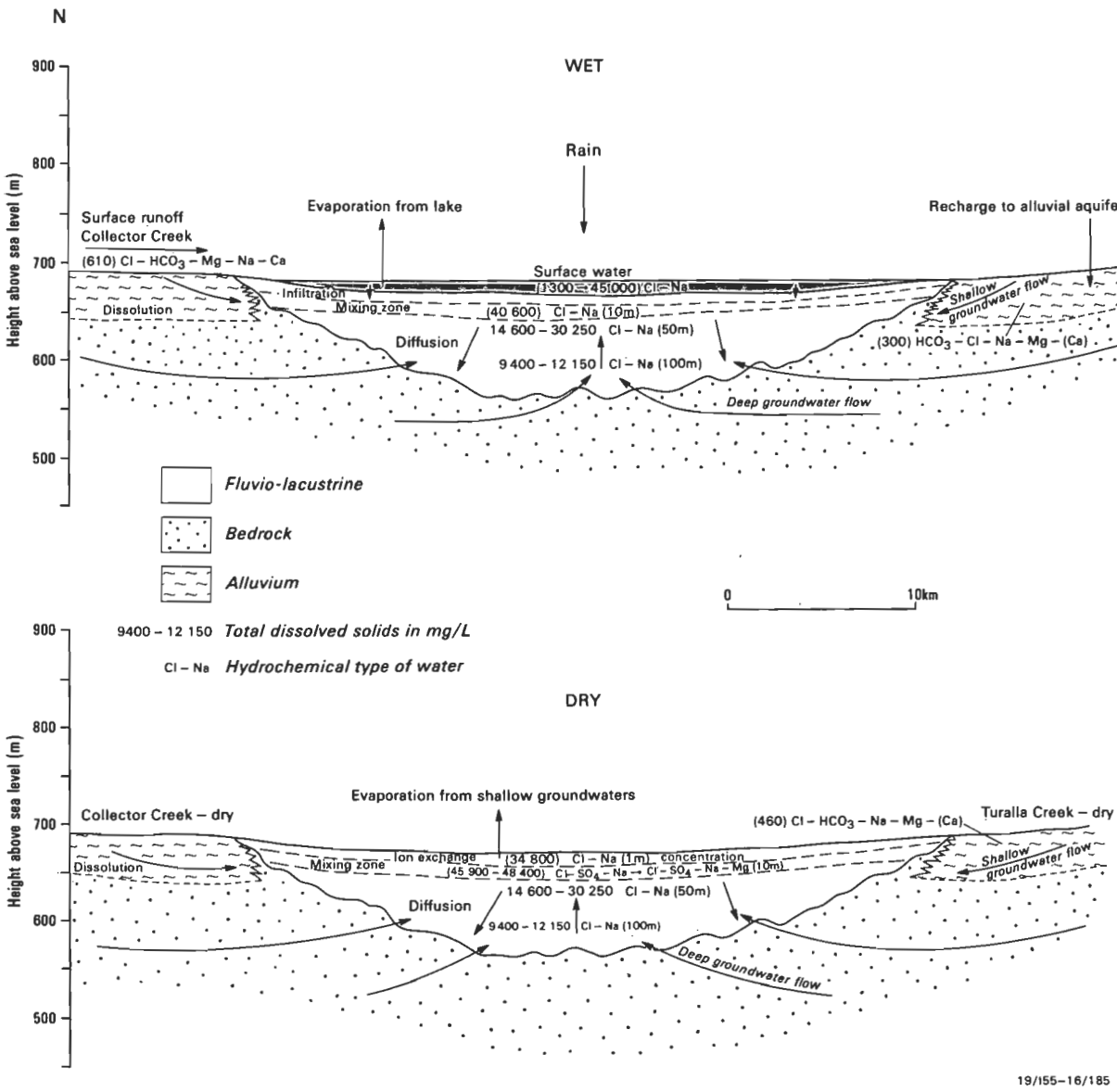

Figure 29. Processes in the wet and dry cycles of Lake George.

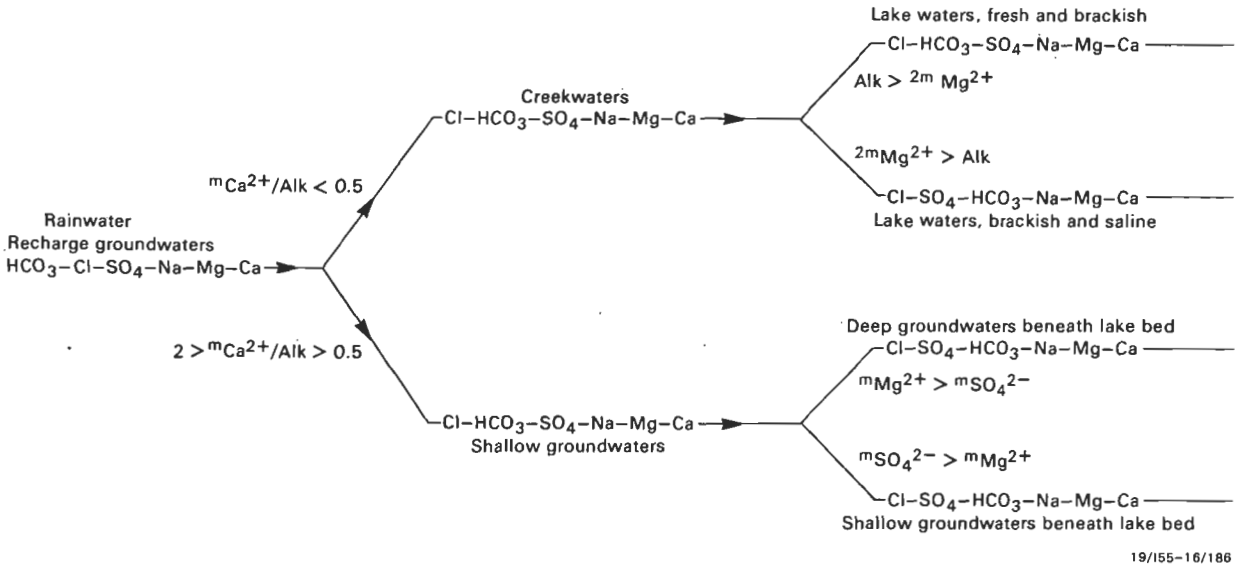

Figure 30. Possible model for hydrochemical evolution.

BMR Journal of Australian Geology & Geophysics, 12, 191–193

Indian Ocean earthquake felt in Australia 19 November 1906

P.J. Gregson[1] & I.B. Everingham[2]

Introduction

One of the difficulties in determining earthquake risk in Australia is the relatively short period of reliable instrumental recording. The Chinese consider that a minimum period of 200 years is necessary as a basis for risk assessment. In Australia, instrumental recording began at Perth in 1901 and Melbourne in 1902 (Doyle & Underwood, 1965). It was not till the 1960s that a reliable network of seismographs began to develop in Australia.

It is therefore important that as much information as possible be collated from historical records and old newspaper reports, to compute magnitudes and epicentres of early large or important earthquakes, to improve the data base used for present earthquake risk assessment. Much information on pre-instrumental earthquakes in Western Australia has been gathered by Everingham (1968) and Everingham & Tilbury (1972).

The authors have investigated a large earthquake which was felt widely in Western Australia in 1906. This earthquake occurred at 0718 UTC (Universal Coordinated Time) on 19 November 1906 and was tentatively located about 400 km offshore from North West Cape. The magnitude was 7¾ (Ms) Gutenberg & Richter (1954).

From a newspaper search, I.B. Everingham identified 21 localities which reported having felt this earthquake and P.J. Gregson prepared an isoseismal map (Fig. 1). Earthquake locations were determined by Gutenberg & Richter (1954) and Stover (1966). The maximum intensity (MM V) was recorded at Carnarvon, where bottles fell from shelves. An intensity of MM IV was felt at Albany, about 1700 km from the epicentre. The following is an extract from the Daily News paper for 19 November 1906.

> 'Telegraphic reports have been received at the Perth Observatory from the various stations:
> Marble Bar — Distinct earth tremor felt here 3.20 p.m. Shook buildings, making loud, rumbling noise. Small particles of plaster fell from the ceiling.
> Cossack — Slight sensation earthquake 3.23 p.m. Duration, 1 ½ minutes.
> Sharks Bay — Experienced slight earth shock, with rumbling noise 3.25 to 3.26 p.m.
> Hamelin Pool — Slight tremor accompanied by dull rumblings lasting from 3.23 to 3.26 p.m.
> Cue — Strong earth tremor lasting nearly 3 minutes felt here, commencing 3.28 p.m.
> Peak Hill — Three severe earthquakes lasting fully 2 minutes commenced 3.28. Felt by all town.
> Geraldton — At 3.24 p.m. an earth tremor passed over Geraldton, shaking all large buildings in the town; also distinctly felt at Narattarra, 11 miles distant from Geraldton.
> Newcastle — Felt an earth tremor at 3.20 p.m. today.
> Bridgetown — Distinct earth tremor felt here today at 3.27 p.m., lasting fully for one minute.
> Busselton — Severe earth tremor, shook lighthouse violently for about 10 seconds at 3.25 p.m.
> Albany — Slight earth tremor felt here at 3.28 this afternoon'.

The earthquake was also felt on board the vessel RMS *Omrah*. The Daily News paper states that

> 'Commander Symons of the R.M.S. Omrah, which arrived at Fremantle from London on Thursday morning reported that at 2.30 p.m. on Monday last, in latitude 21.27° south, longitude 104.50° east, a severe shock was experienced, the vessel trembling violently for two or three minutes. It was at first thought that some wreckage had been struck, or that a whale had got foul of the ship, or that something had gone wrong in the engine-room. These causes not being found correct, the captain told his officers that it was probably a submarine volcano or earthquake. Soundings on the chart at the time showed 1800 fathoms. The nearest point of land was North West Cape, 510 miles eastward. The Greenwich mean time was 7 hours, 18 minutes a.m.'

A Commonwealth Bureau of Meteorology publication (1929) quotes the same extract, except that the ship's location is given as 21° 27'S and 105°50'E. Obviously, minutes and decimal degrees have been confused and a transcription error made by one of the reporters. This discrepancy has not been resolved; the distances quoted from the coast are consistent. It is more likely that the newspaper report is incorrect. Decimal degrees were rarely if ever used then, and the distance from shore is compatible with the position reported by the Bureau of Meteorology (plotted in Fig. 1).

Location

The earthquake origin time and location have been determined previously as follows:

07 18 24 UTC, 22°S 109°E M = 7¾ (Gutenberg & Richter, 1954)

07 18 41 UTC, 19.1°S 111.8°E M = 7¾ (Stover, 1966)

These locations are shown in Figure 1. From the P and S arrival times recorded at the Perth Observatory, the calculated origin time was 07 18 43 UTC, which agrees with the origin time given by Stover.

The S–P time of 1 min 48 s at Perth indicates an epicentral distance of 1120 km from Perth, which is 400 km closer to Perth than the Gutenberg–Richter and Stover locations and the position of the RMS *Omrah*. Using the earliest origin time (17 18 24) and the latest possible time for the shock being felt on the vessel (17 18 30, from the Captain's log) then the shock wave took only 6 s to reach the vessel. If the shock experienced by the vessel was the P-wave, the maximum distance of the vessel from the epicentre would have been about 30 km. If the epicentre was further west than the Gutenberg & Richter location, we consider that the origin time and the Captain's log would tally better. A

[1]Mundaring Geophysical Observatory, Bureau of Mineral Resources, Geology & Geophysics, Mundaring WA 6073
[2]1/38 Riverside Drive, East Fremantle WA 6158

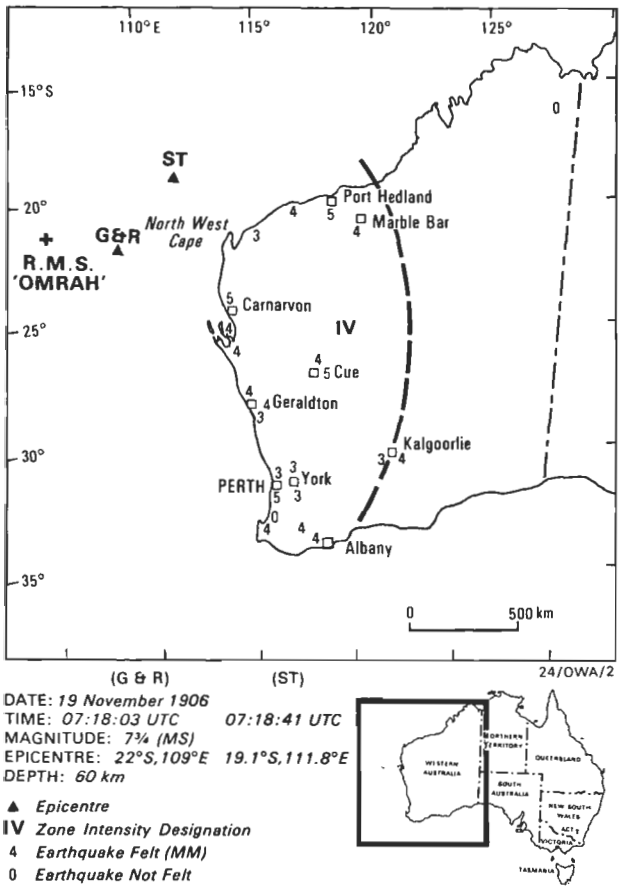

Figure 1. Isoseismal map of the Indian Ocean earthquake 19 November 1906
G & R Gutenberg & Richter (1954) location
ST Stover (1966) location

more westerly epicentre, nearer the position of the RMS *Omrah*, would be consistent with the shape of the MM IV isoseismal.

The mean radius (1700 km) would, however, be about 15% greater than that for a similar-sized earthquake near Indonesia on 19 August 1977 (Gregson & others, 1979). Using the formula given by Greenhalgh & others (1988)

$M_L = 0.38 (\log R_{iv})^2 + 0.49 (\log R_{iv}) + 2.38$

where R_{iv} is the radius of the MM IV isoseismal, the calculated Richter magnitudes for the different locations are:

Gutenberg & Richter	$M_L = 7.7$	(1420 km)
Stover	$M_L = 7.6$	(1290 km)
Omrah	$M_L = 8.0$	(1700 km)

These magnitudes correspond to Ms values of 7.55, 7.5 and 7.8 respectively, using the relationship given by McGregor & Ripper (1976). The magnitudes are consistent with those given by Gutenberg & Richter.

Verse and Worse

The earthquake lead E.G. Murphy to write the following verse in his 'Verse and Worse' column in the Sunday Times, 25 November 1906.

The Dryblower's Doggerel — 'The Quake'

The 'Sunday Times' astronomer tame, set out to trace the 'quake,
That softly sloped as it softly came, with wonderment in its wake;
And climbed the hill where cautious Cooke prepares for ratepayers' meek,
the storms and sunshine cronk and crook that happened yesterday weak,
'O, where,' he asked 'shall I find a guide to traverse the line of 'quake?'
'Go ask of the fusel far and wide', Astronomer Cooke upspake.
He zig-zagged down to the Melbourne big, beloved of Dr Taafe,
and there in the bar where speed gets tight and the bumptious boss-cop offers
to fight he traced a (bar) disturbance slight on his sensitive seismograph.

He traced it down to Daly's pub, and its subterranean rink,
where the girls who want returns of grub are pelted out on their pink,
Then to the 'City' it slewed aside, where the cheap Celestial roams,
and where the barmaids, plump and wide, Hosannqah the name of Holmes;
It swung across to Wilson Dunne's, (of Bungs the burly beau),
which Chaffy Nicholls, sometimes shuns, for geographical show.
And then it slewed to Glowrey's bar, where daily scriveners quaff,
and nonentities shout the bribeful booze for an M.A.P. in the 'Daily Ooze',
while the shock of Ro..?..nns' Penguin cruise assaults the seismograph.

Straight to the shamrock old it tracked, with many a heave and roll,
where Tess and Min. their trunks have packed, large labelled 'Metropole'.
And then with rattle, rumble and jar it richochetted, rocked and roared,
the marble steps to the balcony bar beloved of Milo Maude.
Down to the gay Cremorne it broke, and flew with feverish feet where
Leonard Davis's 'buy-owe' bloke is 'pile'-ing it on a treat,
thence it jumped to Grenike's Cri. whose belle has a bonza calf
then off to Wheatley's parson pub, where beer is (dicken) sold with grub,
but where the language managed to rub big breaks in the seismograph.
The Grosvener heard it rumble by, where the winkful Teddy Wells
oft glues an ardent, amorous eye on pert and passing belles.
Swiftly it shuddered to Goderich Street reminding the bachelor bung
of the days when he heard the war-drums beat at the battle of Dumbleyung
Shocking the earth it passed along to 'Dunks' beside the brine,
where Payne, who once was hot and strong, is ordered to bed at nine.
Ordered to bed, and told that he must never love nor laugh,
but memories pink and memories blue, and thoughts of what he'd like to do —
if it wasn't for jealous number two — unsettled the seismograph.

Conclusion

The information gathered from the search of old newspapers shows that the 1906 earthquake resulted in MM IV intensities up to 1700 km from the epicentre. The epicentre is probably (up to 500 km) further west than that given by Gutenberg & Richter. The isoseismal radius is consistent with a magnitude of MS = 7¾. This is the largest intraplate earthquake known to have occurred in the Australian region.

Acknowledgement

This study was instigated by Kevin McCue (BMR), who provided helpful suggestions during the course of the study.

References

Commonwealth Bureau of Meteorology (1929) — Results of rainfall observations made in Western Australia (for all years of record up to 1927). *Government Printer, Melbourne.*

Doyle, H. & Underwood, R., 1965 — Seismological stations in Australia. *Australian Journal of Science*, 28, 40–43.

Everingham, I.B., 1968 — Seismicity of Western Australia. *Bureau of Mineral Resources, Australia, Report* 132.

Everingham, I.B. & Tilbury, 1972 — Information on Western Australian earthquakes 1949–1960. *Royal Society of Western Australia, Journal*, 55, 90–95.

Greenhalgh, S.A., Denham, D., McDougall, R. & Rynn, J.M. 1988 – Intensity relations for Australian earthquakes. *Tectonophysics*, 166, 255–267.

Gregson, P.J., Paull, E.P. & Gaull, B.A., 1979 — The effects in Western Australia of a major earthquake in Indonesia on 19 August 1977. *BMR Journal of Australian Geology & Geophysics*, 4, 135–140.

Gutenberg, B. & Richter, C.F., 1954 — Seismicity of the earth and associated phenomena. *Princeton University Press, Princeton N.J.* (2nd edition).

McGregor, P.M. & Ripper, I.D., 1976 — Notes on earthquake magnitude scales. *Bureau of Mineral Resources, Australia, Record* 1976/56.

Stover, C.W., 1966 — Seismicity of the Indian Ocean. *Journal of Geophysical Research*, 71, 2575–2581.

New Zealand Journal of Geology and Geophysics

ISSN 0028–8306

For more than 30 years, **NZJGG** has been the standard reference for research in the Earth sciences from New Zealand and the Southwest Pacific. Now there is greater emphasis on relating this research to the whole Pacific Basin — from Antarctica and Australia to Japan and the Americas. This places the journal at the hub of geological investigation within the entire Pacific Rim.

Scope

NZJGG publishes original research papers in all aspects of the Earth sciences, including geology, geophysics, soil science, and the atmospheric sciences, relevant to New Zealand, the Southwest Pacific, and Antarctica. Manuscripts which place this research in a broader Pacific and global context are especially welcome. Review articles, preliminary notes, Letters to the Editor, book reviews and thesis summaries are also published.

All papers are internationally refereed by experts in their respective fields.

NZJGG is abstracted in: Aquatic Science and Fisheries Abstracts; Bibliography and Index of Geology; Biological Abstracts; Bulletin Signaletique; Chemical Abstracts; Current Contents; GeoArchive; INIS Atomindex; IRL Life Sciences Collection; Mineralogical Abstracts; Oceanic Abstracts; Pollution Abstracts; Science Citation Index; SIRIS/STIX.

Subscription rates cover 4 issues of the journal published between January and December.

Back issues are available. The price will be advised upon application.

New Zealand/Australia

1991 Institutional rate	NZ$210.00
1991 Individual rate	NZ$105.00
N.Z./Australian scientific society rate	NZ$ 50.00

Outside New Zealand and Australia

1991 Institutional rate	US$180.00
1991 Individual rate	US$ 50.00

Journals are despatched to subscribers via surface air lift for prompt delivery.

Manuscripts should be submitted to the editor at our New Zealand Office.

To order, fill in this form and return today.

❑ Yes! I want to subscribe to NZJGG.

Subscription Department
DSIR Publishing
P.O. Box 9741
Wellington, New Zealand
Tel. (04) 858-939
Fax. (04) 850–631

North American subscribers send to:
DSIR
810 East 10th Street
P.O. Box 1897
Lawrence, Kansas, USA 66044–8897
Tel. (913) 843-1221
Fax. (913) 843-1274

Payments to this office must be US$ drawn on a US bank or credit card

Name _____

Address _____

City: _____ St/Province: _____ Zip Code: _____ Country: _____

❑ I would like to enter a an individual/institutional subscription to NZJGG. (circle appropriate category)

❑ I enclose payment of NZ$/US$_____
(Payment by bankdraft preferred.)

❑ Please send invoice (institutional orders only)

❑ Please send free sample copy of NZJGG

❑ Please tick if tax receipt required.

❑ Charge my credit card account NZ$/US$_____

My credit card number is: Visa/Amex/Bankcard*/ MasterCard

Expiry date _____

Signature _____

**Bankcard accepted only for non North American orders.*

BMR
GEOLOGY AND
GEOPHYSICS
AUSTRALIA

CONTENTS

9 780644 145220

B91/20418 Cat. No. 91 03431